Systems-level analysis of the mitotic entry switch

María Rosa Domingo Sananes

St John's College

Supervisor: Professor Béla Novák

Dissertation submitted for the degree of Doctor of Philosophy

Department of Biochemistry, University of Oxford

February 2012

Abstract

Entry into mitosis in eukaryotes depends on the activation of the Cyclin-dependent kinase 1 (Cdk1), which phosphorylates many mitotic protein substrates. Activation of Cdk1 requires formation of a complex with Cyclin B (CycB), which gradually rises in concentration during interphase. However, in most organisms Cdk1 activation is not gradual but switch-like, because phosphorylation of the Cdk1-CycB complex by the Wee1 kinase normally keeps Cdk1-CycB inactive during interphase. Mitotic entry is induced when rapid dephosphorylation of Cdk1-CycB by the Cdc25 phosphatase causes abrupt activation of Cdk1-CycB. Cdk1-CycB in turn phosphorylates both Wee1 and Cdc25 leading to Cdc25 activation and Wee1 inhibition. This regulation creates both a positive and a double-negative feedback loop in the system, which are thought to generate a sharp, bistable switch that controls mitotic entry. Bistability is known to require positive feedback and ultrasensitivity, however, how ultrasensitivity arises in the mitotic switch is subject to extensive research efforts both experimentally and theoretically. In this thesis I explore several possible sources of ultrasensitivity in the mitotic switch through mathematical modelling. Based on theoretical considerations and experimental evidence, I show that the existence of multiple positive feedback loops, multisite phosphorylation, and Cdk1-CycB-dependent regulation of Cdk1-counteracting phosphatase activity can all contribute to ultrasensitivity and bistability in the mitotic switch. I analyse models of the mitotic switch including these bistability-generating mechanisms, to simulate and explain experimental data and make testable predictions. I argue that it is unlikely that a single mechanism is responsible for ultrasensitivity in this system, and that bistability requires a combination of different sources, including the ones studied here and others such as enzyme saturation and sequestration effects. I also highlight the importance of network architecture and coherent regulation of opposing reactions in generating efficient biochemical switches. Finally, I draw on recent experimental evidence and ideas derived from this analysis to propose a revised network of the mitotic switch.

Acknowledgements

I would like to thank my supervisor Béla Novák for all his help and unwavering support during my DPhil studies. I am particularly grateful for all the long discussions that gave me the opportunity to share his extensive knowledge about the cell cycle and dynamical systems, and his wonderful and unique perspective on how cells function.

I also thank Orsolya Kapuy, with whom I collaborated with in the phosphatase project, for many interesting and exciting discussions, and for all the time we spent together.

I thank our main collaborators in the work presented in this thesis, John Tyson, Tim Hunt, Liliana Krasinska and Daniel Fisher for their useful advice and for sharing their group's work.

Many thanks to Bernhard Schmierer for his encouragement, proofreading and for many helpful suggestions on this manuscript.

Thanks to all the other full-time and part-time members of the Novák group during my time here, Ahmed, Claude, Elwy, Enuo, Guido, Paula, Tongli, Vinod, for discussions and all the times we have shared. Special thanks to Anael Verdugo who read and commented on large portions of this thesis.

To Dan Best, I cannot thank you enough for your encouragement and help throughout this time, including reading all of this!

I thank my parents Carlos Domingo and Marta Sananes for everything.

This work would not have been possible without the Clarendon Fund and the ORS Award scheme that funded my DPhil studies.

Abbreviations

APC/C	Anaphase Promoting Complex/Cyclosome
CAK	CDK activating kinase
CDK	Cyclin dependent kinase
CKI	CDK inhibitor protein
CSF	Cytostatic factor
CycB	Cyclin B
DNA	Deoxyribonucleic acid
FBL	Feedback loop
FFL	Feedforward loop
IPF	Interphase promoting factor
MPF	M-phase promoting factor
NP	Non-phosphorylatable
ODE	Ordinary differential equation
PM	Phosphomimetic
RNA	Ribonucleic acid
SCF	Skp, Cullin, F-box containing complex

Table of contents

Chapter 1

Introduction: The eukaryotic cell cycle

1.1. Overview

This first chapter is a broad introduction to the eukaryotic cell cycle. I start by describing the general features of the cycle and the cell cycle control system. I also briefly describe the frog egg experimental system, which has been extensively used in studies of the cell cycle and is particularly relevant for the theoretical work presented in this thesis. Finally, I describe our current understanding of a biological switch that controls entry into mitosis in many eukaryotes, which is the main subject of study in this thesis. More detailed aspects of the cell cycle will be introduced, where relevant, in later chapters.

1.2. The eukaryotic cell cycle

All known living organisms in our planet are made of cells, and all of these cells have arisen as a result of reproduction by cell division from the last universal common ancestor to all organisms, which arose 3 to 4 billion years ago. Therefore, the sequence of events leading from one mother cell to two daughter cells, known as the *cell cycle*, is fundamental to life. During the cell cycle, cells must duplicate all their components, including the genetic information contained in chromosomes, and

subsequently distribute them accordingly between the two daughter cells (Nurse, 2000; Nasmyth, 2001; Morgan, 2007)

In eukaryotes, duplication and segregation of chromosomes are separated in time, giving rise to distinct phases of the cycle (Figure 1.1). Cell components, including chromosomes are duplicated during interphase, usually the longest part of the cell cycle, and subsequently distributed between the two daughter cells during M-phase. M-phase comprises nuclear division, or *mitosis*, usually followed by cell division, or *cytokinesis*. Several phases are usually recognized in interphase. In particular, chromosomal DNA is replicated during *S-phase*, when centrosomes are also duplicated. In many organisms S-phase and M-phase are separated further in time by two gap or growth phases; G1, the time between the end of M-phase and the start of the subsequent S-phase and G2, between S-phase and subsequent M-phase. The relative length of these gap phases varies between different organisms and cell types, and in some cases such as in embryonic cells, they can be absent. Other cells, particularly in multicellular organisms, can exit the cell cycle program permanently or for long periods and live in a non-proliferative state normally termed G0 (Nurse, 2000; Morgan, 2007).

M-phase is the most striking phase of the cycle, and is subdivided into several phases, mainly characterized by remarkable changes to cell architecture, visible under the microscope (Figure 1.1). During *prophase*, the replicated chromosomes condense into distinct and separate entities, and in many organisms the nuclear envelope is disassembled. In *metaphase* the chromosomes align on the metaphase plane, usually in the middle of the cell, and the mitotic spindle is assembled. The spindle, a microtubule network, pulls sister chromatids apart and towards opposite poles of the

cell during *anaphase*. Finally, during *telophase* the chromosomes decondense and the nuclear membrane reassembles. This is usually followed by cytokinesis, which gives rise to two daughter cells (Morgan, 2007).

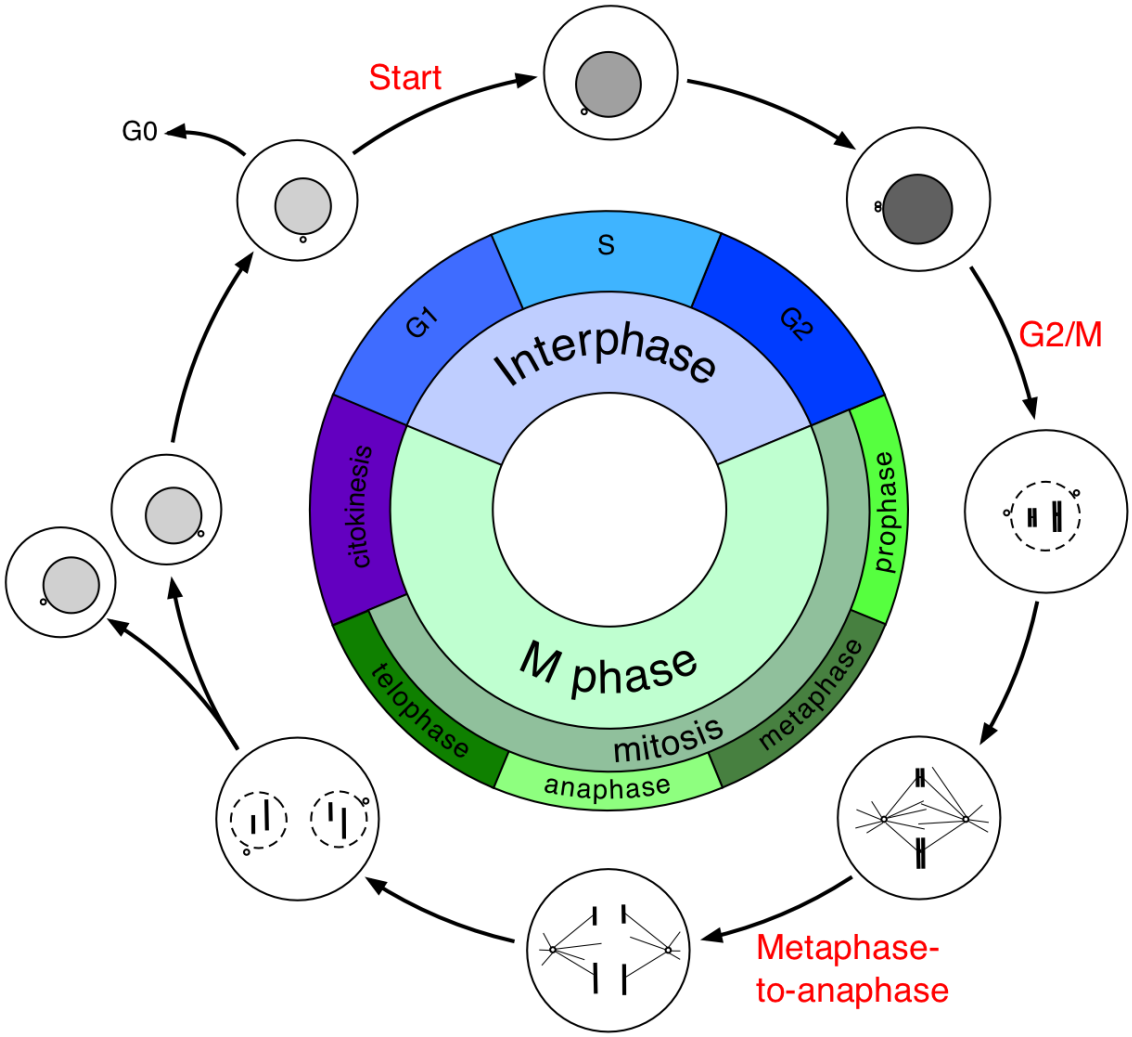

Figure 1.1. *The eukaryotic cell cycle*. The inner circle indicates the phases of the cell cycle, although their size does not necessarily reflect the length of the phase. Cell morphology and the state of chromosomes are represented schematically. The large circles represent the nucleus and the small circles the centrosome. The lines connecting centromeres and chromosomes in metaphase and anaphase represent the mitotic spindle.

All the different events that take place during the cell cycle must be carefully orchestrated and coordinated in order to ensure cell survival. In most cell types, chromosomal DNA must be accurately replicated only once per cell cycle, and this

process must be completed before mitosis takes place. Thus, in general, S-phase precedes M-phase, guaranteeing that each daughter contains one copy of the genetic information (Nurse, 2000, 2002; Pines, 2011). Cells also coordinate growth and cell division, therefore maintaining a constant average cell size through generations (Nurse, 2000, 2002; Goranov and Amon, 2010). However, there are some exceptions to this, such as embryonic division, in which there is no growth and cells get progressively smaller. The opposite happens during egg maturation were a normal cell grows without dividing. Finally, in many cases, and in particular in multicellular organisms, cell proliferation must be carefully controlled to ensure coordinated development and survival. Failure to do so can result in developmental abnormalities and disease, such as cancer (Morgan, 2007).

In most cells the correct ordering of cell cycle events is guaranteed by the existence of particular irreversible transitions during the cell cycle. There are three major transitions: *Start*, the point at which a new cell commits to a new cell cycle during G1, the *G2/M transition*, when cells make an irreversible commitment to enter mitosis, and the *metaphase-to-anaphase transition*, when cells make the decision to separate chromosomes (Figure 1.1). Cell cycle progression can be stopped before any of these three major transitions by signals and surveillance mechanisms, usually referred to as *checkpoints*, which ensure that relevant processes are completed. At Start cells usually check that they have the right size and that DNA is undamaged in order to be replicated. DNA damage and cell size can also impinge on the G2/M transition, which also monitors completion of DNA replication, controlled by the *DNA replication checkpoint*. The metaphase-to-anaphase transition requires correct spindle assembly and attachment of aligned chromosomes at the metaphase plane. This is monitored

by the *spindle assembly checkpoint*, also referred to as the mitotic checkpoint (Hartwell and Weinert, 1989; Novák et al., 2007; Morgan, 2007; Tyson and Novák, 2012).

The relative importance of these transitions, their regulation and the way surveillance mechanisms affect them seems to vary in different organisms and even in different cell types in the same organism. Thus, in most early embryonic cell cycles, surveillance mechanisms are inactive or have little effect on cell cycle transitions, and these early divisions take place even in the presence of unreplicated DNA or unaligned chromosomes (Murray and Kirschner, 1989; Morgan, 2007). There is also variation between unicellular organisms. For instance, fission yeast carefully monitors entry into mitosis at the G2/M transition by ensuring attainment of a critical cell size and completion of DNA replication (Nasmyth, 2001). In contrast, in budding yeast the G2/M transition is not very well defined, but the Start transition is carefully regulated (Dunphy, 1994; Nasmyth, 2001).

Over the last few decades there has been considerable progress in understanding the mechanisms that control the triggering and ordering of cell cycle transitions at a molecular level, commonly known as the cell cycle control system, as well as the surveillance mechanisms that impinge on them (Nurse, 1990; Nasmyth, 2001; Morgan, 2007). These mechanisms have been mostly elucidated using experimental models with relatively simple cell cycle control systems, such as the fission yeast, *Schizosaccharomyces pombe*, and the budding yeast, *Saccharomyces cerevisiae*, as well as early metazoan embryos, like those of the African clawed frog *Xenopus laevis*. However, models with more complicated cell cycle regulation are also widely used, for example *Drosophila* and cultured mammalian cells, including human cells. Despite

differences among different organisms and cells, the core of the cell cycle control system is remarkably conserved (Hartwell, 1991; Nurse, 2002; Nasmyth, 2001). In the next sections I present a summary of the current knowledge of the cell cycle control system, with a particular focus on the G2/M transition, which controls the entry into mitosis.

1.3. The cell cycle control network

The first experiments that started to elucidate the regulation of the cell cycle at a molecular level were carried out in the 1970s and 80s. Masui and Markert initially discovered that a soluble factor promoted egg maturation, by injecting cytoplasm from mature into immature oocytes (Masui and Markert, 1971). The unknown molecule was then named Maturation Promoting Factor. This same factor was subsequently detected in all mitotic eukaryotic cells examined to date, and consequently renamed M-phase Promoting Factor (MPF) (Dorée et al., 1989; Lohka, 1998; Duesbery and Vande Woude, 1998). Purification of MPF led to the demonstration that it was composed of a dimer of the homologue of the Cdc2 protein from fission yeast and B-type cyclin proteins (Lohka et al., 1988; Dunphy et al., 1988; Gautier et al., 1988, 1990; Labbé et al., 1989). Cdc2 and its budding yeast homologue Cdc28, were discovered by Paul Nurse (Nurse et al., 1976) and Lee Hartwell (Hartwell et al., 1974) respectively, and shown to be a serine-threonine protein-kinase (Simanis and Nurse, 1986), conserved in all eukaryotes from yeasts to man, whose activity fluctuated during the cell cycle (Lee et al. 1987; Moreno et al. 1989). The B-type cyclins (CycB) were discovered in fertilized sea urchin eggs by virtue of their abrupt disappearance during mitosis, after steady accumulation during interphase (Evans et

al., 1983; Pines and Hunt, 1987). Since cyclin binding turned out to be essential for Cdc2 protein kinase activity, Cdc2/Cdc28 became the founding member of the Cyclin-dependent protein kinases (CDKs) and was renamed Cdk1 (Nigg, 2001). Since then, other CDKs have been found, many of which have specific functions in cell cycle control. Some organisms have several CDKs, but others, such as the yeasts, have only one (Morgan, 1997; Bloom and Cross, 2007; Hochegger et al., 2008).

Most organisms also contain several classes of cyclins, which activate CDK proteins in different phases of the cell cycle and control specific events by phosphorylating downstream substrates. In particular, G1 cyclins promote entry into a new cell cycle (Start), while G1/S cyclins promote DNA replication (Bloom and Cross, 2007; Morgan, 2007; Hochegger et al., 2008). The most prominent cyclins are the mitotic or type B cyclins, which as mentioned before, in partnership with Cdk1 are considered the trigger for mitosis (M-phase) in all eukaryotic cells (Nurse, 1990; Coleman and Dunphy, 1994; Lohka, 1998). The Cdk1-CycB complex or MPF promotes this state by phosphorylating many downstream mitotic proteins. It is believed that this big increase in protein phosphorylation in M-phase is responsible for bringing about all the changes associated with mitosis. In fact, different studies have identified hundreds of mitotic phosphoproteins, many of which are directly phosphorylated by CDKs (Ubersax et al., 2003; Loog and Morgan, 2005; Dephoure et al., 2008; Holt et al., 2009; Errico et al., 2010).

As expected from their prominent role in controlling cell cycle transitions, the activity of CDKs is tightly controlled during the cell cycle. As further explained below, there are three main mechanisms that cells use to regulate their activity: (*i*) regulation of cyclin abundance, (*ii*) stoichiometric inhibition and (*iii*) posttranslational

modifications, in particular phosphorylation of the CDK subunit (Nurse, 1990; Morgan, 1997, 2007). In general, the concentration of CDKs remains constant throughout the cycle, and control in their abundance is not an important regulatory mechanism of their activity in the cell (Hochegger et al., 2008).

The early experiments in which cyclins were discovered due to their periodic appearance and disappearance, suggested that control of the concentration of different cyclins is a fundamental for regulation of CDK activity (Evans et al., 1983; Bloom and Cross, 2007; Pines, 2011). Cyclin abundance in the cell depends on the relative rates of production and degradation, both of which can be regulated. For example, expression of certain cyclins can be limited to a certain part of the cell cycle (Bloom and Cross, 2007; Hochegger et al., 2008). However, the targeted degradation of cyclins at specific points in the cycle is particularly important. Specific degradation is achieved though the activity of ubiquitin ligases, which can polyubiquitinate cyclins, marking them for proteosomal degradation (Hershko, 2005; Peters, 2006; Pines, 2011). The most important of such ubiquitin-ligases is the Anaphase-Promoting Complex or Cyclosome (APC/C), a multisubunit complex that is activated by CDKs during mitosis, and is responsible for cyclin degradation at the metaphase-to-anaphase transition (Hershko, 2005; Peters, 2006; Pines, 2011). Regulation of APC/C by CDKs creates a negative feedback loop in the cell cycle control system, whereby CDK activity leads to its own inhibition by promoting cyclin degradation (Tyson et al., 2001; Morgan, 2007). The APC/C is able to target particular substrates via its activators Cdc20 and Cdh1. APC-Cdc20 is responsible for degradation of CycB after the metaphase-to-anaphase transition, while APC-Cdh1 is active during G1, and is thought to keep cyclin levels down at this point in the cell cycle (Peters, 2006;

Sullivan and Morgan, 2007; Hochegger et al., 2008). Another important ubiquitin ligase in cell cycle control is the SCF complex, named after its constituent components (Skp1, Cullin and F-box). SCF specifically targets G1 cyclins during late G1 and S phase, among other proteins, and its activity is important for the G1/S transition (Bloom and Cross, 2007).

Cyclin binding is necessary, but not sufficient for CDK activity because the dimers are not necessarily active. In many organisms, CDK-cyclin dimers can be inactivated by binding to small-protein inhibitors, such as Sic1 in budding yeast, Rum1 in fission yeast, or p27 in humans. These stoichiometric inhibitors are commonly referred to as CKIs (CDK inhibitors). They are particularly important during G1 and S, where they inhibit CDKs bound to residual mitotic cyclins, and help to maintain stable G1 and prevent early mitotic entry (Morgan, 1997; Bloom and Cross, 2007).

CDK-cyclin dimers can also be regulated by posttranslational modifications. In particular, phosphorylation of Cdk1 by protein-kinases belonging to the Wee1 family leads to its inactivation. The first member of these inhibitory kinases, Wee1, was discovered in fission yeast by isolation of mutant cells that entered mitosis at a reduced cell size (Nurse, 1975; Thuriaux et al., 1978). Most organisms have duplicates of these inhibitory kinases, for example, Wee1 and Mik1 in fission yeast, and Wee1 and Myt1 in vertebrates (Lundgren et al., 1991; Mueller et al., 1995). The Wee1-dependent inhibitory phosphorylations on Cdk1 are removed by the Cdc25 phosphatase, which therefore acts as a Cdk1 activator (Russell and Nurse, 1986). Both Wee1 and Cdc25 are regulated by CDK-dependent phosphorylation. This results in Wee1 inhibition and Cdc25 activation (Tang et al., 1993; Mueller et al., 1995; Izumi et al., 1992; Kumagai and Dunphy, 1992; Coleman and Dunphy, 1994; O'Farrell, 2001;

Lindqvist et al., 2009). Therefore, the activity of Cdk1-CycB is regulated by a double negative (Cdk1 ⊣ Wee1 ⊣ Cdk1) and a positive (Cdk1→ Cdc25 → Cdk1) feedback loop (Figure 1.2A), that is, Cdk1-CycB activates its activator and inhibits its inhibitor (Solomon et al., 1990; Nurse, 1990; Novák and Tyson, 1993; O'Farrell, 2001). As we will see later this regulation of Cdk1-CycB is particularly important for the G2/M transition. CDKs are also phosphorylated on the T-loop, near their active site by CDK-activating kinases (CAK). This phosphorylation is essential for CDK activity, but it seems to be unregulated and occurs constantly throughout the cell cycle once cyclin has bound to CDK (Morgan, 1997; Lindqvist et al., 2009).

Periodic CDK activity is thought to drive the eukaryotic cell cycle. A simplified view of this control system is summarized in Figure 1.2. In a newborn cell, cyclin concentrations are low but their levels start rising as the cell grows. However, Cdk1 activity is kept low due to Wee1-dependent phosphorylation, because Wee1 is active and Cdc25 inactive. When cyclin levels are high enough, Cdc25 is activated and Wee1 inactivated, resulting in activation of Cdk1-CycB complexes and entry into mitosis. Cdk1 is then able to activate the APC, which leads to cyclin destruction and mitotic exit. This basic picture (Figure 1.2), provides an appealingly simple view of mitotic control in eukaryotes through the regulation of Cdk1-CycB activity (Nurse, 1990; O'Farrell, 2001). This general framework is further validated by the fact that it is conserved, and all studied eukaryotes require Cdk1-CycB activity in order to enter mitosis (Coleman and Dunphy, 1994). In fact in some cases cell cycles seem to be almost that simple. For instance, it has been recently demonstrated that fission yeast can have a normal cell division with a single CDK-cyclin complex (Fisher and Nurse, 1996; Coudreuse and Nurse, 2010), while the link between Cdk1-CycB and mitosis

can be tracked in extracts of *Xenopus laevis* eggs, in which simple embryonic cell cycles, lacking gap phases and checkpoints, can be replicated *in vitro* (Murray and Kirschner, 1989; Brown, 2004; Philpott and Yew, 2008).

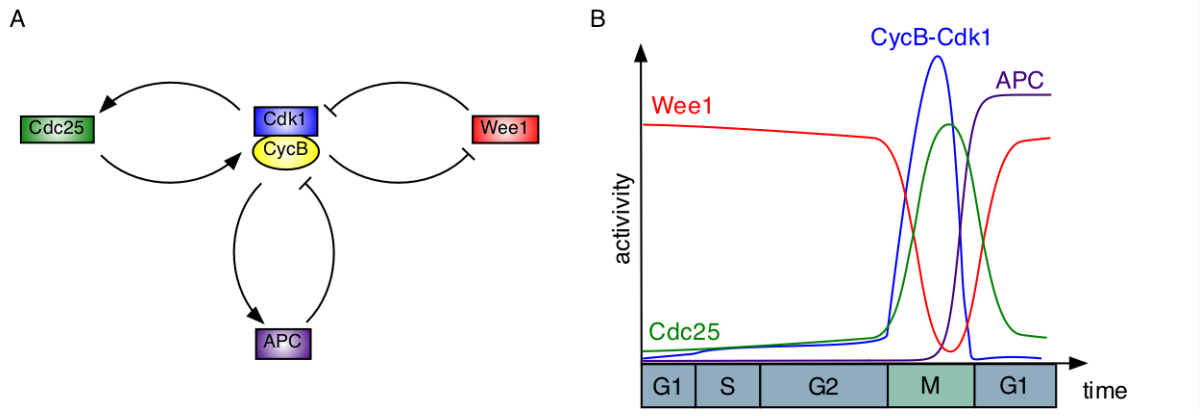

Figure 1.2. *A simple view of the cell cycle control network.* ***A***. Interaction diagram of the main components in the network. Cdk1-CycB, or MPF, is involved in a positive feedback loop with Cdc25, a double negative (positive) feedback loop with Wee1 and a negative feedback loop with the APC/C. **B**. Schematic picture of the activity of the cell cycle control network components in time, during the different phases of the cell cycle. In interphase (G1, S, G2) cyclin levels increase gradually, Wee1 is active and Cdc25 is inactive. At the onset of mitosis, Cdk1-CycB and Cdc25 are activated and Wee1 is inactivated. The APC/C is eventually activated, leading to cyclin destruction and inactivation of Cdk1-CycB. Eventually Cdc25 and APC/C are inactivated and Wee1 is reactivated.

However, in reality, control of the different phases of the cell cycle in many cells tends to be much more complicated. Early events in G1 and S are usually initiated by G1/S cyclins, whose rise is dependent on external and internal signals (such as attainment of a critical size, nutrient availability and presence of growth factors) that convey to the cell that conditions are appropriate to go through the Start transition and start a new cell cycle. In G1 and early S, mitotic cyclin levels and their associated CDK activity (usually Cdk2) is kept low by the action of APC-Cdh1 and CKIs. However, G1 cyclins are insensitive to these regulators and therefore CDK activity associated with these cyclins then usually activates DNA replication (Bloom and Cross, 2007;

Hochegger et al., 2008; Morgan, 2007). Links between sister chromatids are established during replication by proteins called cohesins (Uhlmann, 2003). Checkpoints and surveillance mechanisms then monitor attainment of an appropriate cell size, completion of DNA replication and occurrence of any DNA damage. These mechanisms can delay or block the G2/M transition, usually by interfering with Cdk1 activation by promoting its tyrosine phosphorylation by Wee1 (Morgan, 1997; Perry and Kornbluth, 2007). However, the finer details of how entry into mitosis is achieved are still a matter of much debate. Background CDK activity might eventually lead to Cdk1 and Cdc25 activation, together with Wee1 inhibition, but it is thought that other factors may affect mitotic entry (Lindqvist et al., 2009).

Once Cdk1-CycB is activated, chromosomes usually condense and in many organisms the nuclear membrane is disassembled, the spindle forms and chromosomes align at the metaphase plane (Sullivan and Morgan, 2007). Certain conditions must be met before the cell can go through the metaphase-to-anaphase transition and the cell can exit mitosis. A signaling pathway, usually known as the spindle assembly checkpoint, monitors chromosomal attachment and is believed to keep APC-Cdc20 inactive until the last kinetochore is bioriented. When this happens, APC-Cdc20 is activated and CycB levels start to drop (Peters, 2006; Sullivan and Morgan, 2007; Pines, 2011). APC-Cdc20 also leads to degradation of securin, a protein inhibitor of separase, a protease that cleaves the cohesin molecules that bind sister chromatids together (Uhlmann, 2003). This allows the spindle to pull the chromatids to opposite poles of the cell and anaphase to take place. The drop in cyclin and therefore in CDK activity leads to dephosphorylation of mitotic substrates, reassembly of the nuclear membrane and chromosome decondensation. When cyclin levels and thus CDK activity drop to very

low levels cytokinesis takes place. At this point, replication origins can be licensed for a new round of DNA synthesis. Finally, the activities of APC-Cdh1 and CKIs rise, leaving the new cell back in a stable G1 state (Sullivan and Morgan, 2007; Morgan, 2007).

This description corresponds to a generic eukaryotic cell cycle that includes all the main regulatory mechanisms. However, there are significant differences between organisms. Budding yeast and fission yeast have a single CDK molecule, and fission yeast can even have a functional cycle with a single cyclin (Bloom and Cross, 2007; Hochegger et al., 2008; Coudreuse and Nurse, 2010). Also, different transitions can be more or less important depending on the cell. For example, in fission yeast the Start transition is usually cryptic and cells go through Start as soon as mitosis is completed (before cytokinesis), resulting in a very short G1. In contrast, in budding yeast Cdk1 activity starts rising at Start, while the G2/M transition is not well defined, and the Wee1 and Cdc25 homologues do not have a role in determining the time of mitotic entry (Nasmyth, 2001; Tyson and Novák, 2002; Bloom and Cross, 2007). Moreover, the cell cycle control system of embryonic cells is particularly simple. They are usually very fast, and lack many of the surveillance mechanisms that allow other cells to arrest at particular checkpoints (Nigg, 2001; Morgan, 2007).

Despite these differences, particular transitions in different cell cycles must be irreversible, unmistakable, and coordinated with the rest of the cell cycle. I will focus on the G2/M transition, which I will refer to as the *mitotic switch*. In the next sections I will describe our current knowledge of this switch. But before, because a large amount of research on this topic has been carried out in *Xenopus* egg extracts and

most of the mathematical models presented here are based on data obtained in this system, I will give a brief introduction to the this experimental system.

1.4. The *Xenopus* egg system

Eggs produced by female *Xenopus laevis* have been used for decades in studies of cell cycle control, DNA replication and embryonic development (Ferrell, 1999a; b; Brown, 2004; Philpott and Yew, 2008). Mature eggs remain arrested in metaphase II of meiosis awaiting fertilization. This arrest is characterized by the high kinase activity of Cdk1-CycB, which maintains the metaphase state both in meiosis and in mitosis. The arrest is maintained by the Cytostatic Factor (CSF), now thought to basically be composed of Erp1/Emi2, a protein that inhibits APC/C, preventing cyclin degradation (Hansen et al., 2007; Wu and Kornbluth, 2008). Fertilization, or artificial egg activation by membrane depolarization or addition of a calcium ionophore leads to degradation of Erp1 and exit from meiosis II (Hansen et al., 2007; Wu and Kornbluth, 2008; Philpott and Yew, 2008). After a pause, this is followed, by twelve fast and synchronous cell cycles, of about 20-30min each, after which the embryo reaches the mid-blastula transition. Until this point, there is no transcription from the embryo's chromosomes, and cell division depends on maternal proteins and mRNAs (Philpott and Yew, 2008). Therefore transcriptional regulation has no role in controlling these early embryonic cycles. In fact, translation and degradation of CycB seems to be sufficient to drive these cycles (Minshull et al., 1989; Murray and Kirschner, 1989). After the mid-blastula transition, which is triggered when the nucleocytoplasmic ratio reaches a critical level, cell cycles become slower and less synchronized, surveillance

and checkpoint mechanisms become active and transcription and cell differentiation start (Philpott and Yew, 2008).

These early, and relatively simple cycles are particularly useful for studying the core of the cell cycle regulatory network. Most studies concerning cell cycle control are not carried out on intact eggs, but on highly concentrated cell-free extracts obtained by crushing eggs by centrifugation. These extracts are able to replicate early embryonic cycles and provide a biochemically tractable system in which components can be added or removed by immunodepletion (Hutchison et al., 1988; Murray and Kirschner, 1989; Brown, 2004; Kornbluth et al., 2006). In an extract made from mature eggs, fertilization can be mimicked by addition of calcium ions, which results in the processes typically associated with meiotic exit: dephosphorylation of CDK substrates and cyclin degradation (Kornbluth et al., 2006). If protein synthesis is allowed, "cycling extracts" are obtained. In these, CycB can be resynthesized after mitotic exit, eventually leading to Cdk1 activation and mitosis. The APC/C is eventually activated, resulting in CycB degradation and Cdk1 inactivation, therefore taking the extract back into interphase. Several cycles of CycB synthesis and degradation, and MPF activation and inactivation can usually be followed in these extracts. Exogenously added DNA is also replicated during the cycles, making this system useful to study DNA replication (Brown, 2004; Kornbluth et al., 2006; Philpott and Yew, 2008).

Like many other embryonic cell cycles, the early cycles observed in *Xenopus* extracts as oscillations in Cdk1 activity, lack gap phases and surveillance mechanisms that turn on arrest at checkpoints, which is one of the reasons they are so fast. For instance, during these cycles there are no CKIs and no APC-Cdh1 activity, and

therefore no stable G1 phase. Thus, these are "simplified" cell cycles, very well suited to study the core of the cell cycle control system. Fortunately, the high conservation of the cell cycle control machinery means that many of the features discovered in this system are relevant for other eukaryotes, including humans (Morgan, 2007; Philpott and Yew, 2008).

1.5. The mitotic switch

The decision to enter mitosis is crucial for most cells and accordingly there are multiple mechanisms that ensure that it occurs at the appropriate time and that the cell is capable of carrying the process to completion. It would be disastrous for the cell if it flipped back and forth stochastically between mitosis and interphase. For example, this could lead to division with unreplicated chromosomes, or exit from mitosis before the separation of sister chromatids. Therefore the decision to enter mitosis must be driven by a reliable mechanism that leads to a robust transition into mitosis, and prevents exit until all the necessary processes are completed. Work in the last few years has shown that there is a switch underlying mitotic entry, and further control mechanisms ensuring an appropriate mitotic exit (O'Farrell, 2001; Sha et al., 2003; Pomerening et al., 2003; Sullivan and Morgan, 2007).

The main topic of this thesis is to study properties of this switch using mathematical models. In this section I will introduce the most important features of this biological switch, from both an experimental and a theoretical perspective.

1.5.1. The cyclin threshold for MPF activation

As mentioned in the last section, the early embryonic-like cell cycles in *Xenopus* egg extracts are driven by constant synthesis and periodic degradation of CycB. In these extracts, CycB is synthesized continuously, and at the start of a new cycle its levels increase gradually. However, entry into mitosis is abrupt or switch-like, and only occurs after cyclin reaches a high enough level. This was shown clearly by early experiments that proposed the existence of a CycB threshold for mitotic entry. Solomon et al. (1990) used egg extracts blocked at interphase by addition of the protein synthesis inhibitor cycloheximide and added different amounts of non-degradable CycB (recombinant CycB lacking the destruction box normally recognized by the APC). Therefore, if these extracts enter mitosis, they are blocked in this state, because they cannot destroy CycB (Murray et al., 1989; Solomon et al., 1990). They observed that low cyclin levels did not lead to significant Cdk1 activation, and that a minimum concentration of cyclin, or a *cyclin threshold*, was needed to activate Cdk1. They also showed that there was a time delay in the activation of MPF, which became shorter the more cyclin was added. Finally, they demonstrated that during the delay in MPF activation, or when sub-threshold levels of cyclin were added, Cdk1 was inhibited by Wee1-dependent phosphorylation at tyrosine 15 (Solomon et al., 1990). Therefore, it was proposed that tyrosine phosphorylation of Cdk1 by Wee1 kept MPF activity restrained before mitotic entry, at which point, Cdk1 was rapidly dephosphorylated by Cdc25 and consequently activated (Solomon et al., 1990; Nurse, 1990). It was even proposed that positive feedback loops between MPF and its two regulators could help ensure that this was a switch-like transition (Solomon et al., 1990).

These results led to the proposal by theoreticians that this switch controlling mitotic entry is a *bistable* system (Novák and Tyson, 1993; Thron, 1996). In essence this means that the system has two possible, qualitatively different steady states, where Cdk1-CycB complexes are either active or inactive, and the cell is thus either in mitosis or interphase respectively. This means that the system cannot rest in an intermediate state with partially active Cdk1-CycB. Whether the cell is in mitosis or interphase will depend on the CycB level, but crucially, it will also depend on the history of the system, as explained below. In order to understand the significance of bistability in the mitotic switch, I will first give a brief introduction to this concept and switch-like responses.

1.5.2. Biological switches and bistability

Bistability can be best illustrated by a signal-response curve, which shows the steady state levels of a *response* to different values of a *signal*. In biochemical systems, these *signal-response* curves can have many different shapes, some examples of which are shown in Figure 1.3. A response can be *linear,* (Figure 1.3A) although more commonly in biological systems, responses are usually saturated, which can give rise to *hyperbolic* curves (Figure 1.3B) (Tyson et al., 2003). These are common responses, but do not constitute good switches. A *switch* can be described as a response in which a small change in the signal produces a significant change in the response. A signal-response curve of sigmoid shape provides a better switch, and this type of response is usually called *ultrasensitive* (Figure 1.3C). Such responses are common and important in biological systems (Koshland et al., 1982; Tyson et al., 2003). The most well known example is the response of the concentration of oxygenated haemoglobin with respect to the concentration of dissolved oxygen in the blood. The sigmoid shape

of this curve allows haemoglobin to become fully oxygenated in the lungs where the oxygen concentration is high, but to significantly give up oxygen in the body tissues where the oxygen concentration is lower. This ultrasensitive response of haemoglobin is the result of cooperative interactions between the different subunits that form a haemoglobin molecule (Perutz et al., 1998; Koshland and Hamadani, 2002).

Despite being better switches, ultrasensitive responses are, like linear and hyperbolic responses, graded and reversible (Tyson et al., 2003). That is, the response is a continuous function of the signal, as any small increase in the signal results in an small increase in the response, while if the signal increases and then returns to a lower value, the response will first change, but then also return to its original state, via the same path, as shown by the arrows in Figures 1.3A-C (Tyson et al., 2003). A much better switch can be achieved with a *bistable* signal-response curve, which can be S-shaped (Figure 1.3D) (Tyson et al., 2003). The top and bottom branches correspond to stable steady states and the middle branch to unstable steady states. If the system is initialized at low values of the signal, it will have a single steady state on the lower branch of the diagram. If the signal is increased, it will remain in this lower branch until it reaches the value corresponding to point Q. Beyond this point, the response will jump to the top branch. However, if at this point the signal is decreased, the response will not revert to the lower branch but remain on the top branch until the signal corresponding to point W is reached (see arrows in Figure 1.3D). This discontinuity or irreversibility of the system as the signal is varied, resulting in different paths depending on the direction of movement, is called 'hysteresis' (Laurent and Kellershohn, 1999; Strogatz, 1994; Ferrell and Xiong, 2001; Ferrell,

2002; Tyson et al., 2003; Mitrophanov and Groisman, 2008) , and is a characteristic of bistable systems which has been used to experimentally prove bistability in biological systems (Pomerening et al., 2003; Sha et al., 2003; Ozbudak et al., 2004; Mitrophanov and Groisman, 2008). In some cases, point W can be unreachable again for positive values of the signal, and therefore the transition will be completely irreversible (Figure 1.3E). This is thought to happen in cell differentiation (Hervagault and Canu, 1987; Xiong and Ferrell, 2003; Dubnau and Losick, 2006; Mitrophanov and Groisman, 2008).

In bistable responses, for a range of signal values, the system can be in either the top or lower branch of steady states. Within this *bistability range,* shown in red on Figure 1.3D-E, the final steady state will depend on the history of the system. That is, within the bistable range, if the system is above the unstable steady state branch, it will go to the top branch, if it is below, it will move towards the bottom branch of stable steady states. This is why bistable systems are also referred to as systems with *memory* (Ferrell and Xiong, 2001; Novák and Tyson, 2008). At the extremes of this bistability range, there are two *saddle node bifurcations*, the points where the system can "jump" from one steady state to another (points Q and W in Figure 1.3D) (Strogatz, 1994; Tyson et al., 2001, 2003). Other features of bistable systems will be explained further in Chapter 2, and in the next subsection I will explain bistability in the mitotic switch controlling the G2/M transition.

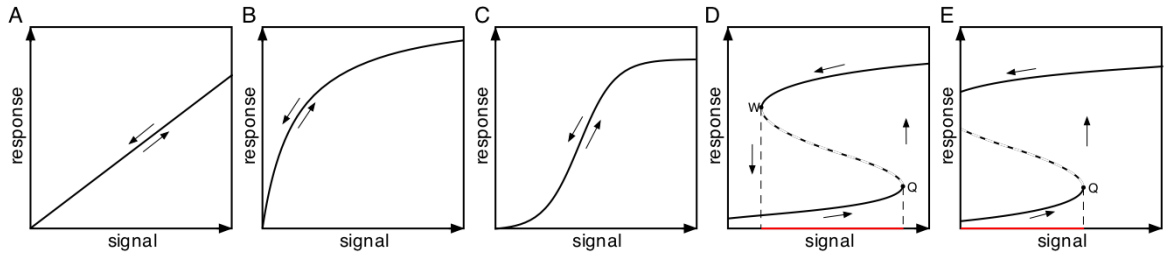

Figure 1.3. *Cartoon of different types of signal-response curves for a biochemical system.* **A**. Linear response. **B**. Hyperbolic response. **C**. Ultrasensitive response. **D**. Bistable response. **E**. Irreversible bistable response. Stable steady states are shown in solid lines and unstable steady states by dashed lines. The arrows indicate the direction of movement of the system when the signal is varied. Points Q and W in panels D and E are saddle node bifurcations. See text for more details.

1.5.3. The bistable mitotic switch

Bistability in the mitotic switch can be revealed if the signal is considered to be the total amount of CycB and the response is Cdk1-CycB (or MPF) activity. A hypothetical signal-response curve for the frog egg extract system, initially proposed by Novák and Tyson (1993) is shown in Figure 1.4. When the total cyclin level is very low, Cdk1-CycB complexes are inactive, due to Wee1-dependent phosphorylation of Cdk1. As cyclin increases, MPF activity increases very little along the lower branch of the curve, because the dimers remain mostly phosphorylated. When the total amount of cyclin reaches point A, the system will jump to the upper branch of the diagram, that is, is activated as a result of Cdc25 activation and Wee1 inhibition. If cyclin increases even more, MPF continues to rise along this upper branch, where most Cdk1-CycB complexes are active. However, if CycB is now reduced, the system will not jump back to the lower branch at point A, but will continue on the upper branch until CycB is reduced to point B.

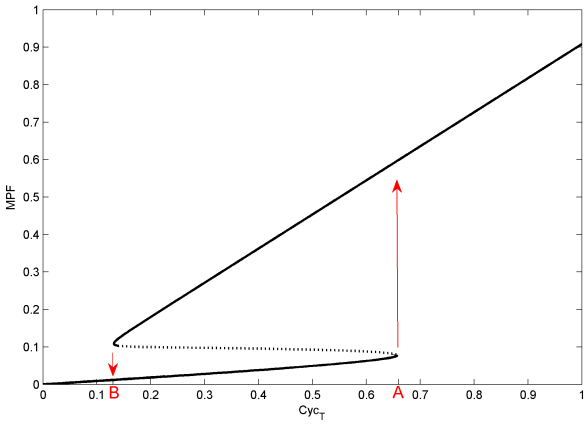

Figure 1.4. *Hypothetical signal-response curve for MPF activity respect to total cyclin levels.* Point A indicates the cyclin threshold for MPF activation and point B the cyclin threshold for MPF inactivation. The dashed portion of the curve shows the branch of unstable steady states.

The saddle-node bifurcations at which the system "jumps" between steady states then correspond to the cyclin thresholds (Novák and Tyson, 1993). In particular, point A corresponds to the cyclin threshold for Cdk1 activation observed by Solomon et al. (1990). Due to bistability in the mitotic switch, a graded signal, the increasing amount of CycB, can be transformed into an almost "discontinuous" response, seen as an abrupt activation of Cdk1-CycB. This model therefore predicted the existence of hysteresis, and thus the presence of a cyclin threshold for MPF inactivation, which is lower than the cyclin threshold for MPF activation (Novák and Tyson, 1993). Furthermore, it also explained the lag time in MPF activation at different cyclin levels, as the time it takes the positive feedback loops involved in MPF activation to become engaged, and predicted that this lag is longer the closer cyclin levels are to the threshold (Novák and Tyson, 1993).

Further work has proposed that most, if not all the irreversible transitions of the cell cycle are based on bistable switches (Chen et al., 2000; Novák et al., 2007; He et al.,

2011), and increasing amounts of experimental evidence seem to suggest that this is the case (Cross et al., 2002; Yao et al., 2008; López-Avilés et al., 2009). Furthermore, bistability seems to be an important characteristic of many other biological systems involved in decision-making in unrelated organisms (Ninfa and Mayo, 2004; Graumann, 2006). Bistable switches in general have properties that are probably useful in many instances and have likely arisen multiple times and then been conserved and tweaked during evolution. Among these properties is robustness to noise, since once the system has moved to a new state, small fluctuations in the signal will not make the system switch back (Laurent and Kellershohn, 1999; Ferrell and Xiong, 2001).

As I will explain in Chapter 3, certain conditions must be met by the system in order to achieve bistability. Among these, the most important is probably the existence of positive feedback, or self-stabilization of the stable states (Ferrell and Xiong, 2001). In the mitotic switch, positive feedback between Cdk1 and its regulators Wee1 and Cdc25 seems to be crucial for bistability, as has been theoretically predicted (Novák and Tyson, 1993; Pomerening et al., 2005) and experimentally demonstrated (Pomerening et al., 2005). The other requirement for bistability is an ultrasensitive response from components of the positive feedback loop. This filters small stimuli, so the system does not switch immediately at small levels of the signal (Ferrell and Xiong, 2001). Most of this thesis will focus on the analysis of this switch from a theoretical perspective to try to understand what the requirements for bistability are and how the mitotic switch meets these requirements.

1.6. Summary

In this chapter I have introduced basic notions about the cell cycle and the cell cycle control system. Cdk1-CycB or MPF has a prominent role in cell cycle control, and its kinase activity is essential for triggering mitosis in all studied eukaryotes. The activity of MPF is regulated in different ways, such as control of CycB levels and inhibition of Cdk1 by Wee1-dependent phosphorylation. These two mechanisms are particularly important in controlling the cell cycle-like oscillations of MPF activity in *Xenopus* egg extracts. Phosphorylation of Cdk1 by Wee1 during interphase and its subsequent Cdc25-catalysed dephosphorylation at mitotic entry are the basis of the abrupt activation of MPF that takes place at the onset of mitosis. Positive feedback between MPF and its regulators creates a bistable switch that guarantees a robust transition into mitosis. The main features of this bistable mitotic switch are the presence of a cyclin threshold for MPF activation and a different, lower threshold for MPF inactivation. In the next chapter, I introduce mathematical concepts important for this thesis and expand on the concepts of bistability and hysteresis introduced in this chapter.

Chapter 2

Mathematical background

2.1. Overview

Information about interactions between molecules in biochemical networks is usually summarized in schematic diagrams, which can be used as starting point for constructing mathematical models. One way these networks can be described is by systems of Ordinary Differential Equations (ODEs), which determine how the concentrations and activities of the different molecules change in time. These systems of ODEs can be analysed in different ways, such as solving them analytically or numerically, but they can also be studied by qualitative methods.

The aim of this chapter is to provide essential mathematical background for later chapters, and it essentially constitutes a Methods section. I will provide a brief introduction to the notion of mathematical modelling using ODEs and their analysis using stability and bifurcation theory, together with numerical simulation. I will also introduce the concept of network motifs, particularly of feedback and feedforward loops, which will be encountered throughout this thesis.

2.2. Ordinary differential equations and steady states

Ordinary Differential Equations are mathematical expressions that relate a dependent variable and its derivative(s) with respect to one independent variable (Jordan and Smith, 2008). In the models of biochemical networks presented here, the independent variable is time and dependent variables will usually correspond to chemical species, particularly proteins. Such ODEs thus define the rate of change of the dependent variables and describe how the concentration or activity of the molecules in the biochemical network fluctuates in time. The equations will include rates of reactions in which the protein is produced (synthesized or activated) and reactions in which the protein is consumed (degraded or inactivated). For the concentration of a protein X, this can be expressed in a general form (Conrad and Tyson, 2006):

$$\frac{dX}{dt} = X' = synthesis + activation - degradation - inactivation \qquad 2.1$$

The terms in this equation correspond to reaction rates, usually described by a rate function and associated parameters. These rate functions describe the kinetic mechanism of the reaction, and are usually dependent on one or more variables (usually the reactants), potentially including X itself. Some types of rate functions relevant for this thesis are described in more detail in the next section, but in the following examples I will use simple mass action laws. For example, the change in concentration of a protein A that is synthesized with a constant rate k_s and degraded with rate k_d can be described by the following ODE:

$$\frac{dA}{dt} = k_s - k_d A \qquad 2.2$$

Thus the positive part of the equation describes the synthesis and the negative term the degradation. This last term also includes the concentration of A itself, since its degradation rate depends on how much of A there is: the higher its concentration, the faster its rate of degradation.

Many ODEs can be solved analytically by integration, that is, it is possible to find a differentiable function that fulfils the ODE. For the example above, the solution can be found by separation of variables and integration, leading to an expression which describes how the concentration of A varies in time, given values for the synthesis and degradation rate constants (k_s and k_d), and an initial condition. This initial condition describes the state of the system at a particular time, that is, the value of the variable at some point in time, which gives enough information to predict the state of the system at all future times. This initial condition is required because the ODE does not specify the state, but only how it changes. For example, if the value of the concentration of A at *t=0* is A_0, an analytical expression for the concentration of A in time can be derived:

$$A = \frac{k_s}{k_d} + \left(A_0 - \frac{k_s}{k_d}\right) e^{-t/k_d} \qquad 2.3$$

Thus, Equation 2.3 is the solution for the initial value problem composed of the ODE in Equation 2.2 and the initial condition $A = A_0$ at $t = 0$. Although many ODEs can be solved analytically, this is not always the case, and it is necessary to use other strategies to study them. The most common alternative strategy is to use numerical approximations to simulate their solution using computers, as will be briefly

explained later. Another approach is to use qualitative methods, such as rate plots and phase plane analysis, which I introduce in the next sections.

Of course most of the models presented in this thesis are for systems with more than one chemical species. Therefore, I will normally deal with systems composed of several ODEs where each ODE describes the rate of change of a single variable. This rate will usually depend on other variables in the system, and the variable itself. In this case, the dimensionality of the system is equal to the number of variables, and the concentration or activity of every one of these variables describes the state of the system.

A relatively simple but informative way to analyse a system of one or more ODEs is to study its steady states or equilibrium solutions. These are values of the variables at which the system remains once it has reached them. At these points the values of the variables do not change as time progresses. That is, their rate of change is equal to zero, and therefore the system is represented by an algebraic equation for each variable. Thus for the example in the previous section (Equation 2.2), at steady state

$$\frac{dA}{dt} = k_s - k_d A = 0 \qquad 2.4$$

and therefore

$$A^* = \frac{k_s}{k_d} \qquad 2.5$$

where A^* is a steady state of the system, in this case the only one.

An important feature of a steady state is their stability. A steady state is stable if small perturbations from it become smaller with time, that is, if the system returns to the

steady state. On the other hand, if disturbances grow, the steady state is unstable. For a more extensive introduction to ODEs and their analysis, the reader is referred to book-length treatments and reviews (Strogatz, 1994; Jordan and Smith, 2008; Tyson et al., 2001; Klipp et al., 2005; Conrad and Tyson, 2006; Kreyszig, 2010).

2.3. Reaction kinetics

An important aspect of constructing a mathematical model of a chemical reaction system is the assumption made for the kinetics of the reaction rates, that is, the functions that form the terms of the ODEs. In this section I briefly describe some relevant kinetic assumptions used in later chapters. For a more extensive treatment of reaction kinetics, the reader is referred to relevant textbooks and reviews (Murray 2002; Voet et al. 2004; Klipp et al. 2005; Cornish-Bowden 2004; Gonze et al. 2011)

2.3.1. Mass action kinetics

The Law of Mass Action states that the rate of a reaction is proportional to the probability of a collision between the molecules involved in the reaction, and thus proportional to the product of the concentrations of the species involved. The rate of the reaction is therefore determined by the reactant concentrations and a rate constant of proportionality. This is usually the simplest assumption, and the most used in this thesis, for reasons that will be discussed later.

Reactions and the rate constants associated with them are classified according to the number of molecules involved (or number of molecules that determine the reaction rate). Thus the rate of a zero-order reaction is independent of the reactant

concentration, such as the synthesis of A in Equation 2.2. A first order reaction is then one which depends on the concentration of only one species, such as the degradation of A in Equation 2.2. Second order reactions are those that involve two reactants whose concentration determines the reaction rate. For example, if a protein B is activated by protein A, its activation rate depends on both proteins, and it is therefore proportional to the product of their concentrations (see for example Equation 2.13). It is also possible that the two reactants are molecules of the same species, in which case the rate is proportional to the square of the reactant concentration.

2.3.2. Michaelis-Menten kinetics

Most reactions in biochemical networks are catalysed by enzymes, which are therefore important in determining the reaction rate. If the simple Law of Mass Action were assumed for these reactions, their rate would be proportional to the concentrations of both enzyme and substrate. However, if the substrate concentration is much higher than the enzyme concentration, the latter is saturated, and the reaction rate depends only on the amount of enzyme, because further increases in substrate concentration do not lead to an increase in the reaction rate. This feature of enzyme-catalysed reactions is normally taken into account by describing their rate using Michaelis-Menten kinetics, usually expressed as the rate of production of the product of the enzymatic reaction:

$$\frac{dP}{dt} = \frac{V_{max}S}{K_m + S} \qquad 2.6$$

where P and S are the concentrations of the product and the substrate of the reaction respectively. V_{max} is the maximum rate of the reaction, which would be realized when the enzyme is completely saturated, and is equal to the product of the reaction rate

constant for conversion of substrate into product and the total enzyme concentration. K_m, usually referred to as the Michaelis constant, is the value of the substrate concentration at which the reaction proceeds at half of the maximum rate.

Figure 2.1 shows the shape of this function, compared to the equivalent reaction rate when the enzyme is not saturated. The rate of the reaction assuming Michaelis-Menten kinetics follows the shape of a rectangular hyperbola, since at high substrate concentration the rate increases very little as the enzyme becomes saturated. Therefore, introduction of Michaelis-Menten kinetics can have important consequences in a model, as it introduces significant nonlinear effects, such as zero-order ultrasensitivity, explained below.

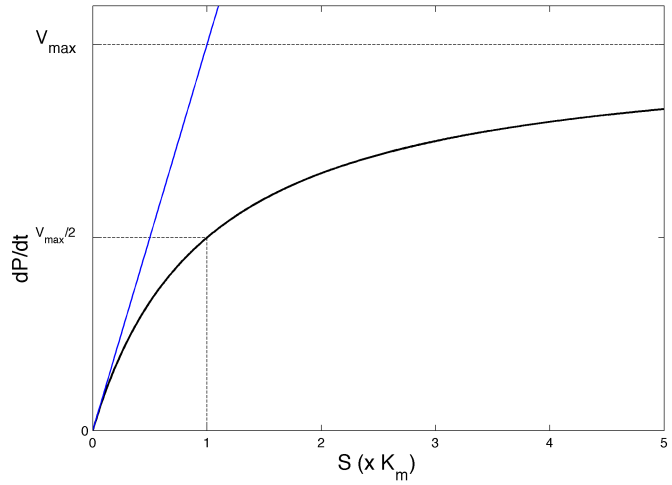

Figure 2.1. *The rate of an enzyme-catalysed reaction as a function of substrate concentration, described by Michaelis-Menten kinetics* (black line). This is a hyperbolic curve, which tends to a maximum rate, V_{max}, as the substrate concentration tends to infinity. Substrate concentration is given as multiples of K_m, the substrate concentration at which the reaction proceeds at half of the maximum rate. The thin blue line shows the rate for the equivalent reaction described by the Law of Mass Action, where the rate is directly proportional to the substrate concentration: $dP/dt = V_{max}S/K_m$. This is only a good approximation if the substrate concentration is significantly less than the K_m.

Equation 2.6 is usually derived by assuming rapid equilibrium in the formation of an enzyme-substrate complex, which is assumed to maintain a steady state. This assumption implies that the reaction rate constants for complex formation are much larger than the actual rate constant conversion of the enzyme-substrate complex into product and free enzyme, or that the amount of substrate is much larger than the total amount of enzyme. These assumptions may not always be true, particularly in signalling networks, where both enzymes and substrates are proteins that may have similar concentration and may even act on one another (Ciliberto et al., 2007; Sabouri-Ghomi et al., 2008). If the substrate concentration is lower than the K_m of the enzyme for the substrate, the reaction rate may be described with mass action kinetics, so the reaction rate increases linearly with substrate concentration, as if the enzyme was never saturated (Conrad and Tyson, 2006).

2.3.3. Goldbeter-Koshland kinetics and zero-order ultrasensitivity

Zero-order ultrasensitivity is a particularly interesting and relevant property that arises as a consequence of the assumption of Michaelis-Menten kinetics in a reaction cycle. This is a pair of opposing reactions catalysed by two different enzymes; such as phosphorylation and dephosphorylation of a protein, S of constant concentration (S_T) catalysed by a kinase, K, and a phosphatase, PP:

$$S \underset{PP}{\overset{K}{\rightleftharpoons}} S_P$$

The ODE describing such a cycle using Michaelis-Menten kinetics:

$$\frac{dS_P}{dt} = \frac{V_K(S_T - S_P)}{J_K + (S_T - S_P)} - \frac{V_{PP}S_P}{J_{PP} + S_P} \quad 2.7$$

where V_K is the maximum rate of the phosphorylation reaction and V_{PP} is the maximum rate of the dephosphorylation reaction. J_K is the Michaelis constant of the kinase for the dephosphorylated substrate and J_{PP} is the equivalent constant of the phosphatase for the phosphorylated substrate. The steady state behaviour of this equation can be analysed by assuming $dS_P/dt = 0$, which leads to a quadratic equation for the concentration of the phosphorylated substrate:

$$S_P = GK(V_{\mathrm{K}}, V_{\mathrm{PP}}, J_{\mathrm{K}}, J_{\mathrm{PP}}) \quad 2.8$$

where *GK* is the Goldbeter-Koshland function defined by:

$$GK(v_1, v_2, J_1, J_2) = \frac{2v_1J_2}{A + \sqrt{A^2 - 4(v_2 - v_1)v_1J_2}} \quad 2.9$$

where

$$A = v_2 - v_1 + J_1v_2 + J_2v_1 \quad 2.10$$

The behaviour of this system was analysed by Goldbeter and Koshland (1981), who showed an interesting property. When at least one of the enzymes is saturated ($S_T \gg J_i$, where J_i is any of the Michaelis constants of the system), this system can behave as an ultrasensitive switch. That is, the steady state concentration of two forms of the substrate will switch drastically with small changes in the amount or activity of the two enzymes (Figure 2.2), resulting in a sigmoidal, ultrasensitive response as described in Chapter 1.

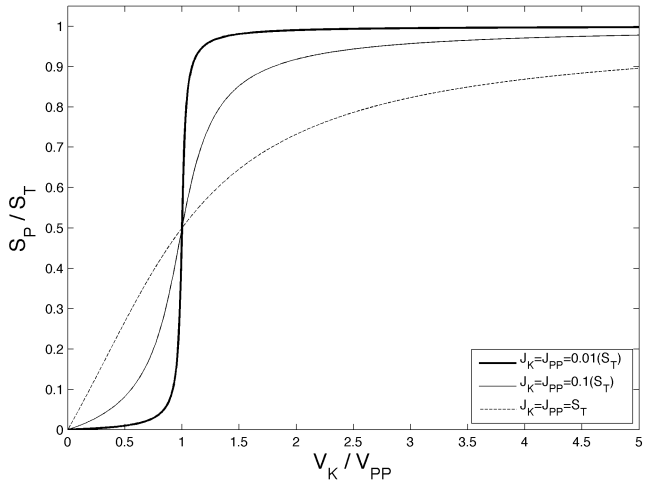

Figure 2.2. *The Goldbeter-Koshland function describing the steady state concentration of a phosphorylated substrate with respect to the ratio of kinase to phosphatase*. The response becomes highly ultrasensitive when the *Js* are much smaller than the total substrate concentration, S_T, that is, when the enzymes are saturated, and the reaction is essentially zero-order with respect to the substrate concentration. However, if the *Js* and S_T are similar, ultrasensitivity is lost.

Goldbeter and Koshland (Goldbeter and Koshland, 1981) referred to this response as zero-order ultrasensitivity, because when the enzymes are saturated, the reactions they catalyse are effectively zero-order with respect to substrate concentrations. This type of kinetics has been used extensively in mathematical models of biological systems (Tyson et al., 2003), and has also been experimentally shown experimentally in a few cases (LaPorte and Koshland; Cimino and Hervagault, 1987). However, because this requires assumption of Michaelis-Menten kinetics, its validity under some circumstances is uncertain, as mentioned previously.

2.3.4. The Hill function

The Hill function is probably the most used function to describe ultrasensitive responses in biological models, and was originally used to model cooperativity in

multi-subunit proteins. The Hill function has the following form, and can describe reaction rates when multiplied by appropriate rate constants:

$$f(x) = \frac{x^n}{J^n + x^n} \qquad 2.11$$

where x is, for example, the substrate concentration of an enzyme-catalysed reaction (or species affecting the reaction rate), J is the substrate concentration at which the reaction rate is half of the maximum rate, and n is the Hill coefficient, which describes the 'sharpness' of the ultrasensitive response. When $n = 1$, the top equation is equivalent to the Michaelis-Menten equation, and the higher the value of n, the steeper or sharper the response (Figure 2.3)

This equation is widely used to phenomenologically describe switch-like changes in mathematical models when the kinetic mechanisms that lead to such switch-like responses are not entirely clear. When used to describe the rate of a reaction, it implies that the rate changes abruptly when x, in Equation 2.11 is close to J (Figure 2.3) In biological responses, the Hill coefficient is also often used to measure the sharpness of ultrasensitive responses, by fitting data to the Hill equation. However, this quantification has been criticized because not all ultrasensitive functions actually fit the Hill function well enough to derive parameter values (Voet et al. 2004; Gunawardena 2005).

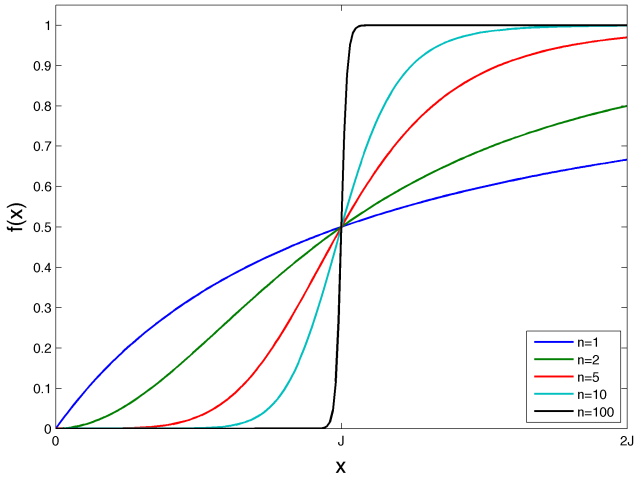

Figure 2.3. *The Hill function with different values of the Hill coefficient, n.* The larger the value of n, the more ultrasensitive the response. If $n = 1$, the response is hyperbolic, the same as with Michaelis-Menten kinetics.

2.4. Qualitative analysis of systems of ODEs

As mentioned previously, it is not always possible to solve an ODE system analytically, particularly when it is nonlinear, that is, when there are terms in the ODEs that depend on more than one variable, or are nonlinear functions of one variable. However, it is still possible to analyse these systems, and one of the most useful ways is to use qualitative methods. Here, I introduce rate plots and phase plane analysis, two tools that will be used in later chapters.

2.4.1. Rate plots

A very simple way to explore stability in systems with one variable is a rate plot, which depicts the absolute value of the derivative of the dependent variable, or terms from the ODE separately, with respect to the variable (Strogatz, 1994; Ferrell and Xiong, 2001; Tyson et al., 2003). Figure 2.4 shows an example of a rate plot for

Equation 2.2 (Section 2.2) where the absolute value of the rates of production and degradation of protein A are plotted independently. In this case, the rate of production of A is a horizontal line, k_s, because the rate of production is independent of the value of A. The rate of degradation is a straight line with slope equal to k_d, since the degradation rate increases as A increases. Where the two lines cross, the rate of production and degradation are the same, therefore $dA/dt = 0$. Thus, the value of A at which this happens is the steady state of the system, $A^* = k_s/k_d$. This plot also shows the behaviour of the system for values of A close to A^*.

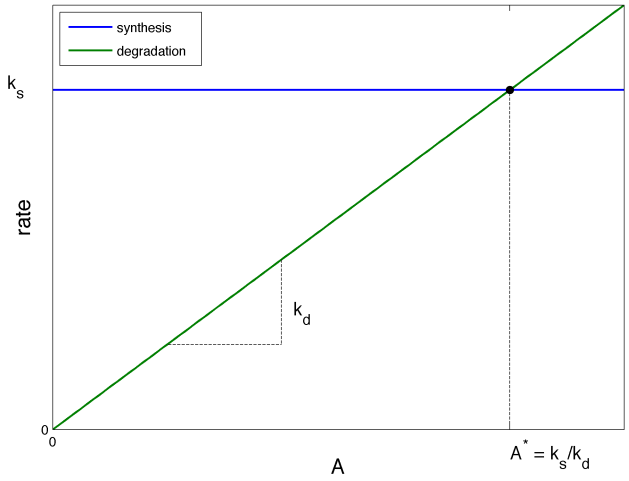

Figure 2.4. *Rate plot for the ODE system described by Equation 2.2*. The rates of synthesis and degradation are plotted with respect to the concentration of A. The rate of synthesis is a horizontal line at k_s, and the degradation rate is a straight line with slope k_d. Where the lines cross, the system is at a stable steady state $A^* = k_s/k_d$, as explained in the text.

If $A < A^*$, the rate of production is greater than the rate of degradation and $dA/dt > 0$, and therefore A increases, approaching the steady state value. On the other hand, if $A > A^*$ then $dA/dt < 0$, and A decreases, again approaching the steady state value. Therefore, A^* is a *stable* steady state, since for values of A around it, A will approach the steady state. In fact, for this example, the system will approach A^* from

any initial value of A, and the steady state is said to be globally stable. However, this is not always the case, since sometimes stability can only be guaranteed in a limited region and the steady state is thus locally stable (Strogatz, 1994).

This type of analysis can also be performed in systems with more than one variable if it is possible to assume that all variables but one are at steady state by making equilibrium approximations. This is done by assuming that the other variables in the system change rapidly relative to the variable of interest. For example, the previous model can be modified by assuming that the rate of synthesis of A is activated by another protein, B. I assume that the total amount of protein B is constant (B_T), and that B is activated by A and inactivated at a constant rate. I denote the concentration of the active form B, while the concentration of the inactive form is $B_{inactive} = B_T - B$. With these assumptions, it is possible to write a set of ODEs to describe this system:

$$\frac{dA}{dt} = k_s' + k_s B - k_d A \qquad 2.12$$

$$\frac{dB}{dt} = k_a A(B_T - B) - k_i B \qquad 2.13$$

where protein A is synthesized with a background rate k_s' and B-dependent rate k_s, and degraded with rate constant k_d. Protein B is activated by A with rate constant k_a and inactivated with rate constant k_i. Assuming that the activation and inactivation of B is fast relative to the production and degradation of A, B can be assumed to be at equilibrium, that is, $dB/dt = 0$ and B can then be expressed using an algebraic expression:

$$B = B_T \frac{k_a A}{k_a A + k_i} \qquad 2.14$$

which can be substituted into the ODE for protein A

$$\frac{dA}{dt} = k_s' + k_s B_T \frac{k_a A}{k_a A + k_i} - k_d A \qquad 2.15$$

resulting in a system described by a single ODE, which can be analysed using a rate plot (Figure 2.5). For this example, there is also a single, globally stable steady state for physically meaningful values of A, although the synthesis rate is now hyperbolic because it depends on A itself.

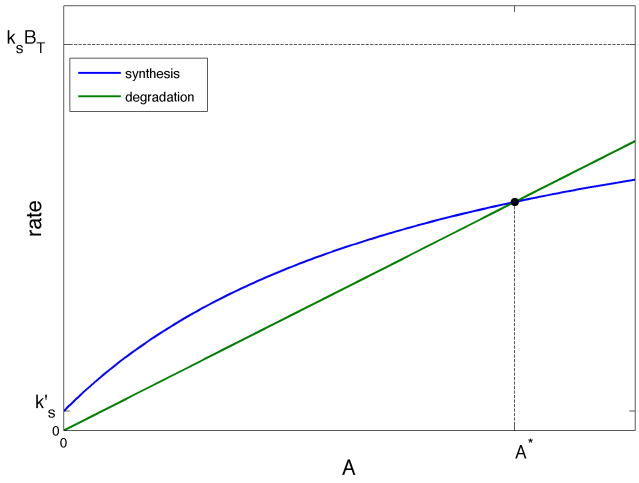

Figure 2.5. *Rate plot for the ODE system described by Equation 2.15*. The rates of synthesis and degradation are plotted with respect to the concentration of A. Where the lines cross, the system is at a stable steady state A^*. See text for details.

2.4.2. Phase planes

The state of a system of ODEs is defined by the values of each of the variables, which allows prediction of all future states. Thus, at any time, the state can be thought of as

a point in an *n*-dimensional space, the state space, where *n* is the number of variables, or dimensionality of the system. At each point in the state space, the ODEs define the rate of change of each variable, and therefore, an *n*-dimensional vector indicates the direction and speed of movement of the system. Therefore, the system of ODEs defines a vector field, which qualitatively shows all possible trajectories of the system. Starting from any point on the state space, it is possible to calculate, or at least estimate, where the system will be after a particular time increment. In this way it is possible to define a trajectory, or solution to the ODE system (Strogatz, 1994; Tyson et al., 2001; Conrad and Tyson, 2006; Jordan and Smith, 2008).

In a two-dimensional system, the state space is a plane where the two variables of the system correspond to each axis. This is referred to as the phase plane, and its analysis gives important information about the stability of steady states and solutions, even for systems that cannot be solved analytically (Strogatz, 1994; Conrad and Tyson, 2006; Kreyszig, 2010). The nullclines, curves along which the time derivative of one of the variables is zero, are important features of the phase plane (Conrad and Tyson, 2006). They can be thought of as a plot of the steady state of one variable with respect to a fixed value of the other variable, both on the same plane. Nullclines are calculated by setting both ODEs to zero and then solving for one of the variables. For the previous example, the A-nullcline is obtained by setting $dA/dt = 0$:

$$B_A^* = \frac{k_d A - k_s'}{k_s} \qquad 2.16$$

and the B-nullcline by setting $dB/dt = 0$:

$$B_B^* = B_T \frac{k_a A}{k_a A + k_i} \qquad 2.17$$

These expressions can now be used to sketch the nullclines in the phase plane of the system (Figure 2.6). Along the nullclines, the vectors can only point up or down for the A nullcline and only left or right for the B nullcline. Similar to the rate plots, where the two lines intersect, the rate of change of both variables is zero, and the system has a steady state, but in this case it is because both variables are at steady state. This picture is not an approximation, since there is no equilibrium assumption. However, as with the rate plots, it is possible to analyse systems of more than two variables using phase planes by using appropriate equilibrium assumptions to reduce the system to two variables. This pseudo phase plane is then an approximation of the behaviour of the system.

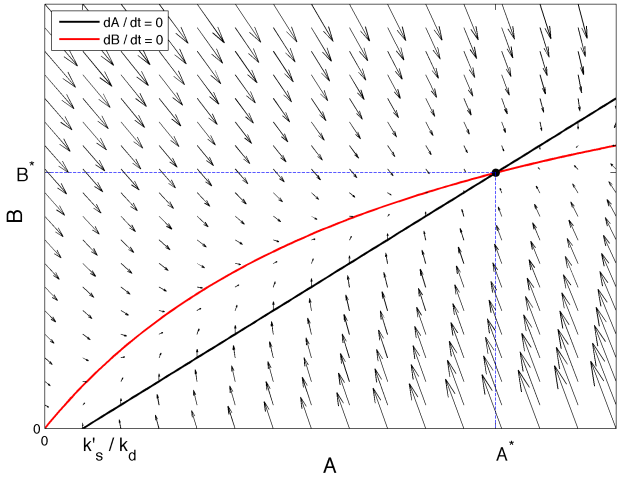

Figure 2.6. *Phase plane for the system described by Equations 2.16 and 2.17*. The nullclines, vector field and steady state are shown. The vector field indicates that the steady state is stable in agreement with the rate plot from Figure 2.5.

The stability of the steady states can be analysed in the phase plane by looking at the vector field, in particular at the vectors close to the nullclines or around the steady state. In this case, the vectors point towards the steady state, which is therefore stable, in agreement with the results for the rate plot in Figure 2.5 for the same system.

The plots presented here are the main tools used in this thesis for analysing the stability of systems. However, a more generalized type of analysis, which can be used for systems with more than two variables and automated on a computer, is linear stability analysis. A full explanation is beyond the scope of this thesis, but it essentially involves predicting how a perturbation to a steady state evolves in time. This is done by deriving an ODE for the perturbation, which is achieved by 'linearizing' the system in some region close to the steady state. This involves approximating the value of the derivative in time of each component of the perturbation by the first term of a Taylor expansion of the differential equation for each variable. Because the perturbation is small, higher order terms can normally be ignored. Linearization is useful because linear systems can be solved analytically, and thus it is possible to transfer the results from this type of system to a local region around the steady state in a nonlinear system. In this way it is possible to construct an orientation matrix by estimating the partial derivatives of each variable with respect to all other variables. This Jacobian matrix describes the time evolution of the perturbation and determines whether the steady state is stable or unstable (Strogatz, 1994). In the next section, I describe the principles of bifurcation analysis, which further expands steady state analysis for systems of ODEs.

2.5. Bifurcation analysis

Bifurcation analysis essentially involves the study of the steady states of a system of ODEs as parameter values are varied. The term bifurcation refers to a qualitative change on the steady state(s) of the system at a particular parameter value. Bifurcation points correspond to parameter values where something 'unusual' happens to the qualitative dynamics of the system, such as appearance or disappearance of steady states, or changes in the stability of steady states (Strogatz, 1994; Tyson et al., 2001).

2.5.1. One-parameter bifurcation diagrams

In Figure 2.2, I showed how the steady state level of the phosphorylated form of a substrate varied with increasing levels of the kinase. If we consider the kinase level as a parameter or signal and the steady state concentration of the phosphorylated substrate as a response, we could refer to this plot as a signal-response curve. This is essentially the principle of a one-parameter bifurcation diagram (Novák and Tyson, 2008), in which we plot the steady state value of a variable of interest with respect to the value of one of the parameters in the system, in this case the kinase level. However, in a one-parameter bifurcation diagram we usually expect to see a bifurcation. This can be illustrated with a simple example: a protein, A, that activates its own production in a nonlinear fashion. A single ODE to describe the concentration of A can be written as:

$$\frac{dA}{dt} = \mathrm{S} + \frac{k_s A^n}{J^n + A^n} - k_d A \qquad 2.18$$

where S is a signal that promotes synthesis of A, k_s is the reaction rate constant for A-dependent synthesis, n is the Hill coefficient, J the concentration of A that gives half of the maximum A-dependent synthesis rate, and k_d the rate constant for A degradation. A rate plot for this system is shown in Figure 2.7A. Due to the Hill function, the rate of synthesis is ultrasensitive with respect to A. The degradation rate is a straight line, and depending on parameter values, can cross the synthesis rate at one or at three points. For values of S where there are three intersections, there are two stable steady states and one unstable steady state, and the system is said to be bistable (Tyson et al., 2003; Conrad and Tyson, 2006; Xiong and Ferrell, 2003).

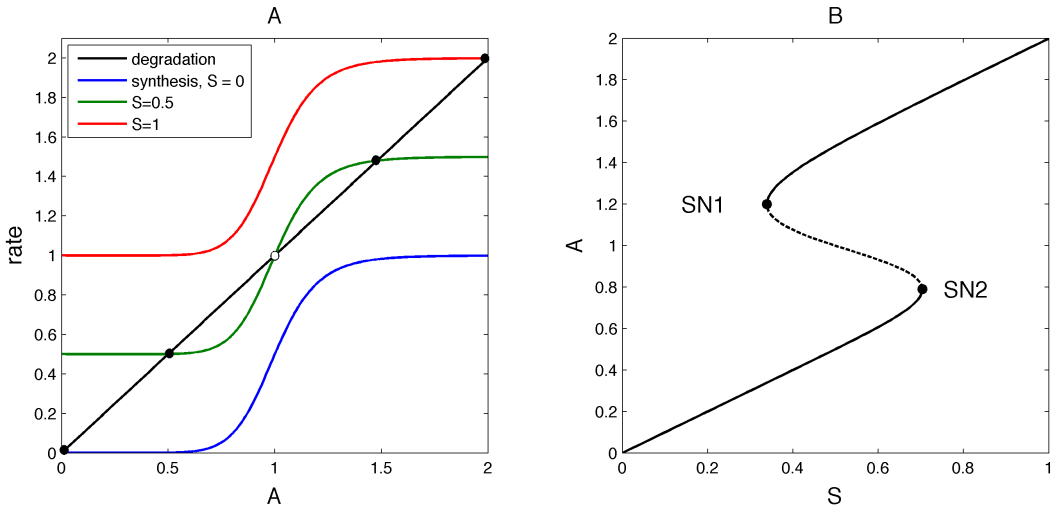

Figure 2.7. *Rate plot (**A**) and one-parameter bifurcation diagram (**B**) for the system described by Equation 2.18*. In A, the rate of synthesis varies with the level of the signal S, a parameter. The degradation rate is constant. In B, the steady states of the system, described the concentration of A, are plotted as a function of the signal. Parameters: $k_s = 1$; $k_d = 1$; $J = 1$; $n = 10$.

A one-parameter bifurcation diagram for this system shows the values for the steady states of A at several values of S. As a convention, stable steady states are plotted with solid lines or filled circles and unstable steady states with dashed lines or empty

circles. In this case it is also possible to obtain a function for this plot by calculating the value of S given a range of values of the steady state for A. The result of this is shown in Figure 2.7B. For small values of the signal, there is a single, stable, steady state where A is low and increases linearly. As the signal increases two more steady states, one stable and one unstable, appear at a higher and intermediate levels of A, respectively. As the parameter increases further, the lower steady state collides with the unstable steady state and they both disappear, leaving only the stable steady state with higher concentration of A. The points where the stable and unstable steady states appear or disappear are bifurcation points, specifically saddle node bifurcations (Strogatz, 1994).

In the following chapters I will only deal with saddle node bifurcations, but other types of bifurcation exist, like transcritical bifurcations, were two steady states exchange stabilities; pitchfork bifurcations, in which a steady state exchanges stability and two new steady states of opposite stability appear; and Hopf bifurcations, where the system starts to oscillate (Strogatz, 1994; Tyson et al., 2003).

2.5.2. Two-parameter bifurcation diagrams

One-parameter bifurcation diagrams show how the steady states of the system change with respect to one parameter and where bifurcation points occur. Two-parameter bifurcation diagrams go one step further, by showing how the bifurcation points change with respect to a second parameter of the system. These diagrams can be useful as 'constraint' diagrams, which show, for example, how the bistable regime of a system varies with other parameters (Novák and Tyson, 2008). Figure 2.8A shows a two-parameter bifurcation diagram for the system described by Equation 2.18. It shows the signal at the saddle-node bifurcations with respect to the Hill

coefficient of the A-dependent synthesis. The bistable region, shaded grey, increases as n becomes larger. Crucially, there is a critical value of n at which the system becomes bistable, a Cusp bifurcation (Strogatz, 1994).

These diagrams can also be thought of as a projection of a surface in a three-dimensional space where the axes correspond to each of the parameter of interest and the steady state value of the variable of interest, as shown in Figure 2.8B. The shaded region in the two-parameter bifurcation diagram corresponds to the bistable regimes of the curves (one-parameter bifurcation diagrams) in the three-dimensional plot.

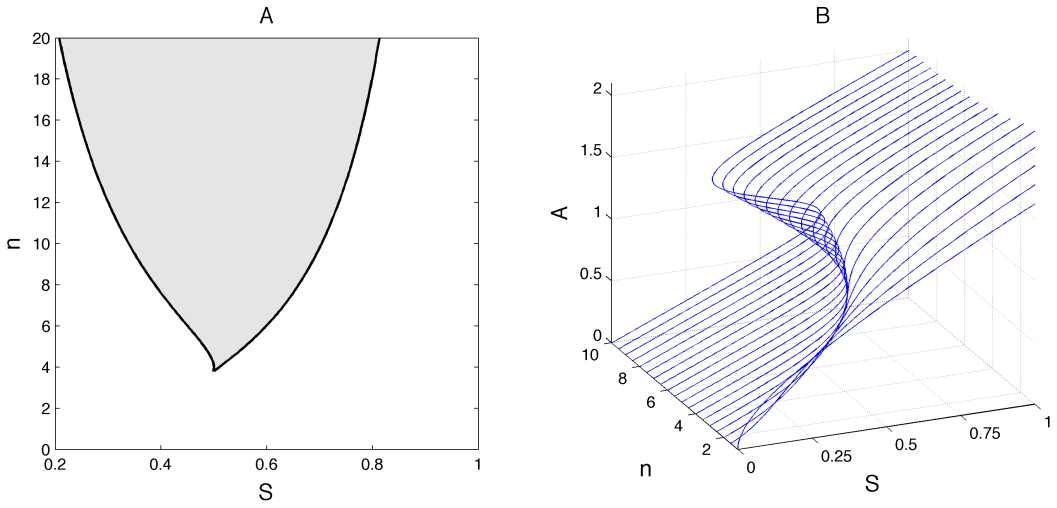

Figure 2.8. A. *A two-parameter bifurcation diagram for Equation 2.18*. The two parameters are the signal *S* and the Hill coefficient for A-dependent synthesis, *n*. The bistable region is shaded. **B.** *A three-dimensional plot showing the surface described by one-parameter bifurcation diagrams at different values of n*. A projection of this surface, showing the boundaries of the bistable region, corresponds to the two-parameter bifurcation diagram in A.

2.6. Computational approaches for ODE analysis

Although some small systems of ODEs can be solved analytically, the majority of analyses of ODE systems rely on computers. All analyses and plots presented in this and following chapters were performed using MATLAB (Mathworks, Natick, MA, USA), a general purpose tool for mathematical computations and XPPAUT (http://www.math.pitt.edu/~bard/xpp/xpp.html), a tool for simulation and analysis of dynamical systems (Ermentrout, 2002). In the simplest case, computers are used to calculate and plot analytically derived functions, which is extensively done in this thesis with MATLAB code.

Systems of ODEs can also be integrated numerically, using more or less complicated solvers. In the simplest sense, these solvers, given an initial condition for each variable, use rate of change given by the ODE of each variable to estimate how much the variable changes in a defined time step. This is the essence of the simplest of these numerical ODE solvers, Euler's method, but more accurate results can be obtained by using more sophisticated methods. Some of these methods also include variable time steps, so the size of the time increment decreases if the rate of change becomes larger. For systems that have differing time scales, it is also useful to use a stiff ODE solver to guarantee the stability and convergence of the solution (Strogatz, 1994; Kreyszig, 2010). The MATLAB function ode15s and the Stiff ODE solver from XPPAUT were used in the time course simulations presented in this thesis.

Stability and bifurcation analysis were mostly performed by deriving the appropriate functions and plotting them using MATLAB. In cases where the relevant functions cannot be derived, and as a check, XPPAUT was also used. XPPAUT provides an interface for AUTO, a tool for bifurcation analysis. AUTO uses automated linearization

of an ODE system to find the stability of steady states and detect bifurcations. It can be used for producing one-parameter and two-parameter bifurcation diagrams (Ermentrout, 2002).

2.7. Constructing mathematical models

The previous sections describe the tools used to construct and analyse the mathematical models of biochemical networks presented in later chapters. This section aims to show how the mathematical models are actually constructed. The starting point is normally a wiring diagram of the biochemical network of interest. These are very similar to the cartoons molecular biologists use to summarize their knowledge of a particular network and depict the regulation of its different components (Tyson et al., 2001; Conrad and Tyson, 2006). In themselves these cartoons constitute a 'model' of the system, as they are abstract representations of the real biological system, which can give initial glimpses of how the network behaves. Mathematical models provide a more precise framework to understand these networks at a deeper level and predict their behaviour and properties.

Since these wiring diagrams are used to construct precise mathematical models, certain conventions are usually adopted for displaying them. I will normally use the following:

- All the different types of molecule in the network to be modelled are present in the wiring diagram. This includes different forms of the same molecule, such as active and inactive forms of a protein.
- All biochemical reactions converting one molecule or form into another are present in the network and displayed with solid lines.

- All regulatory interactions, that is, when a molecule affects the rate of a particular reaction, are shown in the diagram. This is displayed either by placing the relevant regulatory molecule above the arrow indicating the regulated reaction or by a dashed line connecting the regulatory molecule to the regulated reaction.

Once the wiring diagram is completed, it is used to write a system of ODEs for the biochemical network (Tyson et al., 2001). The first step is to define any conservation laws present in the system, such as stating that the active and inactive form of a particular protein sums up to a total. This is important because it normally reduces the number of ODEs required to describe the system, because one of the forms can be defined by an algebraic expression.

It is important to note that by using ODEs to model a biochemical network, some implicit assumptions are made. In particular it is assumed that the system is 'well mixed' and that molecular numbers are large enough so stochastic effects can be neglected and ODEs will accurately describe the behaviour of the system. This is not necessarily true for many biochemical process occurring inside cells, although it is a reasonable assumption for cell extracts, such as those of *Xenopus* eggs (Conrad and Tyson, 2006), which is the experimental system on which most of the models presented here are based.

The next step is to select the type of kinetics to use for each reaction, and write their expressions and associated parameters. This requires careful consideration and depends on different factors, including particular known properties of the system, consideration of the assumptions for the different types of kinetics, and even the aim of the model, as I will demonstrate in the following chapters.

At this point the initial analysis of the system of equations can start. It can be useful to use qualitative methods to analyse the system of ODEs, such as rate plots and phase planes to explore the system and the parameter space. From here, a parameter set that represents the known and desired behaviour can then be chosen to represent the 'wild-type' system and further exploration can continue. In the following chapters, unless otherwise stated all parameters are non-dimensional. Therefore, differences between parameters can be thought of as relative, and the model results as qualitative or semi-quantitative.

As an additional tool for understanding the model behaviour it is often useful to look at simplified versions of the wiring diagram, which I refer to as interaction or influence diagrams. This is because wiring diagrams can have a lot of detail and be too complex to spot interesting regulatory patterns. These interaction diagrams usually contain all the molecules of the network, but not all the forms for each molecule, and the relationships between them indicated by lines. As a convention, an arrow from X to Y indicates that X has a positive effect on Y ($X \rightarrow Y$), while a line starting at X and ending in a bar at Y indicates that X has a negative effect on Y ($X \dashv Y$). An example of such interaction diagram was presented previously in Figure 1.2A. Interaction diagrams are also extensively used by biologists, and are particularly useful for detecting and visualising 'network motifs' such as feedback and feedforward loops. These motifs are described in more detail in the following section.

2.8. Feedback and feedforward loops

Many processes in cells are carried out by large networks of genes and proteins that interact in complex and nonlinear ways (Bray, 1995). Efforts have been made in trying to understand patterns or detect modules in these networks, which might carry out specific functions or have particularly interesting properties. This approach has focused on the understanding of network motifs, which are simple regulatory patterns among a small number of cellular components. Their study has been particularly insightful for understanding gene regulatory networks, but it can also be applied to signalling pathways and other biological networks (Alon 2007a, 2007b; Tyson et al. 2003, 2010). The main idea is to understand the information-processing capabilities of these motifs, which were originally identified as regulatory patterns that occur more often in real networks than in randomly generated ones (Shen-Orr et al. 2002; Alon 2007a). These motifs have been studied from different theoretical and mathematical perspectives, in order to predict if they can in fact carry out particular tasks. In some cases these predictions have been demonstrated experimentally, which encourages the notion that even when these motifs are embedded in large networks they can have defined roles (Mangan et al., 2003, 2006; Alon, 2007a; b; Tyson and Novák, 2010) . In this section, I describe some features of two important motifs that will be relevant throughout this thesis, feedback and feedforward loops.

2.8.1. Feedback loops

Feedback seems to be a particularly prevalent feature in biological systems. Feedback loops (FBLs) arise when the perceived output of a system is also a component of its input. In many cases, this can make it difficult to define which components of the systems are ‘upstream’ or ‘downstream’, making systems with feedback potentially

difficult to understand and showing very complex behaviour. Feedback can be positive or negative, depending on whether the output of the system leads to a further increase, or a decrease in output, respectively (Conrad and Tyson, 2006; Tyson et al., 2003).

The most familiar type of feedback loop in biochemical systems is negative feedback, where the output of the system eventually leads to a decrease in the output, and thus can 'counteract' the effect of the signal. This type of feedback is usually associated with homeostasis, the tendency to keep a system at a constant steady state despite perturbations, and therefore minimize fluctuations in the response of the system (Tyson et al., 2003). A classical example is when high concentrations of the product of a metabolic pathway inhibit initial reactions in the pathway, helping the system to maintain stable levels of the metabolites involved in the pathway. However, negative feedback is also essential for oscillations. Oscillations can be the consequence of 'delayed' negative feedback, where a large increase in the output can occur, before it has a dampening effect on itself. This delay can be a result of the dynamical properties of the system, such as the presence of multiple components (Goldbeter, 2002; Novák and Tyson, 2008; Tyson and Novák, 2010; Ferrell et al., 2011). As described in Chapter 1, the oscillatory nature of the cell cycle is the result of negative feedback, since the signal that promotes mitosis, Cdk1-CycB activates the APC/C after a delay, resulting in CycB degradation and inactivation of Cdk1 (Tyson and Novák, 2008; Ferrell et al., 2011). The circadian cycle is another example of oscillations due to delayed negative feedback (Goldbeter, 2002; Novák and Tyson, 2008). Furthermore, artificial biological networks with delayed negative feedback have been shown to display oscillatory behaviour (Elowitz and Leibler, 2000).

Positive feedback results when the output of a component of the network leads to an amplification or enhancement of the same output. An example is a self-activating enzyme, whose product enhances its activity. Positive feedback is perhaps less familiar than negative feedback, but probably no less common or important. It is usually associated with switch-like, explosive and all-or-none responses and phenomena (Ferrell, 2002; Tyson et al., 2003; Alon, 2007b; Mitrophanov and Groisman, 2008; Pomerening, 2009). A classic example is the action potential in neurons, where a small membrane depolarization causes opening of ion channels, which produces further depolarization and leads to transmission of nerve signals. It is possible to distinguish two different types of positive FBLs, those that involve mutual activation and those with antagonistic relationships between components of the loop. Under appropriate conditions, both can create a discontinuous switch by producing bistability. For example, for two-component loops, either both components are OFF or both ON in the double positive FBL (Figure 2.9E), whereas one component is ON and the other OFF in a double negative FBL. In each case, the system can switch between these two possible states in response to a transient signal (Tyson et al., 2003; Alon, 2007b). These bistable, discontinuous switches seem to be common in biology, and are proposed to be important for cellular differentiation and decision-making (Ferrell, 2002; Tyson et al., 2003; Alon, 2007b).

Figure 2.9 displays several examples of negative (A-C) and positive (D-G) FBLs, and shows that a single or many components can form FBLs. Furthermore, FBLs can be intertwined, creating motifs with interesting behaviours. For example, positive and negative FBLs can be combined to produce very robust oscillators, in which the negative FBLs drive the system around a hysteresis loop created by positive FBLs

(Tyson and Novák, 2008; Tsai et al., 2008; Tyson and Novák, 2010; Ferrell et al., 2011).

An important motif throughout this thesis is the one formed by intertwined double positive and double negative FBLs, shown in Figure 2.9G. This is essentially the central component of the mitotic switch, the motif formed by MPF, Wee1 and Cdc25 as explained in Chapter 1. This motif can produce an efficient bistable switch (Ferrell, 2008) and can even create tristable systems (Tyson and Novák, 2010). The properties of this motif will be explored in later chapters.

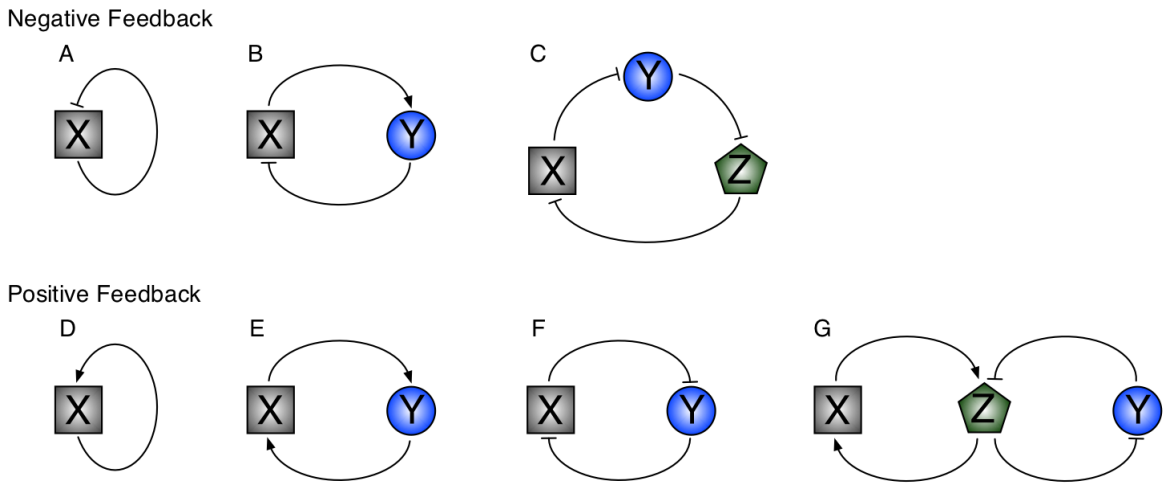

Figure 2.9. *Examples feedback loops*. **A-C**, negative FBLs with one (**A**), two (**B**) and three components (**C**). **D-G**. Positive FBLs. **D**. One-component positive FBL. **E**. Double positive FBL. **F**. Double negative FBL. **G**. Intertwined double positive and double negative FBLs.

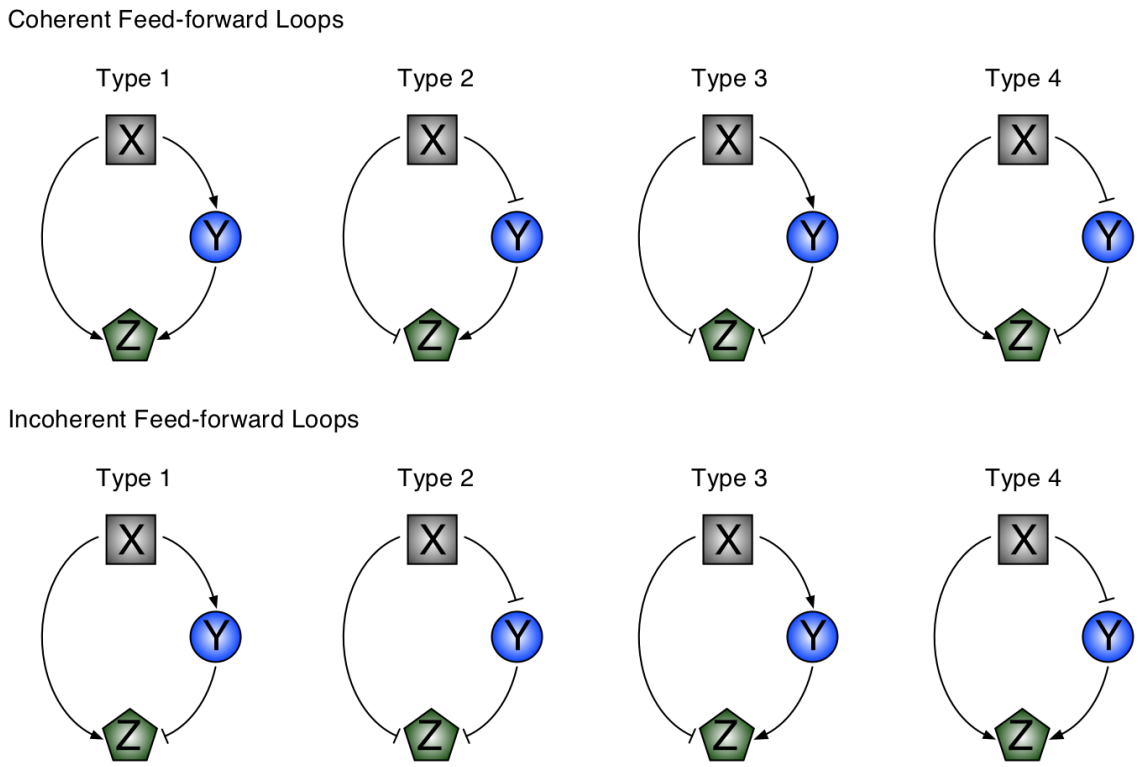

Figure 2.10. *The 8 possible three-component feedforward loops*. See text for details.

2.8.2. Feedforward loops

Feedforward loops (FFLs) are motifs of at least three components, where one component regulates another through two different pathways (Mangan and Alon, 2003; Tyson et al., 2003; Alon, 2007b; Tyson and Novák, 2010). Mangan and Alon (2003) analysed many features of three-component FFLs in the context of gene regulatory networks, where a transcription factor X regulates an output gene Z, both directly and through another transcription factor Y. Each interaction between two components can be positive or negative, resulting in eight distinct FFLs, shown in Figure 2.10. Four of these are coherent (the net effect of X on Z through both branches is of the same sign) and four are incoherent (the two branches have opposite effects on Z). Another important feature of the motif is whether the two transcription factors

function like an AND or an OR logic gate. Particular types of FFLs are prevalent in gene regulatory network, and they are predicted to have particular behaviours. For example, the coherent FFL type 1 with an AND logic gate, the most common in transcription networks can act as a sign-sensitive delay and noise suppression mechanism, and incoherent FFLs can act as mechanisms for perfect adaptation (type 1). Some properties of these FFLs have been confirmed experimentally (Mangan et al., 2003, 2006).

FFLs have also been studied in the context of cell cycle regulation, where CDKs regulate a component of the regulatory network both directly through phosphorylation and indirectly through regulation of its transcription. The evidence indicates that incoherent FFLs can act as triggering modules for required components at particular cell cycle transitions, while coherent FFLs regulate components required during particular phases of the cell cycle (Csikász-Nagy et al., 2009; Tyson and Novák, 2010).

2.9. Summary

In this chapter, I have introduced essential background required for understanding the mathematical models and their analysis presented in the next chapter. I described how to write systems of ODEs for biochemical networks and the kinetic assumptions that can be made for each reaction. I also described different ways to analyse these systems; qualitative tools, such as rate plots and phase plane analysis, and tools that normally require the use of computers, such as bifurcation analysis and

numerical integration. Finally, I introduced the concept of network motifs and described two particularly relevant for this thesis; feedback loops, where one component of the network affects the activity of an 'upstream component', and feedforward loops, where one component of the network is regulated by another through two different pathways.

In the next chapter I start to use the notions presented in this chapter and in Chapter 1 to dissect and understand models of the mitotic switch that use different kinetic assumptions in the ODE systems, and highlight the importance of positive feedback and ultrasensitive responses in the construction of a 'good' biochemical switch.

Chapter 3

Positive feedback and ultrasensitivity in the mitotic switch

3.1. Overview

The previous two chapters have introduced basic notions about cell cycle control and mathematical modelling. In this chapter I draw on this background to construct simple models that demonstrate important features of the mitotic switch. I will focus on which characteristics are necessary and important to produce bistability in this particular switch, but the conclusions are relevant for biochemical switches in general. I begin by revisiting the biochemical network controlling the mitotic entry switch, presented in Chapter 1 and then analyse increasingly complex models, arriving at the core of a previous mathematical model describing this transition (Novák and Tyson, 1993). This description emphasizes the importance of positive feedback loops and nonlinear, ultrasensitive responses for the existence of a robust, bistable mitotic switch. It will also put into focus issues that I deal with in later chapters, such as the sources of ultrasensitivity in biochemical networks. As a start in this direction, I also show that multiple feedback loops can generate ultrasensitive responses. Finally, I discuss this analysis and the importance of ultrasensitivity in bistable switches.

3.2. The biochemical network controlling the mitotic switch

As mentioned in Chapter 1, the regulation of the eukaryotic cell cycle is based on protein phosphorylation and dephosphorylation, catalysed by specific protein kinases and phosphatases (Nigg, 2001; Morgan, 2007; Ma and Poon, 2011; Bollen et al., 2009). In particular, the Cdk1-CycB complex is essentially responsible for bringing about mitosis in all eukaryotes, and is therefore also referred to as M-phase Promoting Factor or MPF (Nurse, 1990; Duesbery and Vande Woude, 1998). The Cdk1 subunit is normally present in excess, and therefore CycB is the rate-limiting component for complex formation (Morgan, 2007; Hochegger et al., 2008). The activity of MPF is itself regulated by phosphorylation (Figure 3.1): the inhibitory kinase Wee1 inactivates MPF by phosphorylation on the tyrosine-15 residue of Cdk1. This phosphorylation is removed by the phosphatase Cdc25, leading to MPF activation and thus mitotic entry (Chapter 1; Lindqvist et al. 2009). I will refer to the phosphorylated, inhibited form of MPF as preMPF.

MPF in turn regulates both Wee1 and Cdc25 by phosphorylating them at multiple sites (Kumagai and Dunphy, 1992; Izumi et al., 1992; Hoffmann et al., 1993; Izumi and Maller, 1993; Tang et al., 1993; Devault et al., 1992; Kim and Ferrell, 2007; Trunnell et al., 2011). Such phosphorylation results in activation of Cdc25 and inactivation of Wee1, and thus creates two feedback loops: (i) a positive feedback loop through Cdc25 (MPF→Cdc25→MPF) and (ii) a double-negative feedback loop through Wee1 (MPF ⊣ Wee1⊣ MPF), as shown in Figure 3.1A. MPF-dependent phosphorylation is reversed by MPF-counteracting protein phosphatases (which I will refer to as PP), which for now are assumed to have constant activity throughout the cell cycle (this

assumption will be challenged in Chapter 5). The chemical interactions in this regulatory network are shown in Figure 3.1B.

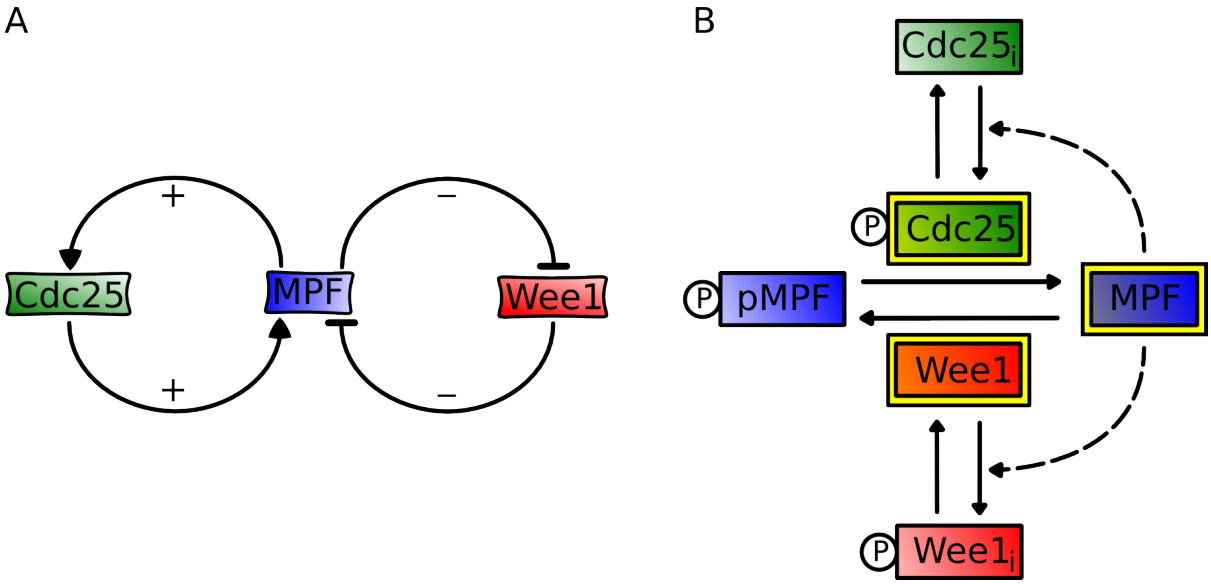

Figure 3.1. *The mitotic switch network*. **A.** Network diagram showing the Cdc25-MPF positive feedback loop and the Wee1-MPF double-negative feedback loop. **B.** Wiring diagram showing biochemical reactions. Yellow boxes indicate the active forms of each of the three species. The dashed lines indicate feedback of MPF on its regulators. (pMPF=preMPF).

As mentioned in Chapter 1, Novák and Tyson (1993) proposed that the two feedback loops in MPF regulation create a bistable switch, and therefore there are two different cyclin thresholds, one for MPF activation and a lower one for MPF inactivation, which correspond to two saddle node bifurcations in the system (Novák and Tyson, 1993). Bistability has been shown experimentally, by demonstrating the occurrence of hysteresis, and thus the existence of the two different cyclin thresholds for MPF activation and inactivation in *Xenopus* egg extracts (Pomerening et al., 2003; Sha et al., 2003). However, the question of how bistability arises in this system is not yet completely resolved, although it is known that bistability requires positive feedback

and a source of ultrasensitivity (Thomas, 1998; Ferrell and Xiong, 2001; Tyson et al., 2003; Angeli et al., 2004). This is demonstrated in the next section, using a graphical approach to analyse increasingly complex models of the mitotic switch, inspired by Ferrell et al. 2001 and Tyson et al. 2003. I will compare three different models of the mitotic switch (Figure 3.2):

1. Model without feedback: MPF is regulated by constant Cdc25 and Wee1 activities. There is no feedback of MPF on its regulators (Figure 3.2A).
2. Model with positive feedback and no ultrasensitivity: MPF is regulated by Cdc25 and Wee1, which are in turn regulated by MPF, creating positive feedback in the system (Figure 3.2B).
3. Model with positive feedback and ultrasensitivity: Besides the positive feedback loops incorporated in Model 2, I also assume a mechanism that generates ultrasensitivity in the response of Cdc25 and Wee1 to MPF (Figure 3.2C).

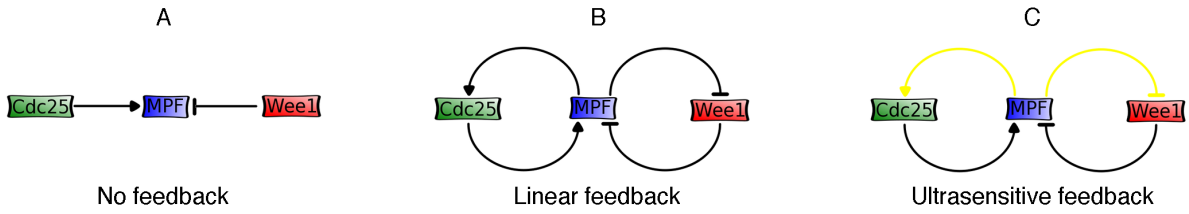

Figure 3.2. *Interaction diagrams for the simple models of the mitotic switch used to analyse the role of positive feedback and ultrasensitivity in the mitotic switch.* **A.** Model with no feedback. **B.** Model with positive feedback and no ultrasensitivity. **C.** Model with positive feedback and ultrasensitivity. The yellow lines indicate the presence of ultrasensitivity in the interaction.

3.3. Positive feedback and ultrasensitivity are important for generating bistability in the mitotic switch

To show the importance of positive feedback and ultrasensitivity for bistability in the mitotic switch, I will start by considering a simple model assuming only mass action kinetics and no feedback. I will then show the effect of progressively incorporating feedback loops and ultrasensitivity in the model, the latter in the responses of Cdc25 and Wee1 to MPF. To begin I state some general assumptions for the mathematical models that will be maintained for the whole section, and in fact for most of this thesis.

First, I assume that the level of Cdk1 is constant throughout the cell cycle, and in excess over the cyclin level. Also, I assume that cyclin binds quickly and strongly to the catalytic subunit (Solomon et al., 1992; Hochegger et al., 2008), so the concentration of free CycB is assumed to be negligible. Therefore, the following mass conservation relationship can be established:

$$Cyc_T = MPF + preMPF \qquad 3.1$$

That is, cyclin is only present as dimers with Cdk1, and the sum of the active (MPF) and inactive dimers ($pMPF$) is equal to the total cyclin level (Cyc_T). This assumption has been used in previous models of the mitotic switch and the cell cycle (i.e. Novák et al. 1993; Trunnell et al. 2011).

Using the algebraic Equation 3.1, and considering the activation and inactivation of MPF, it is possible to write the following ODE for MPF:

$$\frac{dMPF}{dt} = k_{25}(Cyc_T - MPF) - k_{wee}MPF \qquad 3.2$$

Where the activation rate is shown in green and the inactivation rate in red. k_{25} and k_{wee} are functions of *Cdc25* and *Wee1*, respectively, which determine the rates of MPF activation and inactivation. Both Wee1 and Cdc25 have active and inactive forms. However, for reasons that will become clearer later, I assume that the inactive forms actually have a small background activity. This is a reasonable assumption, since the regulation by phosphorylation is probably not absolute, and seems to be supported by recent experimental data (Lorca et al., 2010). However, for simplicity, I will not assume a background activity for preMPF. Thus, I define the rate functions for MPF activation and inactivation,

$$k_{25} = k'_{25}(Cdc25_T - Cdc25) + k''_{25}Cdc25 \qquad 3.3$$

$$k_{wee} = k'_{wee}(Wee1_T - Wee1) + k''_{wee}Wee1 \qquad 3.4$$

Where k'_{25} and k'_{wee} are the rate constants for the background activity of the inactive forms of Cdc25 and Wee1 respectively, and k''_{25} and k''_{wee} are the rate constants for the active forms. $Cdc25_T$ and $Wee1_T$ are the total levels of the two proteins, that is, the sum of the active and inactive forms, which will be assumed to be constant, as in other models for *Xenopus* egg extracts (Novák and Tyson, 1993; Zwolak et al., 2009). The following step is to write differential equations for the MPF regulators Cdc25 and Wee1, which will be modified as positive feedback and ultrasensitivity are incorporated.

3.3.1. Model without feedback

Since the total concentrations of Wee1 and Cdc25 are constant, it is only necessary to write differential equations for their active forms. First, I show how the system would behave with no feedback, that is, without the regulation of Cdc25 and Wee1 by MPF (without the dashed lines in the network diagram in Figure 3.1B). Using mass action kinetics, the differential equations for the two enzymes can be written as:

$$\frac{dCdc25}{dt} = V_{a25}(Cdc25_T - Cdc25) - V_{i25}Cdc25 \qquad 3.5$$

$$\frac{dWee1}{dt} = V_{awee}(Wee1_T - Wee1) - V_{iwee}\ Wee1 \qquad 3.6$$

Where V_{a25} and V_{i25} are the rate constants for Cdc25 activation and inactivation, and V_{awee} and V_{iwee} are the respective constants for Wee1 activation and inactivation. If $Cdc25_T$ and $Wee1_T$ are both equal to 1, *Cdc25* and *Wee1* can be thought of as the fraction of active protein. Equations 3.2-3.4 and 3.5-3.6 constitute the *model without feedback* (Figure 3.2A).

Assuming that the active and inactive forms of Cdc25 and Wee1 are in equilibrium, the steady state for the active forms of the two enzymes can be calculated,

$$Cdc25 = \frac{V_{a25}Cdc25_T}{V_{a25} + V_{i25}} \qquad 3.7$$

$$Wee1 = \frac{V_{awee}Wee1_T}{V_{awee} + V_{iwee}} \qquad 3.8$$

Since the reaction rates and total enzyme concentrations are constant, the steady state levels of active Cdc25 and Wee1 depend only on the values of the rate constants for their activation and inactivation, and therefore their activity is constant. In particular, since there is no feedback, the steady state activities of Cdc25 and Wee1 do not change with different levels of MPF (Figure 3.3A).

Now it is possible to analyse the steady state MPF activity at different Cyc_T levels. As described in Chapter 2, one way to achieve this is with a rate balance plot, shown in Figure 3.3D. Here, I depict the rates of MPF activation (bold green line) and inactivation (red line) as a function of MPF, at a particular Cyc_T level, as described by Equation 3.2. The system is at steady state at the MPF value where the two lines intersect. In this case, there is a single stable steady state, because if MPF is lower than the steady state value, the activation rate is higher than the inactivation rate, and MPF will increase. Similarly, if MPF is higher than the steady state value, inactivation wins and MPF will decrease until it reaches the steady state value.

If Cyc_T increases, the activation line will move upwards (dashed green lines in Figure 3.3D). The inactivation rate does not change because it does not depend on Cyc_T (Equation 3.2). The intersection or steady state of the system will move along the line of the inactivation rate as Cyc_T increases, and therefore *MPF* increases. This is shown in Figure 3.3G, in a signal-response curve, or one-parameter bifurcation diagram with Cyc_T as the signal or bifurcation parameter, and *MPF* as the response (see Chapter 2 for an introduction to bifurcation diagrams). In this model without feedback, *MPF* increases linearly with Cyc_T, which implies that the proportion of active *MPF* with respect to Cyc_T remains constant. The slope of this plot, which dictates the proportion of active Cyc_T is determined by the rate constants. In this case there is no abrupt

activation of MPF, but a gradual increase in MPF activity concomitant with increasing Cyc_T as CycB accumulates. Therefore, this is not a very good model for MPF activation and entry into mitosis, since there is no cyclin threshold for MPF activation.

3.3.2. Adding positive feedback

Next, I examine the effect of incorporating the feedback loops between MPF and its regulators (by including the reactions shown in dashed lines in Figure 3.1B). The simplest approximation is to assume mass action kinetics, and instead of Equations 3.5 and 3.6, the differential equations for *Cdc25* and *Wee1* can be written as,

$$\frac{dCdc25}{dt} = V_{a25}MPF(Cdc25_T - Cdc25) - V_{i25}PP(Cdc25) \qquad 3.9$$

$$\frac{dWee1}{dt} = V_{awee}PP(Wee1_T - Wee1) - V_{iwee}\,MPF\,(Wee1) \qquad 3.10$$

Here, I assume that only MPF can phosphorylate Wee1 and Cdc25 (preMPF is assumed to be completely inactive), with rate constants V_{a25} and V_{iwee}, respectively. A constant phosphatase (*PP*) dephosphorylates the two regulators with rate constants V_{i25} and V_{awee} respectively. Equations 3.2-3.4 and 3.9-3.10 constitute the *model with positive feedback and no ultrasensitivity* (Figure 3.2B). Now, the steady state activities of Wee1 and Cdc25 can be calculated by,

$$Cdc25 = \frac{V_{a25}Cdc25_T\,MPF}{V_{a25}\,MPF + V_{i25}PP} \qquad 3.11$$

$$Wee1 = \frac{V_{awee} Wee1_T}{V_{awee} PP + V_{iwee} MPF} \qquad 3.12$$

Therefore the steady state Wee1 and Cdc25 activities are now hyperbolic functions of MPF (Figure 3.3B) and the MPF activation and inactivation rates are nonlinear (Figure 3.3E). Using the parameter set shown in Table 3.1, the rate curves cross at a single point. However, the signal-response curve is also nonlinear, showing a slight threshold in MPF activation (Figure 3.3H). That is, a small initial increase in Cyc_T results in very little activation, but afterwards the increase is linear. This response is closer to the expected behaviour, but this threshold does not correspond to a saddle node bifurcation and thus the system does not show hysteresis in the activation and inactivation of MPF, which shows that this model can still be improved.

Table 3.1. *Parameter values for the mitotic switch models.*

Parameter	No feedback	Positive feedback, no ultrasensitivity	Positive feedback and ultrasensitivity
k'_{25}	0.01	0.01	0.01
k''_{25}	1	1	1
k'_{wee}	0.01	0.01	0.01
k''_{wee}	1	1	1
$Cdc25_T$	1	1	1
$Wee1_T$	1	1	1
V_{a25}	1	1	1
V_{i25}	0.1	0.1	0.1
V_{awee}	0.1	0.1	0.1
V_{iwee}	1	1	1
PP	1	1	1
J_{a25}			0.1
J_{i25}			0.1
J_{awee}			0.1
J_{iwee}			0.1

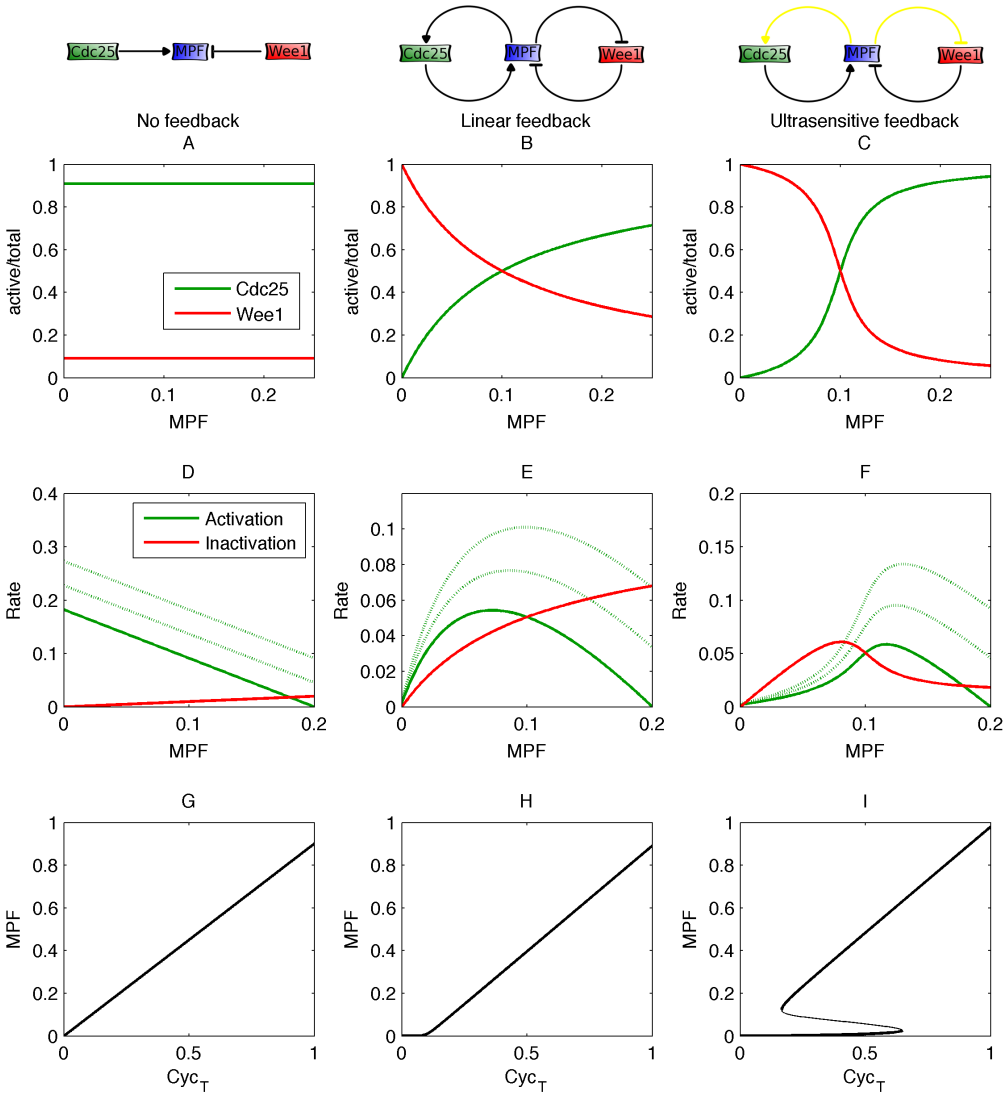

Figure 3.3. *Models of the mitotic switch showing the role of positive feedback and ultrasensitivity*. Panels in each colum correspond to the model indicated by the interaction diagram on top. **A, D, G,** model with no feedback. **B, E, H,** model with positive feedback and no ultrasensitivity (or linear feedback). **C, F, I** model with positive feedback and ultrasensitivity (or ultrasensitive feedback). **A, B, C,** Cdc25 activity (green) and Wee1 activity (red) with respect to MPF activity. **D,E,F,** rate balance plots for MPF activation and inactivation. The thick green line corresponds to the activation rate with $Cyc_T=0.2$ and the green dashed lines to increasing Cyc_T levels. **G, H, I,** Signal-response curves for MPF with respect to Cyc_T. Parameter values were chosen to make a meaningful comparison between models and are given in Table 3.1.

3.3.3. Adding positive feedback and ultrasensitivity

A more extreme switch-like response for MPF can be achieved by assuming that MPF causes a sigmoid or ultrasensitive response on its regulators. This sharper response can be modelled using different assumptions and/or kinetics, such as Hill functions or zero-order ultrasensitivity as described in Chapter 2. With the latter choice, the ODEs for *Cdc25* and *Wee1* become,

$$\frac{dCdc25}{dt} = \frac{V_{a25}MPF(Cdc25_T - Cdc25)}{J_{a25} + Cdc25_T - Cdc25} - \frac{V_{i25}PP.Cdc25}{J_{i25} + Cdc25} \qquad 3.13$$

$$\frac{dWee1}{dt} = \frac{V_{awee}PP(Wee1_T - Wee1)}{J_{awee} + Wee1_T - Wee1} - \frac{V_{iwee}\,MPF\,Wee1}{J_{iwee} + Wee1} \qquad 3.14$$

The rate constants have the same meaning as in Equations 3.9 and 3.10, while the new parameters J_{a25} and J_{iwee} are the Michaelis constants of MPF for Cdc25 and Wee1 and J_{i25} and J_{awee} are the Michaelis constants of PP for Cdc25 and Wee1, respectively. Equations 3.2-3.4 and 3.13-3.14 constitute the *model with positive feedback and ultrasensitivity* (Figure 3.2C). At steady state, *Cdc25* and *Wee1* can be described by,

$$Cdc25 = GK(V_{a25}MPF, V_{i25}PP, J_{25}, J_{25}) \qquad 3.15$$

$$Wee1 = GK(V_{awee}PP, V_{iwee}MPF, J_{wee}, J_{wee}) \qquad 3.16$$

Where *GK* is the Goldbeter-Koshland function (Goldbeter and Koshland, 1981), defined in Chapter 2. As shown in Figure 3.3C, Cdc25 is now activated and Wee1 inactivated by MPF in an ultrasensitive fashion. For a range of Cyc_T values the curves in the rate balance plot can now intersect at 3 points (Figure 3.3F). The rate plot

shows that the two extreme intersections correspond to stable steady states, and the middle one to an unstable steady state. Which steady state is reached will depend on the initial amount of MPF. Therefore, by tuning the feedback loops, the system has become bistable. This is confirmed by the signal-response curve of Cyc_T versus MPF (Figure 3.3I). As explained in Chapter 1, there are two saddle-node bifurcations where the activity of MPF changes abruptly in response to changing Cyc_T. These bifurcation points correspond to the cyclin thresholds for MPF activation and inactivation.

When Cyc_T is low, the system has a single possible steady state, interphase, because it has low MPF activity. If the system starts in this state, MPF activity will initially remain low as Cyc_T increases. However, after the activation threshold is reached, this low steady state disappears and the system is forced to move to a steady state with high MPF activity, or mitosis. Once in this state, cyclin has to decrease below the other saddle node bifurcation in order to inactivate MPF and return the system to interphase. Thus, the system shows hysteresis, and is bistable for Cyc_T levels between the two bifurcations. In this range the two stable steady states coexist along with the middle branch of unstable steady states. This model with feedback and ultrasensitivity conveys the essence of the Novák and Tyson (1993) model of the mitotic switch, which explains the cyclin threshold for mitotic entry.

The reason why ultrasensitivity in the response of Cdc25 and Wee1 to MPF can make the system bistable can be found in the rate plots. In the models with positive feedback (Figure3.3E and F), compared to the model with no feedback (Figure 3.3D), the curves describing the activation and inactivation rates fold back. This is particularly evident in the model with ultrasensitive feedback (Figure 3.3F) in which

it is relatively easy for the curves to cross at three points (Ferrell, 2008). Intuitively, bistability can also be explained by the fact that the ultrasensitive response allows Wee1 to remain active and Cdc25 to remain inactive for small levels of MPF activity. This 'filter for low input' allows the system to have a stable OFF or interphase state. Furthermore, because I assume that inactive Cdc25 has a limited amount of activity, even in interphase there will be a small amount of MPF activity. As cyclin increases, the proportion of active MPF stays the same, but the amount increases. Thus, MPF can eventually turn off Wee1 and turn on Cdc25, engaging the positive feedback loops, ensuring an abrupt MPF activation and entry into mitosis. Therefore, the residual Cdc25 activity allows the turning ON of the switch (Novák and Tyson, 1993; Ferrell and Xiong, 2001).

These simple models illustrate the roles of positive feedback and ultrasensitivity in achieving bistability in the mitotic switch. The importance of positive feedback, has been highlighted previously both experimentally and theoretically (Pomerening et al., 2005). Ultrasensitivity has also been shown in the responses of Cdc25 and Wee1 to MPF in *Xenopus* egg extracts, although the sources of ultrasensitivity in this system are yet to be fully explained (Kim and Ferrell, 2007; Trunnell et al., 2011). Moreover, why there are two feedback loops in this switch is an interesting question that has only recently started to be addressed (Ferrell, 2008).

3.4. Multiple feedback loops may be important in the mitotic switch

In the last section I have shown that positive feedback and high nonlinearity, in the form of ultrasensitive responses of Cdc25 and Wee1 to MPF, are required to achieve

bistability in the mitotic switch. The last two models are based on the known molecular interactions of the this switch, and include both known feedback loops (Dunphy, 1994; Lindqvist et al., 2009). However, both loops are not necessarily required for bistability, but both may be important, as I show in this section.

3.4.1. Bistability is possible with a single feedback loop

The model with positive feedback and ultrasensitivity presented in the last section can be used to show what can happen to bistability if only one feedback loop is present in the system. Figure 3.4A shows the rate plot for this, where the curves for the rates of MPF activation and inactivation cross at three points, exhibiting bistability. If the feedback on Wee1 is removed, so that only the Cdc25-MPF positive feedback loop remains, the inactivation rate becomes a straight line, as in the model without feedback form the previous section (Figure 3.3D and 3.4B). Due to the shape of the curve for the activation rate, three intersections are still possible. A similar outcome is obtained if only the Wee1-MPF double negative feedback loop is considered, and Cdc25 is unregulated, making the activation rate a straight line (Figures 3.4C).

Figure 3.4 therefore shows that in principle only one feedback loop is necessary for bistability, at least when there is ultrasensitivity in the response of the MPF regulator in the remaining loop. Since ultrasensitivity has indeed been shown for the responses of both Cdc25 and Wee1 to MPF (Kim and Ferrell, 2007; Trunnell et al., 2011), it is interesting to consider what, if any, are the benefits of having both feedback loops for the functioning of the mitotic switch. Ferrell (2008) showed that having both feedback loops allows bistability in this system for a much larger parameter space. This highlights the importance of the double feedback regulation of Cdc25 and Wee1

in creating a robust and efficient switch. In fact, this double regulation can in principle bypass the requirement for ultrasensitivity in order to make the system bistable, as I will show next.

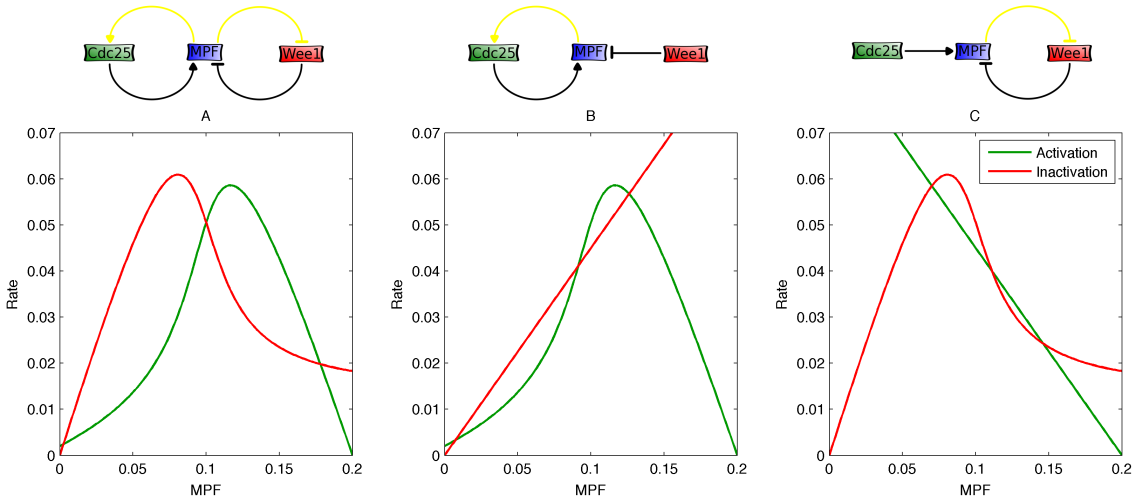

Figure 3.4. *Bistability in the mitotic switch with a single feedback loop*. Interaction diagrams for each plot are shown at the top. Yellow lines indicate ultrasensitivity in the interaction. **A.** Two feedback loops. Parameters as in Table 3.1, model with feedback and ultrasensitivity. **B.** No feedback on Wee1. Parameters: $V_{iwee} = 0$ to eliminate the Wee1-MPF double negative feedback loop, and $k''_{wee} = 0.45$ to show that bistability is still possible, otherwise, parameters as in A. **C.** No feedback on Cdc25. $V_{a25} = 0$ to eliminate the Cdc25-MPF positive feedback loop, and $k'_{25} = 0.45$ to show that bistability is still possible, otherwise, parameters as in A.

3.4.2. Multiple feedback loops can be a source of ultrasensitivity

The second model presented in the previous section, which included positive feedback but no ultrasensitivity in the response of Cdc25 and Wee1 to MPF, did not give rise to bistability with the parameters specified in Table 3.1 (Equations 3.2-3.4, 3.9-3.10, Figure 3.3). However, with the appropriate choice of parameters this model can actually show bistability, as previous examples have indicated (Slepchenko and Terasaki, 2004; Zwolak et al., 2009), although the reasons for this have not been

analysed. Here, I show how that this is possible because there can be a hidden source of ultrasensitivity in the system: the presence of interlinked positive feedback loops.

In the examples of the previous section the parameter choices assumed that the strength of regulation of MPF on Cdc25 and Wee1 is equal, i.e., half of the maximum Cdc25 activity and half of the maximum Wee1 activity are reached at the same MPF level. This is not necessarily the case, but it is a reasonable simplifying assumption for illustrative purposes. For example, if Cdc25 inactivation is stronger than Wee1 activation ($V_{i25} > V_{awee}$) (Figure 3.5A), the mass action model can achieve bistability, as shown by the rate plot and signal-response curve in Figures 3.5B and 3.5C respectively. However, it is obvious that there will be a restricted parameter range in which the rate curves can cross at three points, and that bistability is more easily achieved when there is ultrasensitivity (compare with Figure 3.4A). Furthermore, in this case bistability is not possible with a single feedback loop, because if one of the rates is a straight line in a rate plot, it can only cross the curve for the other rate at a maximum of two places.

The fact that bistability is possible in the model with positive feedback and no ultrasensitivity implies that there is actually a source of ultrasensitivity, because bistability requires both (Ferrell and Xiong, 2001; Tyson et al., 2003; Angeli et al., 2004). The answer is that *bistability is possible because there are two interlinked positive feedback loops*, which together can act as a source of ultrasensitivity. This can be demonstrated by using an approach demonstrated by Angeli et al. (2004) who proved that for a system to be bistable, upon removal of a positive feedback loop, one of the components of the loop must have an ultrasensitive response to another of the components. By removing the MPF-Cdc25 positive feedback loop, for example, we

expect to see either that (i) Cdc25 has an ultrasensitive response to MPF or (ii) MPF has an ultrasensitive response to Cdc25. By definition, in this model with positive feedback but no ultrasensitivity in the responses of Cdc25 and Wee1 to MPF, the first possibility is not true, and therefore, because the system is bistable, the second possibility, must be true: MPF must have an ultrasensitive response to Cdc25 activity.

To show this, I remove the Cdc25-MPF feedback loop but retain the Wee1-MPF feedback loop. Thus, I consider that Cdc25 is not regulated by MPF and therefore constant, so $Cdc25 = Cdc25_T$. Therefore, the system described by Equations 3.2-3.4 and 3.9-3.10 can now be reduced to two ODEs:

$$\frac{dMPF}{dt} = k_{25}^{"} Cdc25_T (Cyc_T - MPF) - k_{wee} MPF \quad (3.17)$$

$$\frac{dWee1}{dt} = V_{awee} PP (Wee1_T - Wee1) - V_{iwee}\, MPF\, Wee1 \quad (3.18)$$

where

$$k_{wee} = k'_{wee}(Wee1_T - Wee1) + k"_{wee} Wee1$$

By assuming steady state levels for *Wee1*, it is possible to calculate the steady state of *MPF* as a function of *Cdc25*, which is then given by a quadratic equation:

$$V_{iwee}\left(k_{25}^{"} Cdc25_T + k'_{wee} Wee1_T\right) MPF^2 + \left[V_{awee} PP\left(k_{25}^{"} Cdc25_T + k'_{wee} Wee1_T + \left(k_{wee}^{"} - k'_{wee}\right) Wee1_T\right) - k_{25}^{"} Cdc25_T V_{iwee} Cyc_T\right] MPF - k_{25}^{"} Cdc25_T V_{awee} PP Cyc_T = 0 \quad (3.19)$$

The physically meaningful solution for this equation can, depending on parameters, produce an ultrasensitive response of *MPF* to *Cdc25*. This function is plotted in Figure 3.5D, using the same parameters that give rise to bistability used for Figure 3.5A-C and two different values of Cyc_T. Therefore, the network architecture of this system,

i.e. the presence of the two feedback loops, can produce the ultrasensitivity required to make the system bistable.

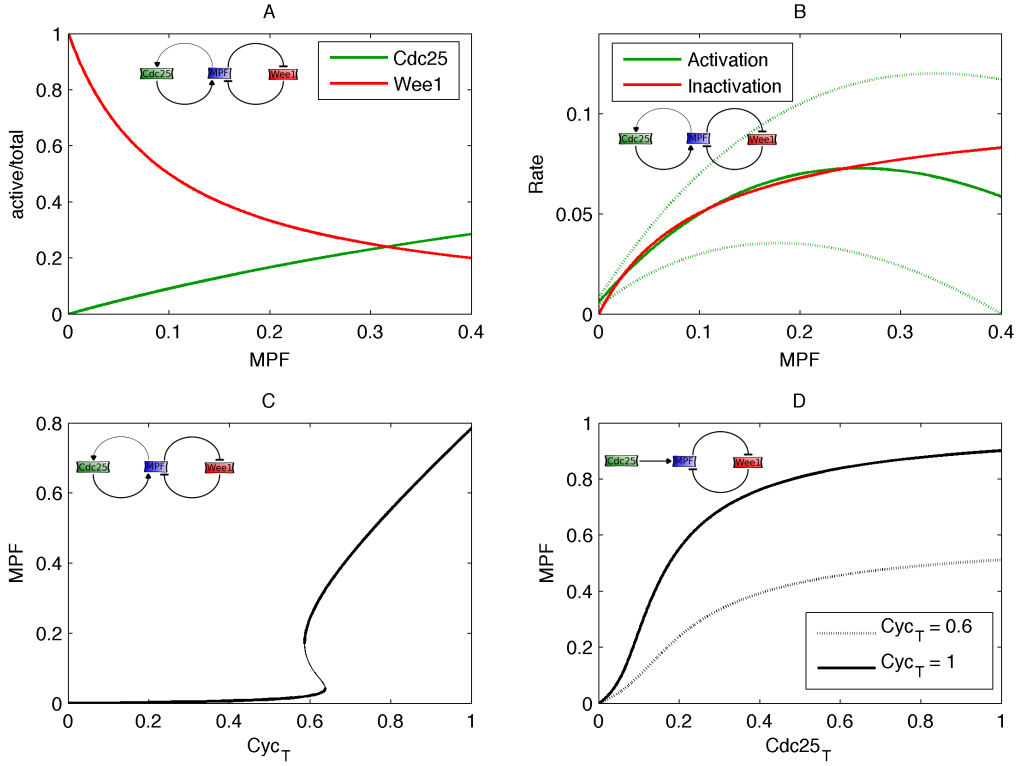

Figure 3.5. *Bistability in the mitotic switch with feedback but no ultrasensitivity*. **A.** Non-ultrasensitive response of Wee1 and Cdc25 to MPF with parameter values that produce bistability. Parameters as in Table 3.1 for the model with feedback and no ultrasensitivity except $V_{i25} = 1$. **B.** Rate plot for the same parameter values. **C.** One-parameter bifurcation diagram. **D.** Ultrasensitive response of MPF to $Cdc25_T$, which demonstrates the source of ultrasensitivity in this model. Interactions diagrams are also shown for each panel.

Equivalent results are obtained if the Wee1-MPF double negative feedback loop is eliminated instead. Importantly however, this source of ultrasensitivity depends on the fact that there is a double negative and a positive feedback loop. If both loops were of the same type, ultrasensitivity is not observed in this model. Therefore, this mix of positive and double negative feedback loops, which are the consequence of coherent regulation of the opposing enzymes Wee1 and Cdc25 by MPF, is likely to be

an important, if relatively minor, source of ultrasensitivity in biochemical systems. This role of interlinked positive feedback loops in generating bistability and ultrasensitivity was also shown by (Chang et al., 2010), and can perhaps be seen as a special type of multistep ultrasensitivity, where an effector acts in more than one place in a reaction network (Koshland et al., 1982; Chang et al., 2010).

Together with the demonstrated ability of coherent regulation of opposing enzymes in generating a robust bistable switch, this analysis indicates that the network architecture of the mitotic switch might be especially suitable for generating a very good switch to control mitotic entry.

3.5. Discussion

During its life, a cell needs to make important decisions, such as commitment to division, apoptosis, differentiation or expression of a particular protein(s). In general, the decision or *response* is taken as a consequence of an internal or external *signal*, such as attainment of correct size for division or the presence of a molecule in the environment. In many cases, the signal can be graded, but the response needs to be all-or-none. Furthermore, in many cases, these decisions must be robust to noise and/or irreversible; that is, they must persist when the original signal triggering the response is diminished or removed. In a sense, systems displaying these characteristics have a memory that 'remembers' the presence of the signal after it is gone (Laurent and Kellershohn, 1999; Ferrell and Xiong, 2001; Ferrell, 2002; Tyson et al., 2003; Slepchenko and Terasaki, 2004; Mitrophanov and Groisman, 2008).

Systems performing such decisions can be described mathematically as *bistable*, which means they are characterized by the presence of two coexisting stable steady states of the response, for a range of values of the signal, as explained in Chapters 1 and 2. The mitotic switch is one of the best-characterized examples of a biochemical bistable switch, and its existence has been experimentally demonstrated (Pomerening et al., 2003; Sha et al., 2003). However, there are other examples of bistable biochemical switches. Other irreversible cell cycle transitions in particular, have been associated with bistability and the switching point with saddle node bifurcations (Novák et al., 2007; Tyson and Novák, 2008; Gérard and Goldbeter, 2009). For example, the Start transition (Chen et al., 2000) and exit in budding yeast (Tóth et al., 2007), the restriction point in mammalian cells (Yao et al., 2008), and the metaphase-to-anaphase transition after the resolution of the spindle assembly checkpoint (He et al., 2011) have been proposed to constitute bistable switches, and this has been experimentally shown for the first three cases (Cross et al., 2002; Yao et al., 2008; López-Avilés et al., 2009).

Besides being a feature of irreversible cell cycle transitions, bistability has also been proposed and in some cases experimentally shown in other biological decision-making systems. Examples are the Lac operon in bacteria (when responding to gratuitous inducers) (Novick and Weiner, 1957; Ozbudak et al., 2004), the lysis-lysogeny switch in phage (Oppenheim et al., 2005) and oocyte maturation in *Xenopus* (Ferrell and Machleder, 1998; Xiong and Ferrell, 2003). Moreover, artificial genetic bistable switches have been even constructed in bacteria using theoretical principles similar to the ones presented here (Gardner et al., 2000; Becskei and Serrano, 2000; Becskei et al., 2001; Chang et al., 2010).

Overall, bistability is likely to be a widespread phenomenon in cell biology, and to be a key property in ensuring irreversible decisions, all-or-nothing responses and biological memory (Ferrell and Xiong, 2001). Therefore, it is extremely important to understand how it arises, and what other interesting properties and features are a result of bistable switches.

In biochemical systems, bistability arises from the way the relevant components are organized or connected in terms of their regulation. In general it requires some sort of positive feedback, which guarantees that only one state is possible and the system cannot rest in intermediate states. A less obvious requirement is the existence of nonlinearity, in the form of ultrasensitivity, which serves as a filter for small inputs, so the system does not switch to the other state immediately, that is, it is necessary for the system to have a stable 'off' state (Ferrell and Xiong, 2001; Ferrell, 2002; Tyson et al., 2003).

In this chapter, I have shown the importance of positive feedback and ultrasensitivity for bistability in the mitotic switch, using simple mathematical models. There is experimental evidence for the importance of positive feedback for bistability and shows the presence of ultrasensitivity in the mitotic switch. For example, positive feedback was experimentally shown to be required for bistability and sustained oscillations of MPF in *Xenopus* egg extracts (Pomerening et al., 2005). This was shown by adding to the extracts a non-phosphorylatable form of Cdk1, which cannot be inhibited by Wee1. This led to dampened oscillations and a reduced bistable regime for the system. Using a similar approach, positive feedback in Cdk1 activation has also been shown to be important in the mammalian cell cycle (Pomerening et al., 2008). These experiments also demonstrated the importance of the difference in

activity between the non-phosphorylated and the tyrosine-phosphorylated forms of Cdk1.

As for ultrasensitivity, several mechanisms commonly found in cells are thought to account for ultrasensitivity, such as cooperativity in allosteric proteins multistep processes, such as multisite phosphorylation, stoichiometric inhibitors and saturation of opposing enzymes, which can lead to zero-order ultrasensitivity (Goldbeter and Koshland, 1981; Koshland et al., 1982; Ferrell, 1996; Gunawardena, 2005; Kapuy et al., 2009a; Novák and Tyson, 2008). Ultrasensitivity has been shown experimentally in the mitotic switch for the response of Cdc25 and Wee1 to MPF (Kim and Ferrell, 2007; Trunnell et al., 2011), although the mechanisms by which it is achieved are not completely clear. The Novák-Tyson model of the mitotic switch assumed zero-order ultrasensitivity for the active forms of Cdc25 and Wee1 (Novák and Tyson, 1993), which implies that MPF and/or its counteracting phosphatase(s) are saturated by their substrates. Although assumption of Goldbeter-Koshland kinetics is a very useful way to model ultrasensitive responses, several questions can be raised about its validity in this system. To obtain a sharp response, at least one of the enzymes has to work at saturation, as explained previously. It is not clear whether this is the case for MPF and its counteracting phosphatase in the cell cycle.

As seen in this chapter, if the enzymes are not saturated, but in the first order regime, as modelled with mass action kinetics, bistability in the mitotic switch can be completely lost or at best be very sensitive to parameter changes (see also Ciliberto et al. 2007; Sabouri-Ghomi et al. 2008). Since the validity of the enzyme-saturation assumption can be difficult to assess, it is worth asking whether there are other sources of ultrasensitivity that could have an important role in the mitotic entry

switch. Experimental work has implicated substrate competition and multisite phosphorylation in the ultrasensitive responses of Wee1 and Cdc25 respectively, although in neither case the proposed mechanism fully accounted for the experimentally observed ultrasensitivity (Kim and Ferrell, 2007; Trunnell et al., 2011).

Since in principle only one of two positive feedback loops would be necessary to achieve bistability, but both are found and conserved in nature, it is likely that this type of regulation is beneficial for the cell. It has been proposed that this reciprocal feedback regulation of both enzymes regulating MPF helps to create a very robust and efficient bistable switch (Ferrell, 2008), but it may also have a role in generating or contributing to nonlinearity in the system, because the presence of multiple feedback loops in the system can be a source of ultrasensitivity, as I showed in the previous section.

In the following chapters I will develop mathematical models of the mitotic switch which assume different sources of ultrasensitivity, to try to understand which mechanisms could be important in the mitotic switch.

3.6. Summary

In this chapter I have shown that positive feedback and ultrasensitivity are essential for bistability in the mitotic switch. I have provided evidence that multiple feedback loops with particular architectures may be a source of ultrasensitivity. However, both from a theoretical perspective and from experimental data, the issue of how ultrasensitivity arises in the mitotic switch, specifically in the responses of Wee1 and

Cdc25, is not fully resolved (Kim and Ferrell, 2007; Trunnell et al., 2011; Tyson and Novák, 2010).

In the next chapter I consider another source of bistability: multistep processes in the form of multisite phosphorylation of the MPF regulators. I develop a model based on this mechanism, and analyse the relative contributions of the two feedback loops in the mitotic switch network.

Chapter 4

The mitotic switch with multisite phosphorylation

4.1. Overview

In the previous chapter I showed the importance of positive feedback and ultrasensitivity to generate bistability in the mitotic switch. I also discussed some of the possible sources of ultrasensitivity in the response of Cdc25 and Wee1 to MPF. In this chapter I develop a model where this ultrasensitivity results from the assumption of multisite phosphorylation for both MPF regulators. I then use this model to explore the roles of the individual feedback loops in the mitotic switch in a biologically meaningful way, by assessing the possible effects of mutations in the phosphorylation sites that control the regulation of Cdk1, Wee1 and Cdc25. Most of this work has been published, and Sections 4.2 to 4.8 (except 4.6) are based on the this publication (Domingo-Sananes and Novák, 2010). Finally, I demonstrate the versatility of multisite phosphorylation for biochemical regulation by developing a model with mixed regulation of Wee1 by MPF, where MPF both activates and inhibits Wee1, which agrees with some recent experimental data. This model, which is presented in Section 4.9, was also published (Novák et al., 2010).

4.2. Introduction

In the previous chapter I presented a simplified version of the Novák-Tyson model of the mitotic switch (Novák and Tyson, 1993) and analysed how positive feedback and ultrasensitivity generate bistability. This analysis showed that positive (or double negative) feedback is necessary, although not sufficient for achieving bistability. To achieve bistability in this model, besides positive feedback it was necessary to assume that the responses of Wee1 and Cdc25 to MPF were ultrasensitive. Ultrasensitivity is achieved, both in the example in Chapter 3 and in the original Novák-Tyson model, by assuming Michaelis-Menten kinetics in the activation and inactivation of Cdc25 and Wee1, which are catalysed by MPF and a constant MPF-counteracting phosphatase, PP. Further assumption of enzyme saturation (using small values for the Michaelis constants), gives rise to the zero-order ultrasensitivity (Goldbeter and Koshland, 1981), as described in Chapter 2.

In contrast to metabolic networks, enzyme saturation may be less common in protein interaction networks, such as the cell cycle control system, where both enzymes and substrates are likely to be present at comparable concentrations (Ciliberto et al., 2007). Furthermore, in these networks feedback loops are common, and as is the case for the mitotic switch network, the components may in turn acts as enzymes and substrates of each other (i.e. Cdc25 is an MPF substrate, and MPF is a Cdc25 substrate) or act on many other substrates (Ciliberto et al., 2007; Sabouri-Ghomi et al., 2008). However, as shown in the previous chapter, without the assumption of zero-order ultrasensitivity, bistability is easily lost in the mitotic switch.

Because ultrasensitivity is required for robust bistability, it is thus important to explore other sources of ultrasensitivity in the mitotic switch. Even if zero-order

ultrasensitivity has a role in bistability in this system, it is unlikely to be the only source, and it is important to assess the contributions of other mechanisms, which may also be relevant for other biochemical systems. As one way to address this issue, I present a model of the mitotic switch in which ultrasensitivity arises from multisite phosphorylation of Cdc25 and Wee1 by MPF, since it has been previously suggested that multistep processes, in particular multisite phosphorylation, can produce nonlinear, ultrasensitive responses which may contribute to bistability (Koshland et al., 1982; Ferrell, 1996; Markevich et al., 2004; Gunawardena, 2005; Salazar and Höfer, 2007; Kapuy et al., 2009a). Moreover, it has been demonstrated that MPF can actually phosphorylate Cdc25 and Wee1 at multiple sites (Kumagai and Dunphy, 1992; Tang et al., 1993; Kim et al., 2005; Trunnell et al., 2011). Parallel to the work presented here, it has been shown that multisite phosphorylation of Cdc25 by MPF in *Xenopus* egg extracts contributes to the ultrasensitive response curve of Cdc25 with respect to MPF (Trunnell et al., 2011).

I will first describe the model and show that multisite phosphorylation is a plausible mechanism that can contribute to ultrasensitive responses, and thus to bistability in the mitotic switch. Furthermore, I use this model to analyse the effects of feedback regulation on the switch, in a way that closely parallels possible experimental approaches, by showing the effects of 'mutations' on the phosphorylation sites. I show that the two feedback loops in this system do not necessarily behave in the same way when perturbed, and that equivalent but independent modifications on them can have distinct effects on the system. I propose that feedback regulation of the Cdc25 phosphatase could have a crucial role in setting the cyclin threshold for MPF activation.

4.3. Multisite phosphorylation can lead to ultrasensitivity

I will first describe the general multisite phosphorylation mechanism used here, which was developed in our group (Kapuy et al., 2009a). Similar approaches have also been derived by Gunawardena (2005) and Hoeffer et al (2007).

The initial assumption is that multisite phosphorylation follows a distributive and ordered mechanism (Kapuy et al., 2009a). In a distributive mechanism, only one catalytic step (phosphorylation or dephosphorylation) occurs during a single enzyme substrate-binding event (as opposed to a sequential mechanism, in which several or all sites are modified during a single enzyme-substrate binding event). In an ordered mechanism, the kinase and the phosphatase modify the sites in a specific sequence and both enzymes work in opposite order. For simplicity, I assume that the different phosphoforms are modified (phosphorylated or dephosphorylated) at the same rate. I refer to the different phosphorylated forms of a substrate X with n phosphorylation sites as XP_0, XP_1, ... ,XP_n. Thus, a protein with n phosphorylation sites has n+1 possible different phosphoforms. I assume that the sum of all the phosphorylated forms of X, X_T, is constant ($XP_0 + XP_1 + \ldots + XP_n = X_T$).

If the kinase and phosphatase activities are denoted by k and h, respectively, the following ODE's can be written for the different phosphoforms of X, assuming mass action kinetics:

$$\frac{dXP_0}{dt} = hXP_1 - kXP_0 \qquad 4.1$$

$$\frac{dXP_i}{dt} = hXP_{i+1} + kXP_{i-1} - (h+k)XP_i \qquad 4.2$$

where Equation 4.2 is valid for $1 < i < n - 1$. Only n ODEs are required since I assume that the total substrate concentration, X_T, is constant. Therefore, the concentration of the n^{th} phosphorylated form can be calculated algebraically by Equation 4.3:

$$XP_n = X_T - \sum_{i=1}^{n} XP_{i-1} \qquad 4.3$$

If the kinase and phosphatase activities, k and h are constant in time, the phosphorylation chain will approach a steady state in which the concentration of various phosphorylated forms of X no longer changes in time. The steady state distribution of the different phosphoforms, shown for n = 5 in Figure 4.1A, can be calculated by the following equation (Kapuy et al., 2009a):

$$XP_i = X_T \frac{\left(\frac{k}{h}\right)^i}{\sum_{j=0}^{n}\left(\frac{k}{h}\right)^j} = X_T \frac{\left(\frac{k}{h}\right)^i \left(1 - \frac{k}{h}\right)}{1 - \left(\frac{k}{h}\right)^{n+1}} \qquad 4.4$$

From Figure 4.1A it is possible to see that the concentrations of the extreme phosphoforms (the fully phosphorylated and completely dephosphorylated) have a sigmoid shape with respect to the kinase to phosphatase ratio. This is already an ultrasensitive response, although it is not extremely sharp, or as described by Gunawardena (2005) a "good threshold but a bad switch". However, because it can function as a filter for small inputs, this response can easily generate bistability (Kapuy et al., 2009a). However, responses more similar to the standard ultrasensitive response in the shape of a Hill function can be achieved by considering that the relevant response does not only depend on the extreme phosphoforms, but that it can also include intermediate phosphoforms. Therefore, if for example, the

concentrations of half of the phosphoforms are summed, a classic sigmoid response is obtained (Kapuy et al., 2009a; Wang et al., 2010), as shown in Figures 4.1B and C. In fact this way of considering the activities of the different phosphoforms can give extremely flexible responses, including bell-shaped curves when only intermediate phosphoforms are considered (Figure 4.1D), which might have biological relevance, as shown in the last section of this chapter.

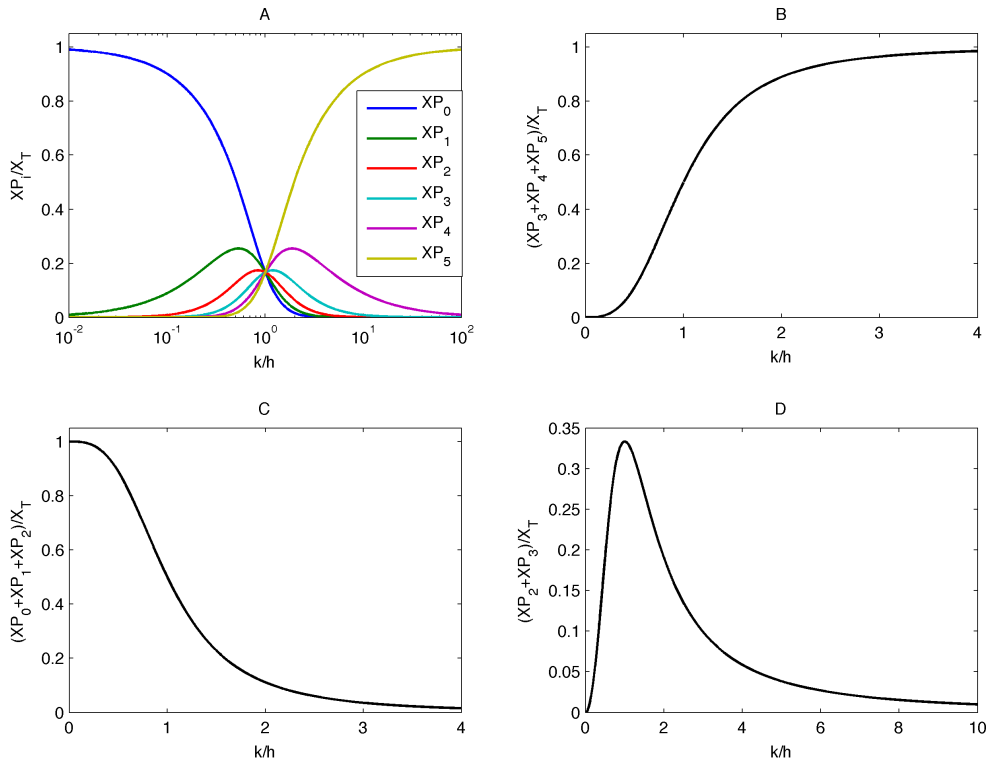

Figure 4.1. A. Concentration of phosphoforms with respect to the kinase to phosphatase ratio in a distributive and ordered multisite phosphorylation mechanism. **B.** Concentration of the sum of the three most highly phosphorylated forms with respect to the kinase to phosphatase ratio. **C.** Concentration of the sum of the three least phosphorylated forms with respect to the kinase to phosphatase ratio. **D.** Concentration of the sum of the forms with two and three phosphorylations.

It is worth mentioning that the ultrasensitivity achieved by assuming this multisite phosphorylation mechanism is independent of enzyme saturation, or zero-order

effects, because the ODEs are written assuming mass action kinetics and ignoring enzyme-substrate complexes. This may not necessarily be the actual biochemical mechanism, but from a modelling perspective allows consideration of multisite phosphorylation as the main source of ultrasensitivity and nonlinearity. In fact, multistep processes can actually enhance zero-order ultrasensitivity (Goldbeter and Koshland, 1984).

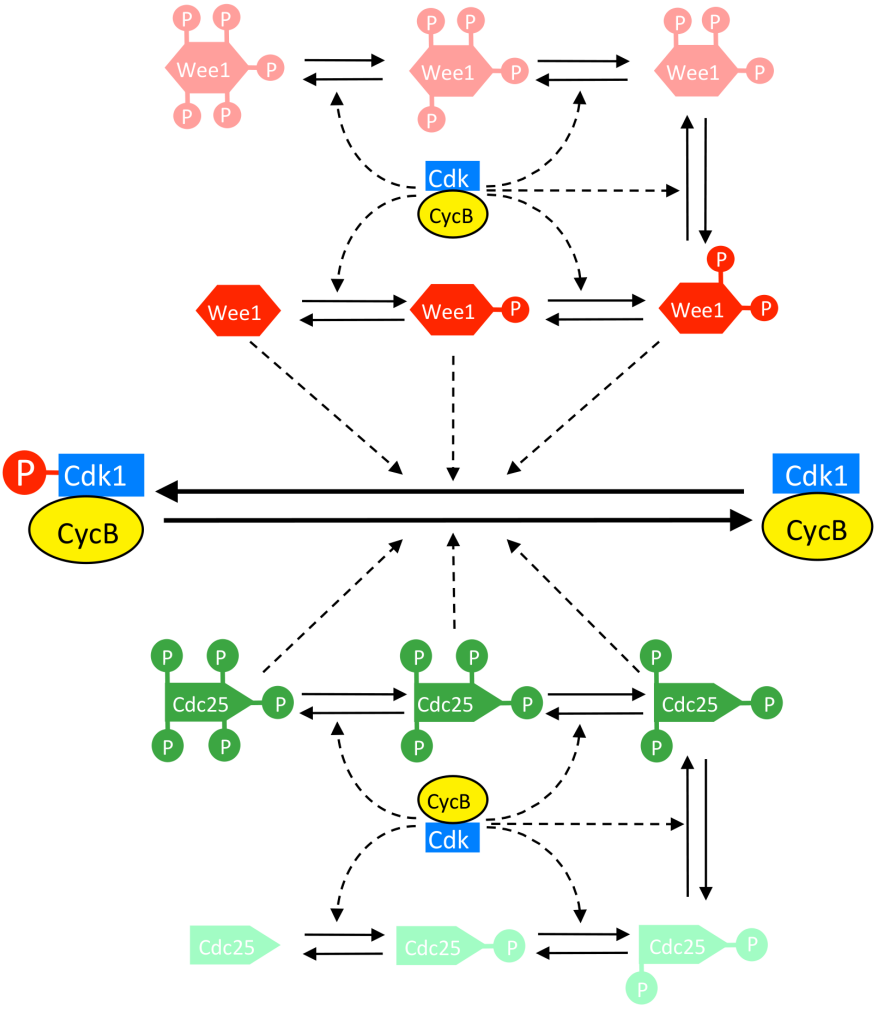

Figure 4.2. *Network diagram of the model of the mitotic switch with multisite phosphorylation*. In the figure, as with the standard parameter set of the model, it is assumed that both Wee1 and Cdc25 have five sites that are phosphorylated by MPF and that half of the phosphoforms of each enzyme are active (dark green and red) and the other half inactive (light green and red).

4.4. A model of the mitotic entry switch with multisite phosphorylation

The essence of the model is shown in the network diagram in Figure 4.2. The model of the mitotic switch with multisite phosphorylation was developed using an approach similar to that in Chapter 3, and therefore, the ODE for MPF is the same as before (Chapter 3):

$$\frac{dMPF}{dt} = k_{25}(Cyc_T - MPF) - k_{wee}MPF \qquad 4.5$$

Where Cyc_T is the sum of active and inactive Cdk1-CycB dimers, ($Cyc_T = MPF + pMPF$), and $k_{25}$and k_{wee} are functions of *Cdc25* and *Wee1*, respectively given by:

$$k_{25} = k'_{25}(Cdc25_T - Cdc25) + k"_{25}Cdc25 \qquad 4.6$$

$$k_{wee} = k'_{wee}(Wee1_T - Wee1) + k"_{wee}Wee1 \qquad 4.7$$

Where k'_{25} and k'_{wee} are the rate constants for the background activity of the inactive forms of Cdc25 and Wee1 respectively, and $k"_{25}$ and $k"_{wee}$ are the rate constants for the active forms. Again, $Cdc25_T$ and $Wee1_T$ are the total levels of the two proteins, the sum of the active and inactive forms, which is still assumed to be constant.

The difference is that in the present model, ultrasensitivity arises from distributive and ordered multisite phosphorylations of the regulatory enzymes Cdc25 and Wee1 by MPF, and dephosphorylation by an MPF-counteracting phosphatase PP, as described above. The maximal number of phosphorylation sites on Wee1 and Cdc25 are labelled as n_w and n_c, respectively. Like in the Novák-Tyson model, the rate of phosphorylation of Cdc25 is $k_{a25}MPF$ and the rate of dephosphorylation is $k_{i25}PP$,

but this now applies at every single phosphorylation site. Likewise, Wee1 is phosphorylated at a rate $k_{iwee}MPF$ and dephosphorylated at a rate $k_{awee}PP$ at each phosphorylation site.

MPF-dependent phosphorylation reduces Wee1 activity while it increases Cdc25 activity. However, little is known about how individual phosphorylations influence their enzymatic activities. Here, I make the simplifying assumption that the activity changes in a stepwise fashion after θ phosphorylations, and sum the relevant forms to calculate the concentration of the active enzymes. For Cdc25, phosphoforms with θ_c or fewer phosphorylations are mostly inactive (their specific activity is k'_{25}) while those with more than θ_c phosphorylations are fully active (their specific activity is k''_{25}). For Wee1, the opposite is true, the forms with θ_w and fewer phosphorylations are fully active (specific activity k''_{wee}) while those with more than θ_w are mostly inactive (specific activity k'_{wee}).

Applying Equation 4.4 to the substrates Cdc25 and Wee1, and summing up the relevant forms, the following algebraic equations can be written to calculate the concentrations of active Cdc25 and Wee1 as a function of *MPF* (*PP* is constant):

$$Cdc25 = Cdc25_T - \sum_{i=0}^{\theta_c} Cdc25P_i = Cdc25_T - Cdc25_T \frac{1 - \left(\frac{V_{a25}MPF}{V_{i25}PP}\right)^{\theta_c+1}}{1 - \left(\frac{V_{a25}MPF}{V_{i25}PP}\right)^{n_c+1}} \qquad 4.8$$

$$Wee1 = \sum_{i=0}^{\theta_w} Wee1P_i = Wee1_T \frac{1 - \left(\frac{V_{iwee}MPF}{V_{awee}PP}\right)^{\theta_w+1}}{1 - \left(\frac{V_{iwee}MPF}{V_{awee}PP}\right)^{n_w+1}} \qquad 4.9$$

Using the parameter values in Table 4.1, these responses of Cdc25 and Wee1 to MPF are shown in Figure 4.3A. From Equations 4.6 and 4.7 together with 4.8 and 4.9 it is

also possible to calculate the cumulative activities of Cdc25 and Wee1, which takes into account the residual activity of the inactive forms of Cdc25 and Wee1 (Figure 4.3A). Both curves have a sigmoid shape with an opposite trend. Thus, multisite phosphorylation can lead to substantial ultrasensitivity and is a plausible mechanism to generate nonlinearity and thus bistability in biological systems. Since I assume that the different phosphorylated forms of Wee1 and Cdc25 are in equilibrium the system is reduced to one differential equation (Equation 4.5) and four algebraic equations (Equations 4.6-4.9). With this new model, it is possible to calculate the response of MPF activity to Cyc_{T}, the one-parameter bifurcation diagram shown in Figure 4.3B. This curve is similar to the one obtained for the original Novák-Tyson model (Figure 3.2I), and therefore with the parameter values specified in Table 4.1, the system is bistable and serves as our standard model of the mitotic switch.

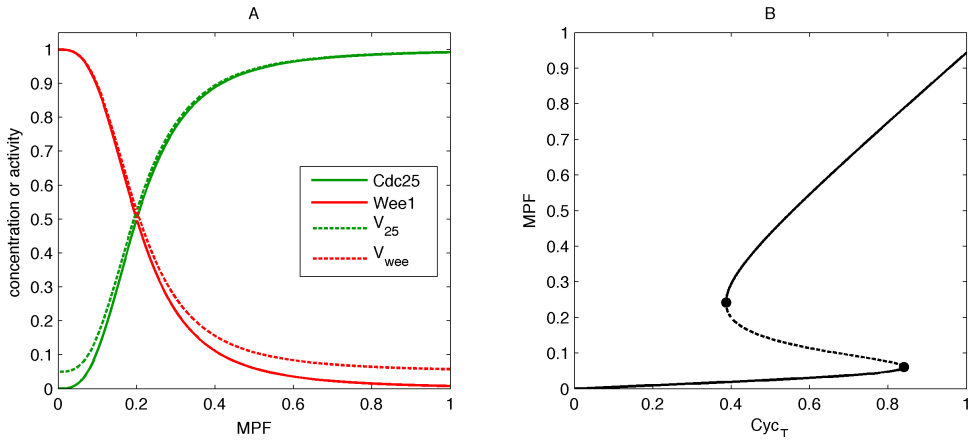

Figure 4.3. A. Response of Cdc25 and Wee1 active forms and cumulative activities with respect to MPF in the model of the mitotic switch with multisite phosphorylation. **B.** One-parameter bifurcation diagram of MPF activity with respect to Cyc_T levels. Parameters values are given in Table 4.1.

Table 4.1. *Parameter values for the MPF switch model based on multisite phosphorylation.* These parameter values were used for the standard model, unless specified otherwise.

Parameter	Description	Value
k'_{wee}	Rate of MPF inactivation by inactive Wee1	0.05
k''_{wee}	Rate of MPF inactivation by active Wee1	1
k'_{25}	Rate of MPF activation by inactive Cdc25	0.05
k''_{25}	Rate of MPF activation by active Cdc25	1
V_{awee}	Rate of Wee1 activation by PP	0.2
V_{iwee}	Rate of Wee1 inactivation by MPF	1
V_{a25}	Rate of Cdc25 activation by MPF	1
V_{i25}	Rate of Cdc25 inactivation by PP	0.2
θ_c	Number of phosphorylations of the last inactive form of Cdc25	2
θ_w	Number of phosphorylations of the last active form of Wee1	2
n_c	Total number of phosphorylation sites on Cdc25	5
n_w	Total number of phosphorylation sites on Wee1	5
PP	Constant, MPF-counteracting phosphatase	1
$Cdc25_{\mathrm{T}}$	Total Cdc25 (sum of all phosphoforms)	1
$Wee1_{\mathrm{T}}$	Total Wee1 (sum of all phosphoforms)	1

4.5. The role of the individual feedback loops in the mitotic switch

Using the model of the mitotic switch with multisite phosphorylation, I analysed the role of the feedback loops in the mitotic switch. In a previous theoretical analysis, Pomerening *et al* (2005) showed that reducing feedback on both Wee1 and Cdc25 in a model of *Xenopus* egg extracts reduced the width of the bistable region and led to damped MPF oscillations. They confirmed their findings experimentally, by using a CDK that could not be inhibited by Wee1 due to mutation of CDK tyrosine 15 to a non-phosphorylatable residue. This is equivalent to elimination of both feedback loops, and results in constitutively active MPF, regardless of Wee1 and Cdc25 activity. However, both loops were analysed together, and implicitly assumed to be equivalent. To test this assumption, I aimed to analyse the role of each of the feedback loops individually, by perturbing or eliminating them, to assess their individual contributions to the bistable mitotic switch.

One of the advantages of the multisite phosphorylation model is that the effect of mutation of the phosphorylation sites, which determine how all the molecules in the network are regulated, can be analysed and predicted. The amino-acid residues acting as phospho-acceptor sites can be mutated in two different ways: (1) to a residue which cannot be phosphorylated (such as alanine), a modification which locks the protein in its unphosphorylated state, or (2) to a 'phosphomimetic' residue (such as aspartate or glutamate) which cannot be phosphorylated either but mimics permanent phosphorylation due to its negative charge. This is referred to as a "phosphomimicking" mutation. I refer to these two types of mutant proteins as NP (non-phosphorylatable) or PM (phosphomimetic). WT indicates the 'wild type' or normal form of the protein.

All the MPF-phosphorylation sites on Cdc25 can be eliminated in the model by setting $n_c = \theta_c = 0$, representing the non-phosphorylatable Cdc25 mutant (NP-Cdc25). Thus $Cdc25 = 0$ (see Equation 4.8), and all Cdc25 permanently remains in the unphosphorylated, mostly inactive form (specific activity k'_{25}). Therefore, the positive feedback loop is eliminated. This 'mutation' has a dramatic effect on the cyclin threshold for MPF activation. Although the system is still bistable, due to double negative feedback through Wee1, Cyc_T needs to increase to much higher levels in order to activate MPF (Figure 4.4A, compare WT and NP-Cdc25).

On the other hand, elimination of all the MPF-phosphorylations sites on Wee1 by setting $n_w = \theta_w = 0$, results in non-phosphorylatable Wee1 (NP-Wee1), which is locked in its active form (thus $Wee1 = Wee1_T$, see Equation 4.9). This eliminates the double negative feedback loop but leaves the Cdc25 positive feedback loop intact. Surprisingly, this barely has an effect on the cyclin threshold for MPF activation,

although it results in reduced MPF activity in the upper steady state (Figure 4.4A). MPF activity is decreased because the Cdc25 positive feedback loop now works against constitutively active rather than phosphorylated and inhibited Wee1.

The effect of phosphomimicking modifications can also be studied if I assume that they have the same effects on protein activity as normal phosphorylations. Mutating all the MPF-target sites on Wee1 and Cdc25 to a phosphomimetic residue creates constitutively active Cdc25 (PM-Cdc25, setting $n_c = 0$, $\theta_c = -1$) or inactive Wee1 (PM-Wee1, setting $n_w = 0$, $\theta_w = -1$), respectively. As shown in Figure 4.4B, both modifications result in loss of bistability. This is because Wee1 activity is not high enough to cause substantial MPF inhibition, even at low Cyc_T, either because it is inactive or because it is opposed by a fully active Cdc25, which results in MPF activation a low Cyc_T levels.

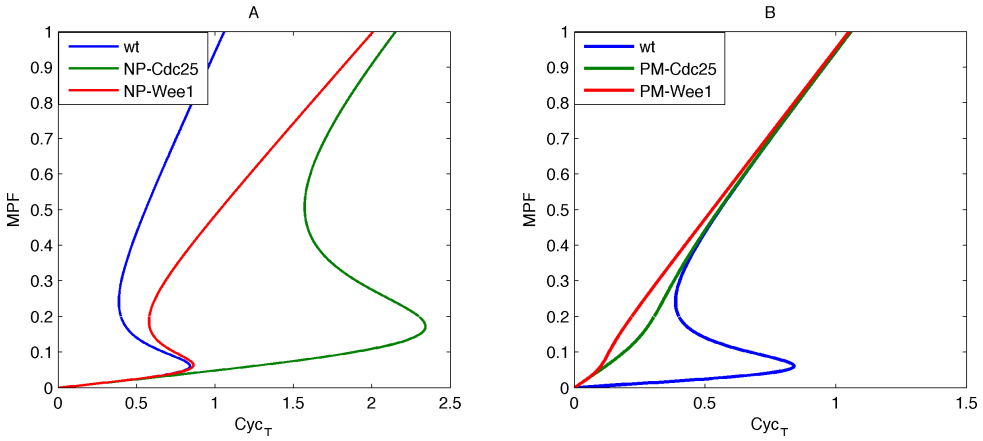

Figure 4.4. *Effect of mutations of all the MPF phosphorylation sites on Cdc25 or Wee1*. **A.** Elimination of sites: one-parameter bifurcation diagrams for the WT case (same as Figure 4.3B), and non-phosphorylatable Cdc25 (NP-Cdc25) or Wee1 (NP-Wee1). For NP-Wee1 only the Cdc25 positive feedback is functional. For NP-Cdc25 only the double negative feedback operates. **B.** Phosphomimicking of all phosphorylation sites: one-parameter bifurcation diagrams for the WT (same as Figure 4.3B), and phosphomimetic Cdc25 (PM-Cdc25) or Wee1 (PM-Wee1). This also results in a single functional feedback loop in the mutant cases but the activities of the mutant proteins are the opposite. Parameters as in 4.1 except*:* $\theta_c = 0$, $n_c = 0$ for NP-Cdc25; $\theta_w = 0$, $n_w = 0$ for NP-Wee1; $\theta_c = -1$, $n_c = 0$ for PM-Cdc25; $\theta_w = -1$, $n_w = 0$ for PM-Wee1.

I can compare these results of modifications to individual loops, to the effects of using a similar 'mutation' strategy to perturb both loops together. The first option is to consider the same perturbation performed by Pomerening et al (2005), of adding a non-phosphorylatable, constitutively active form of Cdk1 to *Xenopus* egg extracts. This can be modelled here by preventing MPF inactivation by Wee1 ($k'_{wee} = k''_{wee} = 0$), which is equivalent to having a non-phosphorylatable Cdk1 (NP-Cdk1). As expected, this leads to complete loss of bistability, as all the Cdk1-CycB dimers are now fully active (Figure 4.5). However, it is possible to modify both feedback loops together in other ways. One possibility is a phosphomimetic version of Cdk1 (PM-Cdk1), which prevents MPF activation by Cdc25. Because in this case MPF is always inactive, the signal-response curve becomes a horizontal line at *MPF=0* and bistability is lost (Figure 4.5).

Another way to alter both loops together is to combine mutations on both Cdc25 and Wee1. Elimination of all the sites in both Wee1 and Cdc25 (NP-Wee1 & NP-Cdc25) causes, as might be expected, loss of bistability (since all positive feedback is eliminated). In this case, Wee1 is always active and Cdc25 always inactive, so the system can only move along the lower branch of the signal-response curve (Figure 4.5). The slight rise in MPF depends on the background rate of dephosphorylation of inactive Cdc25, k'_{25}. If k'_{25}=0, there would be no rise and the system would move along the horizontal line at *MPF=0*, just like PM-Cdk1 in this model. In reality, a slight rise in activity could be expected for a stably phosphorylated Cdk1, due to residual activity.

Phosphomimicking on all the sites of both Wee1 and Cdc25 (PM-Wee1 & PM-Cdc25) leads to constitutively active Cdc25 and inactive Wee1. This also causes loss of

bistability, but in this case the system can only move along the upper branch of the signal-response curve, where MPF is mostly active, because of the constitutively high Cdc25 and low Wee1 activities. In this case, the low proportion of inactive MPF depends on the background phosphorylation of inactive Wee1 k'_{wee}. If $k'_{wee} = 0$, the system would move along the diagonal with slope 1, equivalent to NP-Cdk1.

Finally, if all the phosphorylation sites are eliminated on one of the MPF regulators and phosphomimicked on the other, both enzymes will be either fully active or fully inactive. The complete loss of feedback again results in loss of bistability, but now the signal-response curve is between the two branches of the original (PM-Cdc25 and NP-Wee1, or NP-Cdc25 and PM-Wee1). This is because in either case, the activities of the two opposing regulators are of similar magnitude. Because in the parameter set used here (Figure 4.3A, Table 4.1) the responses of Cdc25 and Wee1 to MPF are symmetrical, half of MPF will be active for all values of Cyc_T.

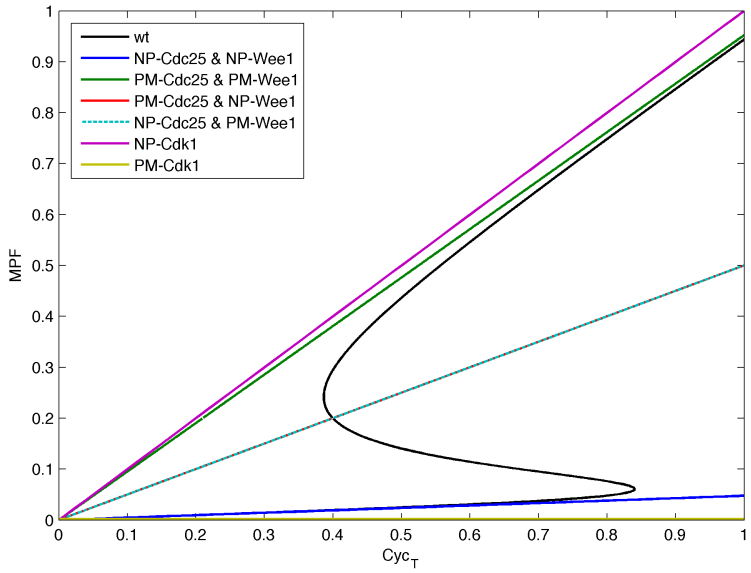

Figure 4.5. *Effects of mutations that disrupt both feedback loops in the model of the mitotic switch with multisite phosphorylation.*

This analysis shows that elimination of both feedback loops always results in loss of bistability, but hysteresis is not always lost when the feedback loops are compromised individually. This is because, as shown in Chapter 3, bistability in this system is possible with only one feedback loop if there is enough ultrasensitivity in the system, which in this model is mainly the result of an ultrasensitive response of Wee1 or Cdc25 to MPF, due to multisite phosphorylation. Moreover, Figure 4.4A shows that elimination of the phosphorylation sites on Wee1 and Cdc25 has different effects on the position of the cyclin threshold for MPF activation. With the parameter set from Table 4.1, elimination of the Cdc25 positive feedback loop drastically increases the threshold, while elimination of the Wee1 double negative feedback loop has almost no effect.

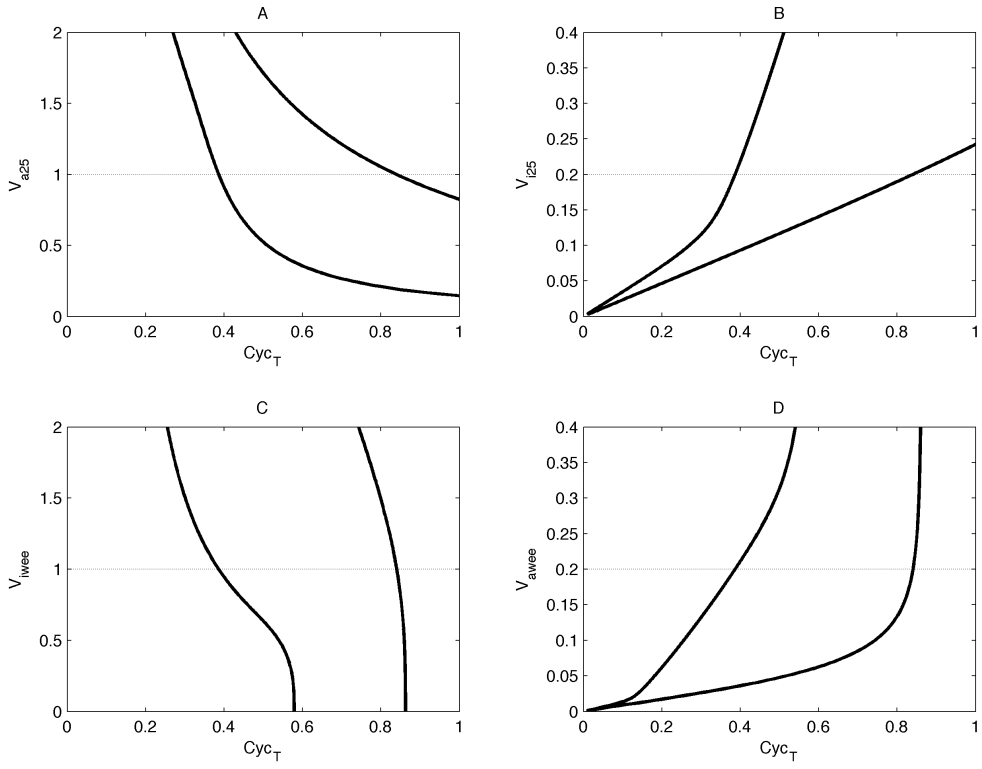

Figure 4.6. Two-parameter bifurcation diagrams for the model of the mitotic switch with multisite phosphorylation for Cyc_T versus the rates of **(A)** Cdc25 activation, V_{a25}; **(B)** Cdc25 inactivation, V_{i25}; **(C)** Wee1 inactivation, V_{iwee} and **(D)** Wee1 activation V_{awee}. The grey horizontal line shows the original value of the second parameter, from Table 4.1.

The independent effects of the two feedback loops on the cyclin thresholds can also be analysed in terms of the rate constants for the activation and inactivation of Wee1 and Cdc25, which determine the 'strength' of the feedback of MPF on its regulators. This can be illustrated by two-parameter bifurcation diagrams (Figure 4.6). In these plots the values of the two cyclin thresholds are plotted as a function of different rate constants for activation and inactivation of Cdc25 (V_{a25} and V_{i25}) and Wee1 (V_{awee} and V_{iwee}). A steep slope in these diagrams is an indication that the position of the saddle node bifurcation changes little with the parameter. In contrast, a flat slope indicates that the position of the saddle node bifurcation is very sensitive to the parameter. If I compare the MPF activation threshold for V_{a25} and V_{i25} with those for V_{awee} and V_{iwee}, the differences in slope are evident for a significant part of the parameter range (Figure 4.6). Similar results are obtained with the original Novák-Tyson model, which does not assume multisite phosphorylation (not shown), indicating that the different effects of the two feedback loops on the lower saddle node bifurcation is not dependent on the multisite phosphorylation mechanism that I have described.

4.6. Mutations on individual phosphorylation sites on Cdc25 and Wee1

We can also have a closer look at how individual mutations might affect the system, although this is slightly more complicated and requires careful consideration of the model and additional assumptions. There is a semi-hidden assumption in the model, that phosphorylation at the third site is the one that causes the activity to actually change. Phosphorylation of the third site changes the activity and then further phosphorylation on sites 4 and 5 has no effect on the activity of Cdc25 or Wee1.

Therefore, if site 5 is mutated, the end of the phosphorylation chain (Figure 4.2) is truncated, so that now for Cdc25, for example, there will only be two active forms (those with 3 and 4 phosphorylations) and 3 inactive forms as before (those with 0, 1 and 2 phosphorylations). This is equivalent to setting $n_c = 4, \theta_c = 2$. Since I assume an ordered mechanism for the phosphorylations, mutation of site 4 also prevents phosphorylation of site 5, leading to further truncation of the chain, so that now $n_c = 3, \theta_c = 2$. Mutation at site 3, besides preventing phosphorylation at sites 4 and 5, also eliminates MPF feedback on Cdc25, as the protein can no longer change its activity in response to its regulator. This can be expressed by setting $n_c = 2, \theta_c = 2$, which is equivalent to the case described previously where all the sites are mutated and *Cdc25=0*. Therefore in this model, elimination of sites 1, 2 and 3 is equivalent to elimination of all the sites.

The signal-response curves for these mutants can be seen in Figure 4.7A for Cdc25 and Figure 4.7B for Wee1. This shows that mutations on sites 4 and 5 have much smaller effects than mutations on sites 1, 2 and 3. This is expected, since elimination of sites 4 and 5 changes the Cdc25 and Wee1 activity curves with respect to MPF only slightly, making the feedback less sharp. However, this has an unexpected biological significance of showing how mutations on a single, functional phosphorylation site might show very little or no biological effect, even though they are still important for the kinetics of the system. This was also shown, in a general context but with a similar mechanism by Wang et al. (2010).

The effects of introducing individual phosphomimicking mutations can also be analysed in this model. I keep the assumption that phosphomimicking has the same effects as a natural phosphorylation, and therefore the ordered phosphorylations can

still take place if a previous site has a phosphomimicking mutation. Therefore, introducing the modification at site 1 truncates the chain from the non-phosphorylated form, which is equivalent to a model with $n_w = 4$ and $\theta_w = 1$ for Wee1 and similarly for Cdc25. If site 2 is permanently phosphorylated, this truncates the chain further, and the model is described by $n_w = 3$ and $\theta_w = 0$. Permanent phosphorylation at site 3 again causes the activity of the protein to change permanently, so I can write $n_w = 2$ and $\theta_w = -1$, as for the case where all the sites 3, 4 and 5 are mutated. This is because since dephosphorylation is also ordered, I can assume that if site 1 and 2 are not modified but can become phosphorylated, they stay permanently so. By the same logic, I could assume that phosphomimicking of sites 4 and 5 eventually results in permanent phosphorylation of site 3, which causes the protein to permanently switch its activity. The signal-response curves for these mutants (Figure 4.7C for Cdc25 and 4.7D for Wee1) show that in this case, the mutations of both proteins contribute to changing the cyclin threshold for MPF activation and loss of bistability. For both enzymes, phosphomimicking of all sites results in loss of bistability as seen in Figure 4.4B. However, when the first two sites are modified to phosphomimicking residues, the reduction in the cyclin threshold is more significant for Cdc25 than for Wee1.

It is important to mention that these results depend on the assumptions made for this model, in particular the ordered phosphorylation mechanism and the stepwise activity change. If these are changed, the way in which the mutations are modelled needs to be carefully considered. For example, in a disordered mechanism mutations of individual sites would be equivalent, and it would be possible to consider mutations that increase the number of phosphorylation sites. Also, in a mechanism

where the activity changes gradually with the number of phosphorylations, all the mutants will have slightly different curves.

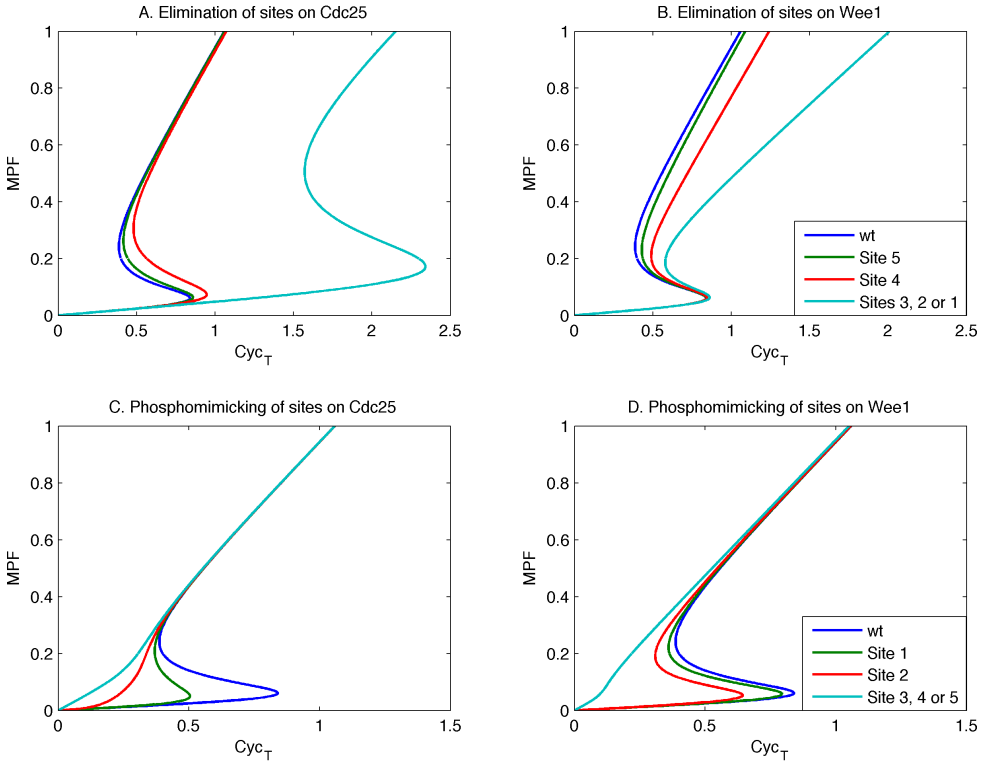

Figure 4.7. *Effects of mutations of single phosphorylation sites on Wee1 and Cdc25, on the signal-response curves of the model of the mitotic switch with multisite phosphorylation*. **A**. Elimination of sites on Cdc25, legend as in B. **B.** Elimination of sites on Wee1. **C.** Phosphomimicking on Cdc25 phosphorylation sites, legend as in D. **D.** Phosphomimicking on Wee1 phosphorylation sites.

4.7. Mutation analysis with different feedback strength on the two loops

As shown in Section 4.5, changes in the Cdc25 positive feedback loop have a pronounced effect on the position of the saddle node bifurcation that determines the cyclin threshold for MPF activation, while changes in the Wee1 double negative feedback loop can have little effect. This suggests that Cdc25 activation can be more important than Wee1 inactivation in setting the value of this threshold. In the model,

this means that the parameters that determine the rate of Cdc25 activation have a more significant influence on the cyclin threshold for MPF activation than the parameters that determine the rate of Wee1 activation. However, these results might depend on particular assumptions. In particular, for simplicity I have assumed that the effect of MPF feedback on its regulators (Wee1 and Cdc25) is 'symmetric'. That is, 50% of Wee1 and Cdc25 are in their active forms at the same MPF level. This implies that the strength of MPF regulation, or feedback, is the same on both of its regulators. This may or may not be a good assumption, although recent data from cultured human cells suggests that Wee1 may be more sensitive to MPF than Cdc25 (Deibler and Kirschner, 2010), but in *Xenopus* egg extracts both regulators appear to be equally sensitive (Trunnell et al., 2011), as in the present model.

To address this issue, I repeated the mutational analysis in a situation where the strength of the two feedback loops is different. I will first consider a situation where Wee1 is more sensitive to MPF, by decreasing the rate constant for Cdc25 activation by MPF, V_{a25} (Figure 4.8A-C). As the feedback on Cdc25 becomes weaker (as V_{a25} decreases), Wee1 regulation has a more significant effect on the cyclin threshold for MPF activation. In particular, elimination of the phosphorylation sites on Wee1 produces an increase in the cyclin threshold for MPF activation (Figures 4.8D and 4.8F, note different scale). In contrast, in the standard model where the strength of the two loops is equal, this modification has little effect on the position of the saddle node bifurcation (Figure 4.8B, the same as Figure 4.4A). As expected, changing the rate of phosphorylation on Cdc25 has no effect on the signal-response curve of the non-phosphorylatable Cdc25 mutant (because by definition this mutant is not affected by MPF activity). However, as expected from the two-parameter bifurcation

diagram in Figure 4.6A, changing V_{a25} also changes the curve of the 'wild type', increasing the cyclin threshold for MPF activation. As V_{a25} decreases, the 'wild type' curve approaches the curve for the non-phosphorylatable Cdc25 mutant, because higher MPF levels are required to activate Cdc25. In this situation, the cyclin threshold for MPF activation depends more and more strongly on Wee1 regulation.

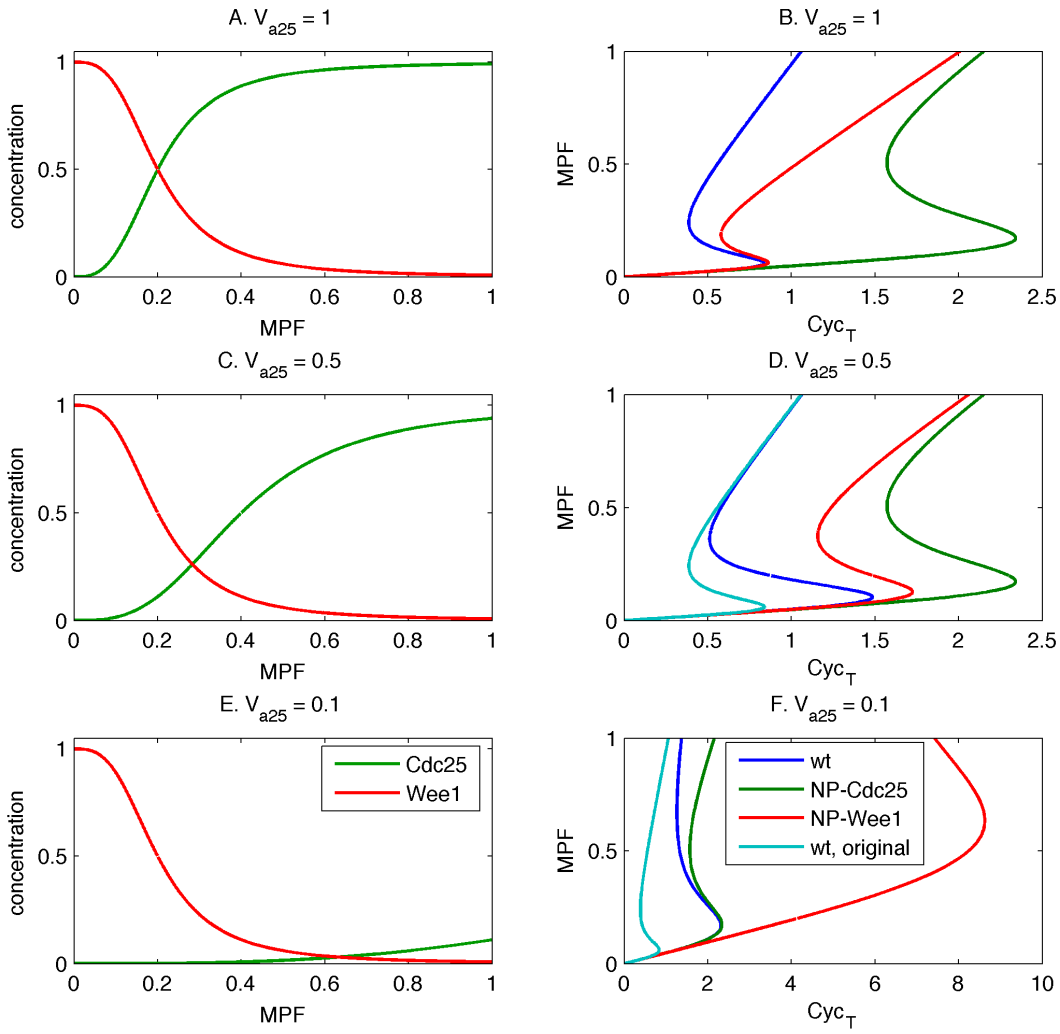

Figure 4.8. *Effect of elimination of all the MPF phosphorylation sites on Cdc25 or Wee1 with stronger feedback on Wee1 than on Cdc25.* The plots on the left (**A, C, E**) show the concentrations of Wee1 and Cdc25 with decreasing values of the rate constant for Cdc25 activation by MPF (V_{a25}) and the plots on the right (**B, D, F**) the corresponding one-parameter bifurcation diagrams for the 'wild type' (WT) with normal phosphorylation sites on both Wee1 and Cdc25 and the non-phosphorylatable mutants NP-Cdc25 and NP-Wee1. In D and F, the fourth curve also shows the original wild type curve, which corresponds to the wild type in B. Therefore A and B are the same as Figure 4.3A and 4.4A respectively. C and D are the same as A and B except that $V_{a25} = 0.5$. E and F are the same as A and B except that $V_{a25} = 0.1$.

A similar analysis can show the effects of the opposite case, where Cdc25 is more sensitive to MPF than Wee1. This is shown in Figure 4.9 by decreasing the rate of Wee1 inactivation by MPF V_{iwee}. As expected from the two-parameter bifurcation diagram, this barely changes the cyclin threshold for MPF activation of the wild type curve, and has no effect on the non-phosphorylatable Wee1 mutant. However, as the feedback on Wee1 becomes weaker, mutation of the MPF-phosphorylation sites on Cdc25 has a more and more dramatic effect on the threshold.

Thus, if the strength of the two feedback loops is similar, or if the Cdc25 positive feedback loop is stronger than the Wee1 double negative feedback loop, Cdc25 activation determines the cyclin threshold for MPF activation. Similar results are obtained with a model assuming a disordered mechanism for multisite phosphorylation of Cdc25 and Wee1 (not shown), and bifurcation analysis also produces similar results with the Novák-Tyson model (not shown). Thus, the importance of Cdc25 regulation for setting the position of the saddle node bifurcation is most likely independent of particular kinetic assumptions, but dependent on the architecture of the system and the relative strength of the two feedback loops.

4.8. An explanation for the different effects of the Wee1 and Cdc25 feedback loops

An explanation for the different effects of the two feedback loops on the cyclin threshold for MPF activation can be found in the rate plots for the system (Figure 4.10), where the absolute values of the rate of MPF activation by Cdc25 and inactivation by Wee1 are plotted as a function of *MPF*.

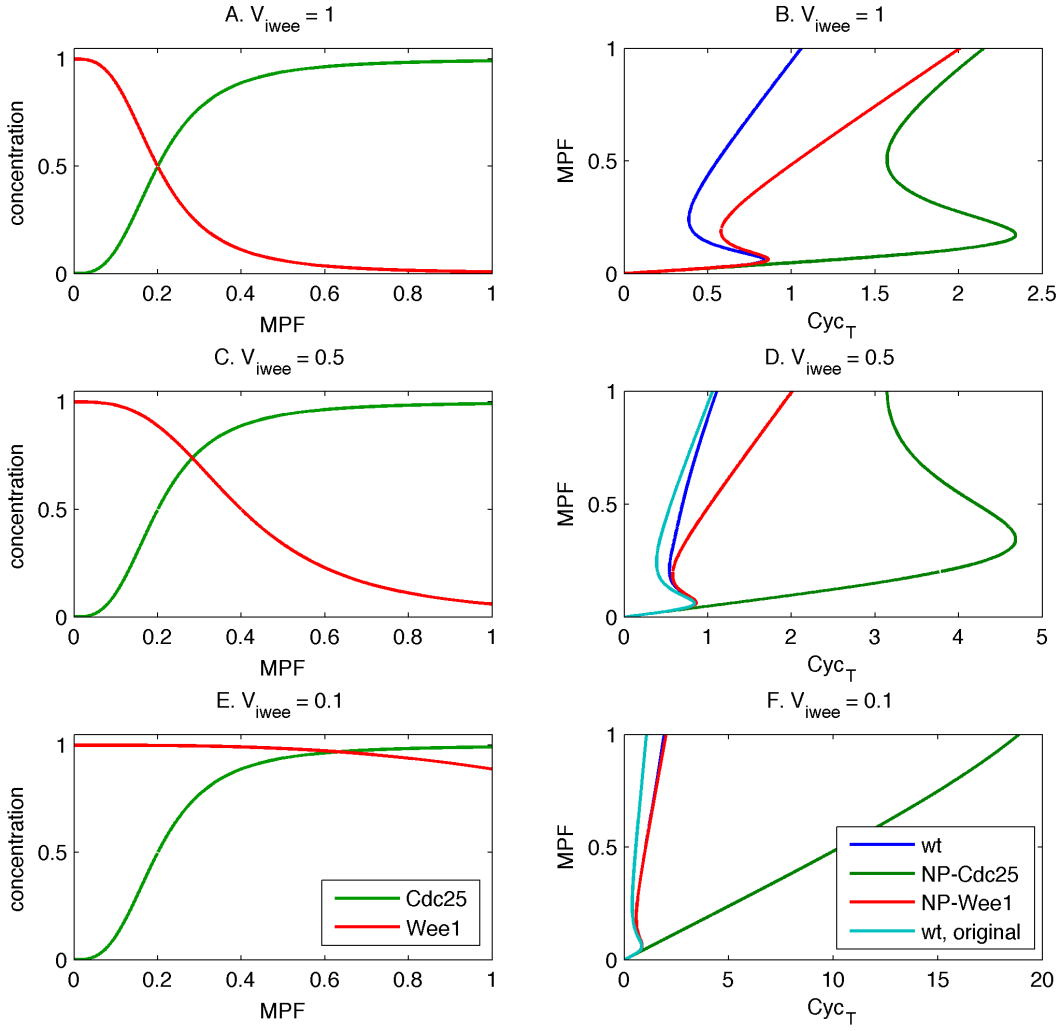

Figure 4.9. *Effect of elimination of all the MPF phosphorylation sites on Cdc25 or Wee1 with stronger feedback on Cdc25 than on Wee1.* The plots on the left (**A, C, E**) show the concentrations of Wee1 and Cdc25 with decreasing values of the rate constant for Wee1 inactivation by MPF (V_{iwee}) and the plots on the right (**B, D, F**) the corresponding one-parameter bifurcation diagrams for the 'wild type' (WT) with normal phosphorylation sites on both Wee1 and Cdc25 and the non-phosphorylatable mutants NP-Cdc25 and NP-Wee1. In D and F, the fourth curve also shows the original wild-type curve, which corresponds to the wild type in B. Therefore A and B are the same as Figure 4.3A and 4.4A respectively. C and D are the same as A and B except that $V_{iwee} = 0.5$. E and F are the same as A and B except that $V_{iwee} = 0.1$.

Each rate curve corresponds to the cumulative activity of Cdc25 or Wee1 (shown in Figure 4.3A) multiplied by the amount of available substrate ($Cyc_T - MPF$ or *preMPF* and *MPF*, respectively). In the absence of feedback in the system, the MPF inactivation and activation curves would be straight lines with positive and negative slopes respectively, as seen in Chapter 3. The feedback loops cause the "kinks" in the MPF activation and inactivation rates. The positive feedback on Cdc25 and the double negative feedback on Wee1 determine the MPF value where the activation curve turns upwards and the inactivation curve turns downwards along the MPF axis, respectively, in Figure 4.3. The stronger the feedback, the lower the MPF value at which this turning occurs (not shown). The rate of MPF activation depends on the total cyclin level (Cyc_T), but the rate of MPF inactivation is independent of this parameter and thus the same for all cyclin levels.

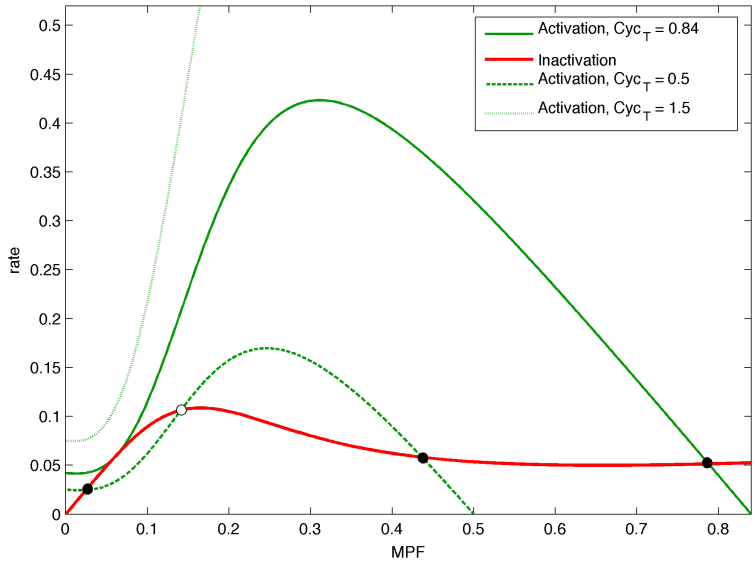

Figure 4.10. *Rate plot for the model of the mitotic switch with multisite phosphorylation.* The rate of MPF activation is plotted at three different Cyc_T levels. The rate of MPF inactivation does not change with cyclin level. Wherever the rate curves intersect with each other, the system is in steady state since the activation and inactivation rates are equal. The steady state is stable (filled circles) if the activation rate is higher than the inactivation rate to the left of the steady state, and it is unstable (open circle) if the opposite is true. Parameters as in Table 4.1 and Cyc_T values are specified for the relevant curves.

In Figure 4.10, the MPF activation rate is shown at three different cyclin levels. The bottom curve and the top curve (dashed green lines with Cyc_T = 0.5 and Cyc_T = 1.5) correspond to Cyc_T values below and above the cyclin threshold for MPF activation, respectively. The activation rate corresponding to the value of the cyclin threshold lies between the previous two curves (solid green line with Cyc_T = 0.84). Wherever the rate curves intersect, there is a steady state for MPF because activation and inactivation balance each other. There are three steady states at the cyclin level below the MPF activation threshold, the two extreme ones, at high and low MPF are stable, while the intermediate one is unstable, as shown previously in the signal-response curves. At the cyclin level equal to the threshold for MPF activation, the unstable and the low-MPF activity stable steady states collide and disappear. At higher cyclin levels only the high MPF steady state is left. Observe that the saddle-node bifurcation happens along the MPF inactivation curve where Wee1 activity is high and not inhibited by MPF yet. As a consequence the double negative feedback, which determines the position where the inactivation curve turns downwards, has little effect on the bifurcation point (i.e. the MPF activation threshold). In contrast the positive feedback, which determines where the activation curve turns upwards, has a major effect of the cyclin level where the bifurcation happens.

4.9. A model of the mitotic switch with multisite phosphorylation and mixed regulation of Wee1 by MPF

For some organisms there are suggestions that initial phosphorylation of Wee1 by MPF actually causes activation, and that only further mitotic MPF-dependent phosphorylation leads to Wee1 inactivation (Harvey et al., 2005; Deibler and

Kirschner, 2010). One line of evidence comes form experiments carried out by Deibler et al. (2010), who prepared human cell extracts blocked in interphase and then added increasing amount of a non-degradable version of CycB, similar to the experiments that established the existence of the cyclin threshold for mitotic entry in *Xenopus* egg extracts (Solomon et al., 1992) explained in Chapter 1. The signal-response curve of MPF activity with respect to cyclin levels obtained from these experiments showed an initial rise in MPF activity, followed by a plateau of more or less constant MPF activity, and then an abrupt increase, which corresponds to the cyclin threshold for MPF activation. Deibler et al. (2010) proposed that this shape could be the result of initial activation of Wee1 by MPF, followed by Wee1 inactivation at higher levels of MPF activity. Here I present a modification of the previous model, which takes into account this mixed regulation of Wee1 by MPF, and shows that this could be a plausible mechanism to explain the shape of the signal-response curve obtained in these experiments. This model also exemplifies the versatility of multisite phosphorylation as a regulatory mechanism.

The model was developed using the multisite phosphorylation kinetics described in Sections 4.3 and 4.4. As before, the total amounts of Wee1 and Cdc25 are assumed to be constant and I maintain the same assumptions for Cdc25, so the concentration of its active form is therefore described by Equation 4.8. However, for Wee1 I now assume that phosphorylation first activates and then inactivates Wee1. Therefore the concentration of active Wee1 is the sum of the forms that have more than the number of phosphorylations required for activation and less than the number of phosphorylations required for inactivation. Thus, to write the algebraic equation for Wee1 in terms of MPF, I assume that the forms with 0 to q_{w1} phosphorylations are

inactive, those with $q_{w1} + 1$ to q_{w2} are active, and those with $q_{w2} + 1$ to n_w phosphorylations are again inactive (see the simplified wiring diagram in Figure 4.11). Hence, the concentration of active Wee1 is

$$Wee1 = \sum_{i=\theta_{w1+1}}^{\theta_{w2}} Wee1P_i = Wee1_T \frac{\left(\frac{V_{iwee}MPF}{V_{awee}PP}\right)^{\theta_{w1}+1} - \left(\frac{V_{iwee}MPF}{V_{awee}PP}\right)^{\theta_{w2}+1}}{1 - \left(\frac{V_{iwee}MPF}{V_{awee}PP}\right)^{n_w+1}} \qquad 4.10$$

where $Wee1_T$ is the total concentration of Wee1, n_w the total number of phosphorylation sites on Wee1, V_{iwee} the rate constant of Wee1 phosphorylation by MPF, V_{awee} the rate constant of Wee1 dephosphorylation by PP. This generates a bell-shaped response of the concentration of Wee1 with respect to MPF activity (4.12A).

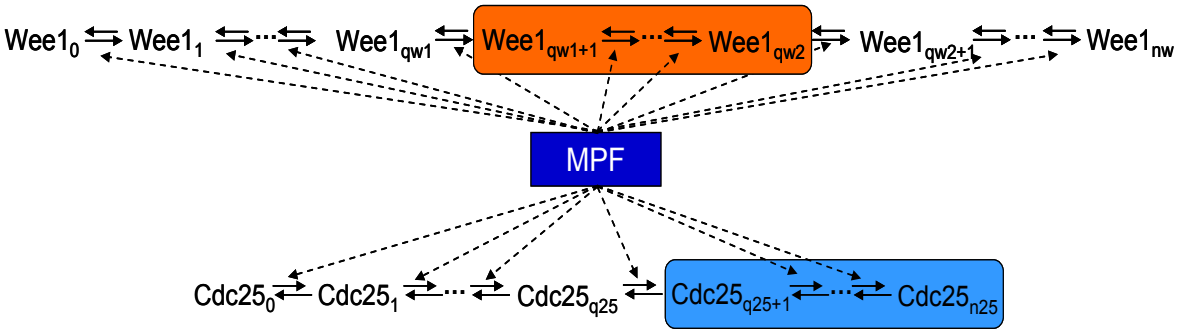

Figure 4.11. *Simplified wiring diagram for the model of the mitotic switch with multisite phosphorylation and mixed regulation of Wee1 by MPF.*

In principle, just replacing Equation 4.9 by the above equation (4.10), results in a model of the mitotic switch, which explains the initial shape of the signal-response curve obtained by Deibler et al. (2010) in human cell extracts, as shown below. However, in their results, as cyclin increases beyond physiological levels, MPF activity plateaus again, which suggests that the Cdk1 subunit in the extracts becomes saturated. In order to take this into account I modified the equations for MPF to

consider a limiting amount of Cdk1 and obtain a better fit to the experimental data. To do this, I assume that Cdk1-CycB dimers (whose concentration I label as MPF_T) are formed by reversible binding of Cdk1 to CycB:

$$\frac{dMPF_T}{dt} = k_a CycB_F Cdk_F - k_d MPF_T \qquad 4.11$$

where $CycB_F$ and Cdk_F are the concentrations of the free (uncomplexed) forms of CycB and Cdk1, and k_a and k_d the association and dissociation constants of the complex, respectively.

Since for each measurement the total amounts of CycB and Cdk1 are constant in the cell-free extracts where the signal-response curve was determined, $Cyc_T = CycB_F + MPF_T$, where Cyc_T, is the amount of added CycB. Likewise, $Cdk_T = Cdk_F + MPF_T$, where Cdk_T, is the constant amount of Cdk1 in the extracts. Therefore, the previous equation (Equation 4.11) can be rewritten as:

$$\frac{dMPF_T}{dt} = k_a(CycB_T - MPF_T)(Cdk_T - MPF_T) - k_d MPF_T \qquad 4.12$$

Assuming equilibrium for the complex formation, the following quadratic equation is obtained:

$$(MPF_T)^2 - (CycB_T + Cdk_T + K_d)MPF + CycB_T Cdk_T = 0 \qquad 4.13$$

where $K_d = k_d/k_a$, is the dissociation constant of the complex. Equation 4.13 is easily solved for MPF_T as a function of $CycB_T$ and Cdk_T.

Then, the differential equation for the concentration of the active form of MPF is

$$\frac{dMPF}{dt} = k_{25}(MPF_T - MPF) - k_{wee}MPF \qquad 4.14$$

where $MPF_T - MPF = pMPF$, which is the concentration of the phosphorylated (inactive) form of MPF. Again, k_{25} and k_{wee} are functions of Cdc25 and Wee1 described by Equations 4.6 and 4.7 respectively.

This model accounts for the results in Figure 7A of Deibler et al. (2010). Again, in this experiment, different amounts of His_6-Cyclin B are added to a somatic-cell extract for which no cyclin synthesis or degradation occurs. After an incubation period, the extract is assayed for H1 kinase activity (corresponding to MPF). Figure 4.12B shows the experimental data and a superimposed one-parameter bifurcation diagram for MPF activity as a function of Cyc_T. This model of mixed-mode regulation of Wee1 by MPF explains the small initial rise in MPF activity with added cyclin followed by a plateau and a cyclin threshold for MPF activation.

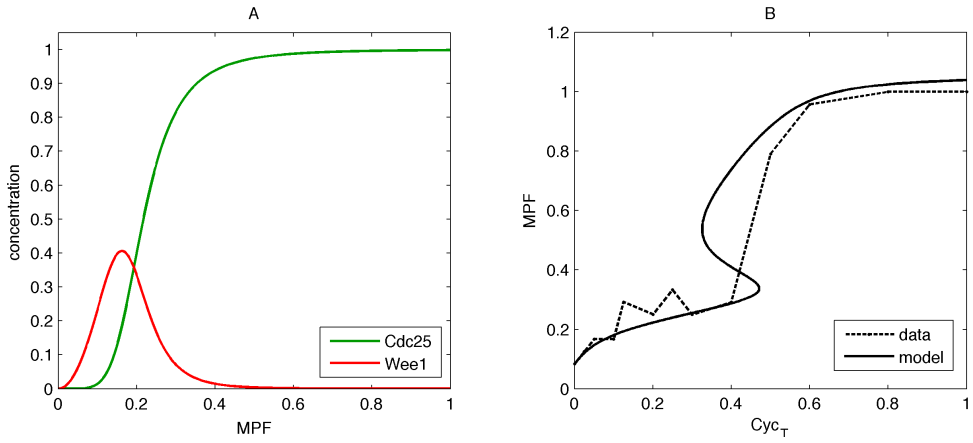

Figure 4.12. *Model of the mitotic switch with multisite phosphorylation and mixed regulation of Wee1 by MPF.* **A.** Wee1 and Cdc25 activities as functions of MPF activity. **B.** Signal-response curve for the model (solid line) fitted to the normalized data (dashed line) from Figure 7A in Deibler et al (2010). To fit the theoretical curve to the experimental data, *'MPF' = 1.8 [MPF] + 0.09* while Cyc_T was scaled to 1. Parameter values: $V_{awee} = V_{i25} = 0.2$, $V_{iwee} = V_{a25} = k''_{wee} = k''_{25} = 1$, $k'_{wee} = 0.01$, $k'_{25} = 0.1$, $k_{as} = 10$, $k_{dis} = 0.1$, $n_{25} = 9$, $n_w = 11$, $q_{25} = 5$, $q_{w1} = 1$, $q_{w2} = 5$, $PP = 1$.

4.10. Discussion

In this chapter, I presented and analysed a model of the mitotic switch where bistability arises as a result of positive feedback and ultrasensitivity due to multisite phosphorylation. I have shown that multisite phosphorylation can potentially generate varied responses, from ultrasensitive to bell-shaped, as has been shown by us and others (Gunawardena, 2005; Kapuy et al., 2009a; Salazar and Höfer, 2007; Wang et al., 2010). I demonstrate that multisite phosphorylation combined with positive feedback can generate bistability, as has also been shown previously (Markevich et al., 2004; Krishnamurthy et al., 2007; Kapuy et al., 2009a). Furthermore, by considering additional sources of nonlinearity, it is even possible to generate multistability by multisite phosphorylation without explicit positive feedback loops (Markevich et al., 2004; Ortega et al., 2006; Thomson and Gunawardena, 2009). This demonstrates that multisite phosphorylation is a mechanism potentially capable of generating extremely flexible responses in biochemical networks, which is perhaps the reason it seems so widespread, as it is estimated that up to 30% of proteins can be phosphorylated, many of them at multiple sites (Cohen, 2000; Mann et al., 2002).

In the models of the mitotic switch presented in this chapter I have considered a particular mechanism for multisite phosphorylation; distributive, ordered phosphorylation and dephosphorylation, with rates described by mass action kinetics and ignoring the concentration of enzymes substrate complexes, as in Kapuy et al. (2009a). This is not necessarily the actual mechanism of phosphorylation for Cdc25 and Wee1, but it is probably the simplest possible mechanism and a good starting point for mathematical modelling. Other possibilities are also plausible, such as

disordered phosphorylation and a gradual change in activity of the target protein as the number of phosphorylations increases (Kapuy et al., 2009a; Salazar and Höfer, 2009). However, there is currently little experimental data supporting a particular mechanism in the mitotic switch system.

In the model of the mitotic switch presented in this chapter, the main role of the multisite phosphorylation mechanism is to substitute the assumption of zero-order ultrasensitivity present in the original Novák-Tyson model with a perhaps more plausible source of ultrasensitivity in this system. Other models of the cell cycle have also exploited multisite phosphorylation as a source of interesting dynamic behaviour (Yang et al., 2004; Barik et al., 2010). In fact, there is recent experimental evidence that multisite phosphorylation is an important source of ultrasensitivity in the response of Cdc25 to MPF (Trunnell et al., 2011). However, the exact phosphorylation mechanism remains to be determined, that is, whether it really occurs in a distributive manner, whether it is ordered or disordered and how phosphorylation changes Cdc25 and Wee1 activities. Furthermore, it is very likely that other sources of ultrasensitivity are involved in this response, possibly including zero-order ultrasensitivity, the presence of multiple positive feedback loops in the system, and competition between different MPF substrates, as proposed for Wee1 (Kim and Ferrell, 2007).

Despite these uncertainties, there are obvious benefits of the mitotic switch model with multisite phosphorylation for analysing the system and making experimentally testable predictions. The analysis carried out by mutating the MPF phosphorylation sites in Cdc25 and Wee1 suggests an asymmetry in the redundant feedback loops controlling the MPF bistable switch. Equivalent modifications in the Cdc25-controlled

positive and the Wee1-regulated double negative feedback loops can have different effects on emergent properties such as the cyclin threshold for MPF activation. In particular the results suggest that elimination of the MPF phosphorylation sites on Cdc25 will have a more pronounced effect on the cyclin threshold for MPF activation than elimination of the phosphorylation sites on Wee1. There is actually some experimental evidence in *Xenopus* egg extracts suggesting this might be the case. The cyclin threshold seems to be substantially affected by non-phosphorylatable Cdc25, but the effect seems very small for non-phosphorylatable Wee1 (Izumi and Maller, 1993; Kim et al., 2005). However, these two studies use different methodologies to assess the cyclin threshold and are therefore difficult to compare.

An actual experiment to test our predictions could be carried out with *Xenopus* egg extracts, where the signal-response curve of MPF versus cyclin levels can be experimentally determined, as explained in Chapter 1, by using interphase extracts in which protein synthesis is blocked, followed by addition of non-degradable cyclin. One approach would be to deplete these extracts of either endogenous Cdc25 or Wee1 and add back similar amounts of non-phosphorylatable versions. Different amounts of non-degradable cyclin can then be added and MPF activity monitored to determine the cyclin threshold for MPF activation. The results presented here indicate that more cyclin would be required if Cdc25 is substituted by the non-phosphorylatable version than when the same is done with Wee1. However, if that is not the case, I expect that the changes in activity of Wee1 and Cdc25 with respect to MPF occur over significantly different MPF levels; specifically that Wee1 is inactivated at lower MPF activity levels than those required for Cdc25 activation. This would in turn allow the possibility that the existence of the two redundant positive

feedback loops in the system could help generate ultrasensitivity and thus bistability in the mitotic switch, as shown in Chapter 3. Therefore, the results presented here show that when positive and double negative feedback work at the same time, they do not necessarily do so in the same way, and independent but equivalent modifications on these feedback loops can have different effects. It is likely that the two types of loop are not necessarily functionally equivalent, and therefore, in a sense they are not actually redundant, but both important in their own right. This may have important implications in biological regulation.

In addition to modelling the result of elimination of the phosphorylation sites on Cdc25 and Wee1, I also showed the effect of phosphomimicking on Cdc25 and Wee1, that is, where Cdc25 is constitutively active and Wee1 has very low activity. Experimentally, this should potentially lead to loss of bistability, because MPF would be constitutively active. In reality, the effect of these mutations would of course depend on their actual consequences on protein activity and regulation. Therefore, this could lead to results similar to those seen by Pomerening et al. (2005) who observed damped oscillations due to reduction of the bistable regime in the system, when they added non-phosphorylatable CDK to cycling *Xenopus* egg extracts. Experimental determination of the signal-response curves under these conditions would also allow a comparison between a graded and a discontinuous response of MPF to total cyclin.

The results of this analysis strengthen the notion that feedback regulation of both Cdc25 and Wee1 is important for the operability of the switch for mitotic entry. The double regulation creates a robust switch, as shown by Ferrell (2008), and can allow the switch to work without ultrasensitivity, as shown in Chapter 3 and in examples by

others (Slepchenko and Terasaki, 2004; Zwolak et al., 2009). Again, this also agrees with the notion that the occurrence of multiple feedback loops is a possible mechanism for achieving bistability, as shown in Chapter 3 and previously suggested (Chang et al., 2010). Also of possible importance is the fact that this type of regulation allows almost complete, switch-like activation of MPF and may reduce futile cycles of simultaneous phosphorylation and dephosphorylation, which could potentially be energetically costly for the cell. Double regulation could also allow the system to switch faster between states, although a rigorous dynamic analysis is required to establish this. Therefore, it is possible that opposite regulation of antagonistic enzymes is widespread in biological systems that behave in a switch-like manner and/or use a considerable amount of energy.

The analysis presented in this chapter illustrates that even though the roles of positive and double negative feedback have been regarded as equivalent, the difference in their architectures can lead to differences in their effects on the system. In particular, in our model, which possesses one loop of each type, both of similar strength, perturbation of the positive feedback loop has a major effect on the position of one of the saddle-node bifurcations of the system, but perturbation of the double negative feedback loop can have almost no effect on this property. I propose that this might be a general feature of systems with this architecture, which could be relatively common in biological networks because, as mentioned above, regulation of opposing enzymes is likely to be widespread in nature. It is also possible that differing architecture of feedback loops has further consequences for other system-level properties.

To complement the analysis of mutation of all the phosphorylation sites on Cdc25 and Wee1, I also showed the effect that mutations of single sites could have in the mitotic switch. There are actually several possibilities of how to model the effect of the mutations, which strongly depends on the assumed mechanism. Regardless of the limitations of this approach, an interesting result from this analysis is the observation that mutations of biologically relevant individual phosphorylation sites may show no significant effects. Wang et al. (2010) also made this observation for a multisite phosphorylation mechanism outside the context of the mitotic switch. These results may help to explain the lack of significant biological effect of such mutations in some cases (Wang et al., 2010).

In addition to the analysis of the mitotic switch model, and taking advantage of the flexibility of multisite phosphorylation, I have shown a modification of the original model, where initial phosphorylation activates, and further phosphorylation inactivates Wee1. Assumption of this mechanism gives rise to a bell-shaped response of Wee1 activity to MPF (Figure 4.12A), and this modified model seems to fit experimental data from human cell extracts (Deibler and Kirschner, 2010) relatively well. However, it is not clear what benefits this type of regulation could bring to this system. Further experimental and theoretical work is required to address this issue, probably focusing on other features of the switch, such as dynamics. Moreover, this type of regulation of Wee1 might be a particular feature of the mitotic switch in specific cells or organisms, and it would be important to discern if there is a reason for differences in the regulation.

Finally, since bistability is likely to be an evolutionarily conserved feature of the mitotic entry switch, it is perhaps not surprising that cells use several mechanisms to

achieve it, since this might provide robustness to this property. The model presented in this chapter includes multiple, redundant feedback loops, reciprocal regulation of antagonistic enzymes and multistep processes, such as multisite phosphorylation, all of which have been experimentally shown in the mitotic switch (Morgan, 2007; Trunnell et al., 2011). In general, if bistability and ultrasensitivity are indeed important properties of biological systems that make decisions or transitions, it is likely that several mechanisms that can theoretically generate it are used together to construct robust switches.

4.11. Summary

In this chapter I presented a model of the mitotic switch with multisite phosphorylation of Cdc25 and Wee1 by MPF. I showed that multisite phosphorylation could create ultrasensitivity required for bistability in the mitotic switch. I also analysed the effects of individual perturbations of the two feedback loops, showing that they can have different effects and making testable predictions. In particular, I showed that equivalent but independent modifications on these feedback loops can have different effects on the system. This analysis suggests that feedback regulation of the Cdc25 phosphatase could have a crucial role in setting the cyclin threshold for MPF activation. In addition, analysis of mutations of individual phosphorylation sites showed that mutation of biologically relevant, individual phosphorylation sites could have very little effect on important properties of a biological system. Finally, I also looked at how multisite phosphorylation can result in more complex responses, which can also help explain biological data, by modifying the model of the mitotic

switch with multisite phosphorylation to incorporate mixed regulation of Wee1 by MPF.

In the next chapter, I will show yet another possible source of ultrasensitivity in the mitotic switch: the cell-cycle-dependent regulation of MPF counteracting phosphatases.

Chapter 5

The mitotic switch with MPF-regulated CDK-counteracting phosphatase activity

5.1. Overview

In the previous chapter I showed that multisite phosphorylation could contribute to ultrasensitivity in the responses of Cdc25 and Wee1 to MPF, and thus generate bistability in the mitotic switch. In this chapter I will show that MPF-dependent inhibition of CDK-counteracting phosphatase activity could also contribute to ultrasensitive responses of MPF regulators and thus to bistability in the mitotic switch. In a more general framework, I will show that coherent feedforward loops in biochemical networks can generate ultrasensitivity. Most of this work has been published (Novák et al., 2010). As in Chapter 3, the analysis presented here contributes to the notion that coherent regulation of opposing enzymes can be an important mechanism for constructing efficient switches in biochemical networks. Finally, I use these ideas to develop a model of the mitotic switch that explains experimental data of the effects that perturbations to CDK-counteracting phosphatase activity have on the mitotic switch. This model was published together with L. Krasinska, D. Fisher and their collaborators, who performed experiments with *Xenopus* egg extracts (Krasinska et al., 2011). I would also like to acknowledge the

assistance and collaboration of Orsolya Kapuy in the work shown in this chapter. Before presenting the mathematical analysis, I will briefly introduce the CDK-counteracting phosphatases and review some previous and current work about their cell cycle roles. Parts of this introductory section and the chapter's discussion have also been published as a review article (Domingo-Sananes et al., 2011).

5.2. CDK-counteracting phosphatases and their regulation

As mentioned in Chapter 1, it is widely accepted that entry into mitosis is driven by the activation of the Cdk1-CycB complex, which phosphorylates dozens of target substrates which carry out the processes associated with mitosis (Nigg, 2001; Morgan, 2007; Ma and Poon, 2011). However, phosphorylations on CDK substrates must be removed after mitosis, so that these proteins can return to their unphosphorylated, interphase state. It is possible that protein turnover is partially responsible for returning CDK substrates to their hypo-phosphorylated state, by degradation of phosphorylated proteins and re-synthesis of unphosphorylated ones. However, for CDK substrates with long half-lives, the most likely explanation is that dephosphorylation carried out by phosphatases is responsible for reverting proteins to their interphase state (Sullivan and Morgan, 2007; Hochegger et al., 2008; Bollen et al., 2009; De Wulf et al., 2009). Furthermore, dephosphorylation of CDK substrates is probably also necessary to prevent their premature phosphorylation during interphase, as explained later on.

In fact, long standing evidence suggests that regulated phosphatases (other than Cdc25) are important in controlling cell cycle transitions. The clearest example so far

is Cdc14 regulation in budding yeast. This phosphatase is kept inactive during mitosis by sequestration in the nucleolus and is released at mitotic exit, its activation indirectly promoted by MPF. Cdc14 can then dephosphorylate several MPF substrates, and promote chromosome segregation, spindle disassembly and cytokinesis. The release of this phosphatase is essential for mitotic exit in budding yeast; elimination of CDK activity alone is not sufficient. However, even though Cdc14 orthologues still have mitotic roles in other organisms, their function does not seem to be crucial, because their elimination is not lethal. For example, the fission yeast Cdc14 homologue, Clp1/Flp1 is important for septation, but not for mitotic exit, although it might be involved in mitotic entry. In *C. elegans*, Cdc14 is required for cytokinesis, but not mitotic exit (Stegmeier and Amon, 2004; Trinkle-Mulcahy and Lamond, 2006; Queralt and Uhlmann, 2008; Clifford et al., 2008).

Other phosphatases have been shown to have important cell cycle functions in other organisms. Experiments with *Xenopus* egg extracts have shown that phosphatases of the PP2A family are active in interphase, because addition of the inhibitor okadaic acid brings about M-phase, suggesting that one or more of these phosphatases reverse the small amount of CDK-dependent phosphorylation that can take place in interphase (Goris et al., 1989; Félix et al., 1990; Lorca et al., 1991; Maton et al., 2005). This is because inhibition of CDK-counteracting phosphatases facilitates phosphorylation of Cdk1-target proteins, which can be then phosphorylated even at low kinase activities. Moreover, inhibition of these phosphatases could also result in MPF activation due to Wee1 inhibition and Cdc25 activation (Clarke et al., 1993; Novák and Tyson, 1993). However, at higher concentrations, okadaic acid also inhibits other phosphatases, such as PP1, which could therefore also be involved in

reversing mitotic phosphorylation (Lorca et al., 1991; Mochida et al., 2009; Wu et al., 2009). Thus, there has been confusion as to the identity of CDK-counteracting phosphatases, and probably for this reason, little was known about their regulation, although there were some early hints that CDK-counteracting phosphatase activity was reduced during mitosis in *Xenopus* egg extracts (Kumagai and Dunphy, 1992; Clarke et al., 1993; Lee et al., 1994). Besides, in principle CDK counter-acting phosphatases would not seem to require regulation, since their activity could be constant throughout the cell cycle, and overcome by the fluctuating Cdk1 activity in mitosis.

Therefore, there has been an often unspoken assumption, in both theoretical and experimental research, that CDK-phosphorylations are reversed by constitutive, unregulated, unspecific phosphatases. Consequently, their analysis was probably considered too complicated and perhaps not that interesting, leading research into mitotic phosphatases to lag considerably behind that on mitotic kinases (Trinkle-Mulcahy and Lamond, 2006; De Wulf et al., 2009; Bollen et al., 2009). There are various reasons for this belief, the most important one probably being that there are significantly fewer phosphatases than kinases in cells. There are about 500 genes coding for kinases in the human genome, compared to about 40 coding for phosphatases. Also, deletion of many of these phosphatases has pleiotropic effects, so that it is difficult to identify those with specific mitotic roles (Trinkle-Mulcahy and Lamond, 2006; Queralt and Uhlmann, 2008; Virshup and Shenolikar, 2009; De Wulf et al., 2009; Bollen et al., 2009).

Nonetheless, it is now becoming clear that phosphatases can actually be highly specific and regulated. This is achieved through specific interaction of catalytic

subunits with targeting subunits and modulators, as well as regulation of subcellular localization (Trinkle-Mulcahy and Lamond, 2006; Queralt and Uhlmann, 2008; Virshup and Shenolikar, 2009; De Wulf et al., 2009; Bollen et al., 2009). Furthermore, recent research has begun to unveil the identity and regulation of CDK-counteracting phosphatases.

An enzyme assay showed that phosphatase activity against a model Cdk1-CycB substrate fluctuated in the cell cycle of *Xenopus* egg extracts, being high in interphase and low in mitosis (Mochida and Hunt, 2007). Further work identified PP2A bound to the B55δ regulatory subunit as the specific and regulated CDK-counteracting phosphatase in these extracts (Mochida et al., 2009). Depletion of PP2A-B55δ from cycling extracts advanced entry into mitosis and compromised exit from mitosis via CycB degradation. The mitotic advancement was caused by premature activation of Cdk1 and phosphorylation of mitotic substrates. Addition of extra, purified phosphatase delayed and blocked Cdk1 activation (by Wee1-dependent phosphorylation of Cdk1) and entry into mitosis in a dosage dependent manner (Mochida et al., 2009). In a similar way to addition of okadaic acid, the simultaneous effects of promoting Cdk1 inhibitory phosphorylation, and dephosphorylation of Cdk1 substrates in interphase suggested that PP2A-B55δ acts on both downstream Cdk1 substrates and in the Cdk1 auto-activation loops (on Wee1 and Cdc25) (See Figure 5.1 where PP can be regarded as PP2A-B55δ). More recent work is also starting to shed light on the regulatory mechanisms of PP2A-B55δ during the cell cycle.

Greatwall, a novel mitotic kinase important for proper timing of G2-M transitions was discovered in *Drosophila* (Yu et al., 2004). Subsequent work with *Xenopus* extracts

revealed that this kinase is required for both establishment and maintenance of M-phase (Yu et al., 2006; Zhao et al., 2008). This kinase was shown to be phosphorylated by Cdk1-CycB and its activity increased in mitosis, suggesting that Greatwall is activated by MPF (Zhao et al., 2008). Addition of the activated form of the kinase promoted M-phase entry in cycling extracts, while depletion prevented mitotic entry and Cdc25 activation. Depletion from CSF extracts (oocyte extracts blocked in metaphase of meiosis II) caused dephosphorylation of mitotic phosphoproteins and loss of M-phase state. Greatwall depletion was accompanied by Wee1-dependent inactivation of Cdk1 without any cyclin degradation, suggesting that Greatwall regulates the Cdk1 auto-amplification loop (Yu et al., 2006; Zhao et al., 2008). The M-phase extract was resistant against Greatwall depletion in the presence of okadaic acid, however, suggesting that Greatwall inhibits an okadaic sensitive (i.e. PP2A-family) phosphatase in M-phase. Furthermore, addition of okadaic acid allowed mitotic entry in Greatwall-depleted cycling extracts, also suggesting that Greatwall had an inhibitory effect on an okadaic sensitive phosphatase (Zhao et al., 2008; Castilho et al., 2009). However, simultaneous depletion of Greatwall and Wee1 from M-phase extracts still led to mitotic exit, even though Cdk1 activity remained high (Vigneron et al., 2009), suggesting that the activated phosphatase overcomes Cdk1-CycB activity on CDK substrates.

These two initially independent lines of research, on Greatwall and PP2A-B55δ, finally converged, by the demonstration that Greatwall down-regulates PP2A-B55δ activity (Castilho et al., 2009; Vigneron et al., 2009). This finding produced a further surprise, the fact that Greatwall inhibition of the phosphatase is not direct, but mediated by the low molecular-weight phosphatase inhibitors, α-Endosulfine and

Arpp19 (I refer to both as ENSA in the following) (Gharbi-Ayachi et al., 2010; Mochida et al., 2010). The level of ENSA is constant during early embryonic cycles in the frog, but it is extensively phosphorylated in mitosis, probably by several kinases. In particular, Greatwall-dependent phosphorylation converts ENSA into a highly specific inhibitor of PP2A-B55δ. As expected from its function as a PP2A inhibitor, addition of thio-phosphorylated (stably-phosphorylated) ENSA promotes mitotic entry in cycling and interphase extracts, similar to addition of okadaic acid and its depletion blocks mitotic entry, like depletion of Greatwall (Gharbi-Ayachi et al., 2010; Mochida et al., 2010).

Other studies have also implicated the B55α and/or B55δ regulatory subunits of PP2A as a CDK-counteracting phosphatase, and Greatwall and ENSA as important in the regulation of mitosis in humans (Schmitz et al., 2010; Manchado et al., 2010; Voets and Wolthuis, 2010; Burgess et al., 2010) and *Drosophila* (Mayer-Jaekel et al., 1994; Yu et al., 2004; Chen et al., 2007; Archambault et al., 2007; Wang et al., 2011; Rangone et al., 2011). This suggests that the identity of the CDK-counteracting phosphatase(s), and the system for regulating its activity could be more or less conserved in many organisms and important for cell cycle regulation.

The Greatwall/ENSA regulatory network would ensure that when Cdk1-CycB activity is low, its counteracting phosphatase is active, keeping mitotic substrates dephosphorylated. In contrast, in the mitotic state Cdk1-CycB down-regulates its counteracting phosphatase by promoting the activities of Greatwall and ENSA, ensuring that while kinase activity is high, the phosphatase is low. These findings have important consequences for the functioning of the mitotic switch, as shown by the mathematical models presented in this chapter.

5.3. Role of phosphatase regulation on the mitotic switch

As seen in previously published models, and those presented in the previous chapters, CDK-counteracting phosphatase activity is absolutely necessary in the mitotic switch, and experimental evidence implies that this activity is also crucial for mitotic exit and for maintaining the hypo-phosphorylated state of CDK substrates during interphase (Novák and Tyson, 1993; Hochegger et al., 2008; Queralt and Uhlmann, 2008). Furthermore, as described in the previous section, recent data indicate that the phosphatase activity that reverses CDK-dependent phosphorylation fluctuates during the cell cycle, being high in interphase and low in mitosis. To understand the consequences of this regulation in the cell cycle control system, and specifically in the mitotic switch, I will first analyse a simple mathematical model. An early version of this model was previously used to explain observations about mitotic exit, but was not analysed in greater detail (Kapuy et al., 2009b). Here I present the analysis of this model from the context of bistability in the mitotic switch (Novák et al., 2010).

The wiring diagram for the model is presented in Figure 5.1. As in Chapters 3 and 4, I consider that MPF is inactivated by Wee1-dependent phosphorylation, and activated by dephosphorylation catalysed by Cdc25. MPF activates Cdc25 and inhibits Wee1, forming a positive and a double negative feedback loop. The difference in the wiring diagram is that now the phosphatase that reverses MPF-dependent phosphorylation of Cdc25 and Wee1, which I still refer to as PP, is now shown explicitly as a molecule. Furthermore, PP can be in an active (*PP*) and inactive (PP_i) form, which together sum up to a constant total concentration, PP_T, similar to all the other molecules in the system. Because the activity of PP is high in interphase and low in mitosis, I assume

that MPF is responsible for its inhibition, as this kinase activity is opposite to PP, high in mitosis and low in interphase. Phosphorylation of PP by MPF must be reversed by a phosphatase, which can be represented by a constant reaction rate. However, since I assume that PP is now a CDK substrate, it should, by definition be dephosphorylated by the CDK-counteracting phosphatase, PP. Consequently, I will allow the possibility that PP can auto-dephosphorylate in an intermolecular reaction and analyse the consequences of this assumption. It is now known, that inhibition of the CDK-counteracting phosphatase PP2A-B55δ does indeed depend on MPF activity, although the regulation is actually indirect, through the MPF-dependent activation of the Greatwall kinase, which in turn activates ENSA (Castilho et al., 2009; Vigneron et al., 2009; Gharbi-Ayachi et al., 2010; Mochida et al., 2010). However, to understand the effects of PP regulation, it is useful to analyse the simplified version of the network presented here (Figure 5.1).

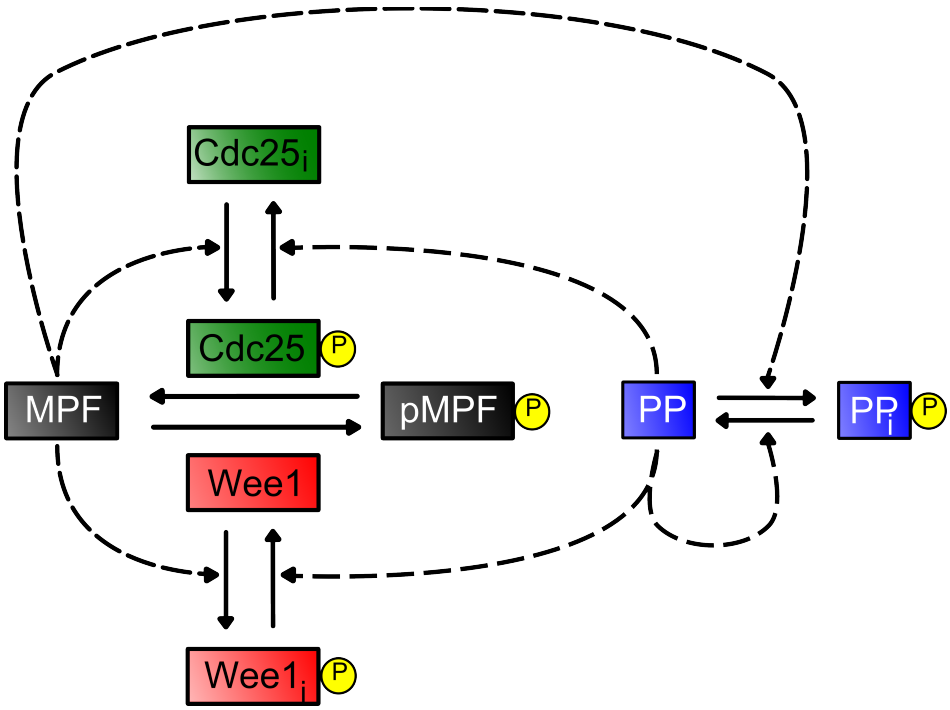

Figure 5.1. *Network diagram for the model of the mitotic switch with MPF-regulated CDK counteracting phosphatase activity*.

The general equations for the model were derived from Figure 5.1 using mass action kinetics. As in the previous two chapters, assumption of mass action kinetics allows analysis of the system without introduction of additional ultrasensitivity in the steady state responses of individual network components. Therefore, the nonlinearity present in the model is the consequence of network architecture. The differential equations for each of the four species can then be written as:

$$\frac{dMPF}{dt} = k_{25}(CycB_T - MPF) - k_{wee}MPF \quad 5.1$$

$$\frac{dPP}{dt} = k_{app}(PP_T - PP) - k_{ipp}PP \quad 5.2$$

$$\frac{dCdc25}{dt} = V_{a25}MPF(Cdc25_T - Cdc25) - V_{i25}\,PP\,Cdc25 \quad 5.3$$

$$\frac{dWee1}{dt} = V_{awee}PP(Wee1_T - Wee1) - V_{iwee}\,MPF\,Wee1 \quad 5.4$$

This system of differential equations is very similar to that for the model of the mitotic switch with positive feedback but no ultrasensitivity for the response of Cdc25 and Wee1, presented in Chapter 3 (Equations 3.2-3.4 and 3.9-3.10). The difference is the extra differential equation for PP, which is no longer constant. As before, the rates of MPF activation and inactivation, k_{25} and k_{wee}, are described by algebraic equations:

$$k_{25} = k'_{25}(Cdc25_T - Cdc25) + k"_{25}Cdc25 \quad 5.5$$

$$k_{wee} = k'_{wee}(Wee1_T - Wee1) + k"_{wee}Wee1 \quad 5.6$$

I also write algebraic equations for the rate functions for PP activation (k_{app}) and inactivation (k_{ipp}):

$$k_{app} = k'_{app} + k''_{app}PP \qquad 5.7$$

$$k_{ipp} = k'_{ipp} + k''_{ipp}MPF \qquad 5.8$$

where k'_{app} and k'_{ipp} are background rates of activation and inactivation, respectively. k''_{app} is the rate at which PP dephosphorylates itself (auto-activation) and k''_{ipp} is the rate at which MPF phosphorylates and inactivates PP.

To look at the effects of phosphatase regulation, I will focus on the activities of MPF and assume steady state for Cdc25 and Wee1. In order to understand the role of regulation of PP in the mitotic switch, I will actually consider and compare three possibilities or models (their interaction diagrams are shown in Figure 5.2):

1. Model with no PP regulation (Model A): This is the same as the model of the mitotic switch with no ultrasensitivity in the response of Cdc25 and Wee1, which was presented in Chapter 3. It is obtained from the above equations by setting $k'_{ipp} = k''_{ipp} = 0$, and therefore $PP = PP_T$ (Figure 5.2A).
2. Model with PP regulated by MPF (Model B): Here PP is inhibited by MPF and activated by another, constant phosphatase activity. This regulation creates coherent feedforward loops in the network, as Wee1 and Cdc25 are now regulated by MPF both directly and through the MPF-regulated phosphatase (see Chapter 2 and the next section, 5.4). In this case, $k''_{ipp} > 0$, $k'_{app} > 0$ and $k''_{app} = 0$ (Figure 5.2B).
3. Model with PP regulated by MPF and PP (Model C): In this case, besides the coherent feedforward loops, another positive feedback loop is created in the network, since PP activates itself. Here, $k''_{app} > 0$. (Figure 5.2C).

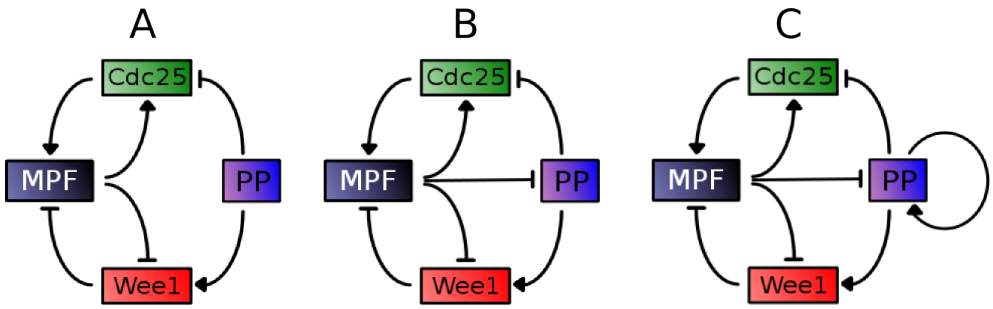

Figure 5.2. *Interaction diagrams of the three models considered for analysis of the role of PP regulation in the mitotic switch*. **A.** Model with no PP regulation (Model A). **B.** Model with PP regulated by MPF (Model B). **C.** Model with PP regulated by MPF and PP (Model C).

Figure 5.3 shows the results of analyses of these models using some of the tools described in Chapter 2. Table 5.1 shows the parameter values for each model, chosen to make the comparison as consistent and meaningful as possible. The first row of panels on Figure 5.3 (A, B and C) shows the phase plane for each model at an intermediate Cyc_T value. The *MPF* nullcline (shown in black) is the same for all the models, because PP has the same effect on Cdc25 and Wee1, and therefore on MPF, in all three cases. This nullcline shows that in general, as PP increases, MPF decreases, because more PP tends to lead to Wee1 activation, Cdc25 inhibition and thus MPF inactivation. The MPF nullcline is nonlinear, due to the Cdc25-MPF-Wee1 positive feedback loops. This nullcline is shown for particular Cyc_T value, equal to the intersection with the *MPF* axis, i.e., the maximum possible *MPF* value, when $PP = 0$. In contrast, the *PP* nullcline (blue) is different in each model. For model A, with no PP regulation, $PP = PP_T$, and the nullcline is a horizontal line. Here the MPF and PP nullclines cross only once, creating a single stable steady state (see also the rate plot for the same model in the second row, panel D). However, if *PP* is inhibited by *MPF* (Model B), the phosphatase activity decreases with increasing *MPF*, and the nullcline is a hyperbola, due to the assumption of mass action kinetics in this inhibition (Figure

5.3B). This qualitative difference in the shape of the PP nullcline allows it to cross the MPF nullcline at three points. Therefore, PP regulation by MPF allows bistability to arise in the system. This is also demonstrated in the rate plots on the second row in Figure 5.3 (Panels D, E and F), from which is also easy to determine the stability of the possible steady states (Chapter 2). Bistability is also confirmed by the signal-response curves or one-parameter bifurcation diagrams of Cyc_T versus MPF shown in the third row (Panels G, H and I).

Bistability arises in Model B because PP regulation by MPF results in a slight ultrasensitive response of Cdc25 and Wee1 to MPF (Figures 5.3K), in contrast to the hyperbolic responses when PP is considered constant (Figure 5.3J). As I will show in the next section, the source of ultrasensitivity is the creation of coherent feedforward loops in the network, where Cdc25 and Wee1 are regulated through two different branches by MPF, directly by phosphorylation and indirectly due to the MPF regulation of PP.

Table 5.1. Parameter values for the three models of the mitotic switch with PP regulation.

Parameter	Model A	Model B	Model C
k'_{25}	0.01	0.01	0.01
k''_{25}	1	1	1
k'_{wee}	0.01	0.01	0.01
k''_{wee}	1	1	1
V_{a25}	1	1	1
V_{i25}	1	1	1
V_{awee}	1	1	1
V_{iwee}	1	1	1
$Cdc25_T$	1	1	1
$Wee1_T$	1	1	1
k'_{app}	0.1	0.1	0.01
k''_{app}	0	0	0.1
k'_{ipp}	0	0	0
k''_{ipp}	0	1	1
PP_T	0.5	1	1

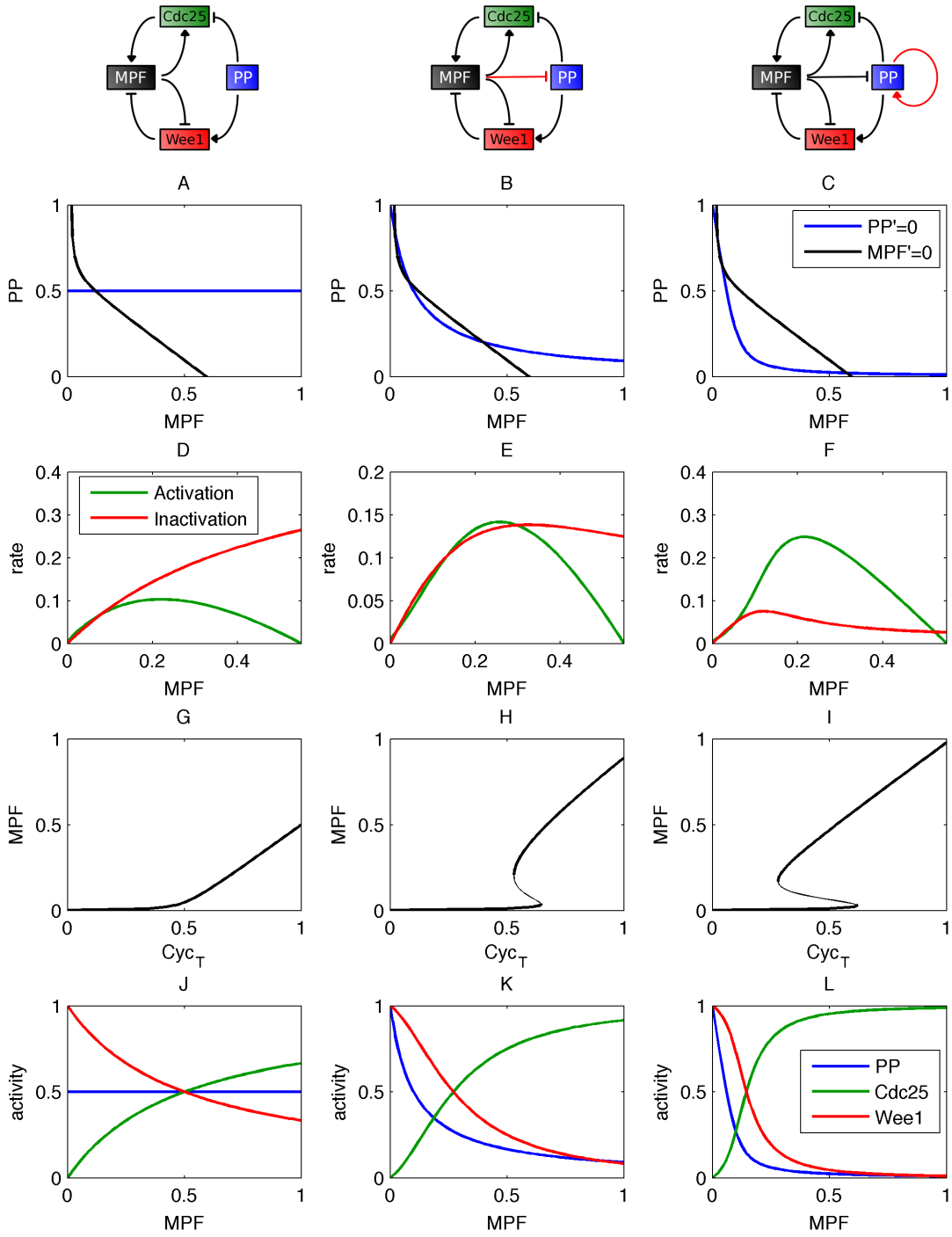

Figure 5.3. *Models of the mitotic switch with different types of PP regulation*. The interaction diagram for each model is shown above its corresponding panels. **A, B, C**. Nullclines. $Cyc_T = 0.6$. **D, E, F**. Rate plots. $Cyc_T = 0.6$. **G, H, I**. One-parameter bifurcation diagram showing the response of MPF to Cyc_T. **J, K, L.** Response of PP, Cdc25 and Wee1 to MPF**. A, D, G, J**. Model with no PP regulation (Mode A). **B, E, H, K**. Model with PP regulated by MPF (Model B). **C, F, I, L**. Model with PP regulated by MPF and PP (Model C). Parameters as in Table 2.1

The third column in Figure 5.3 shows the corresponding plots for Model C, in which PP is regulated by both MPF and PP. Like in Model B, bistability is also possible in this case, and depending on parameter values, the bistable regime can be even wider when PP is auto-activated, as shown by the Cyc_T versus MPF bifurcation diagram (Figure 5.3I). Therefore, the presence of this additional positive feedback loops in the network could make bistability more robust in the system.

It is important to highlight that the effect of the different types of PP regulation depends not only on the connections established in the network, but also on the parameter values assumed in the model. The effect of the crucial parameters relating to PP regulation can be analysed with two-parameter bifurcation diagrams.

Incorporation of PP regulation implies that the rate of MPF-dependent phosphorylation of PP is greater than zero ($k''_{ipp} > 0$). A two-parameter bifurcation diagram for k''_{ipp} (Figure 5.4A) shows that as this parameter increases, there is a critical value at which the system becomes bistable (a Cusp bifurcation). As it increases more, the bistable region becomes wider, and at yet higher values it remains more or less the same (although eventually it is reduced again). Of course, if MPF inhibits PP, it is crucial that the phosphatase can also be activated. In Model B, this activation is assumed to occur at a constant, background rate, k'_{app}. Therefore, when $k''_{ipp} > 0$, then $k'_{app} > 0$ also. The two-parameter bifurcation for k'_{app} (Figure 5.4B) for Model B shows that bistability requires that this parameter is greater than zero. As the value of this parameter increases, at first the region of bistability becomes wider. However, as the activation of PP becomes stronger, the bistable regime is eventually reduced, and bistability is lost when k'_{app} reaches values of a similar magnitude to k''_{ipp}. This is because as the constant phosphatase activation

increases, the inhibitory effect of MPF on PP becomes less and less significant. Therefore, most PP remains active, and the situation is similar to Model A, where PP is not regulated.

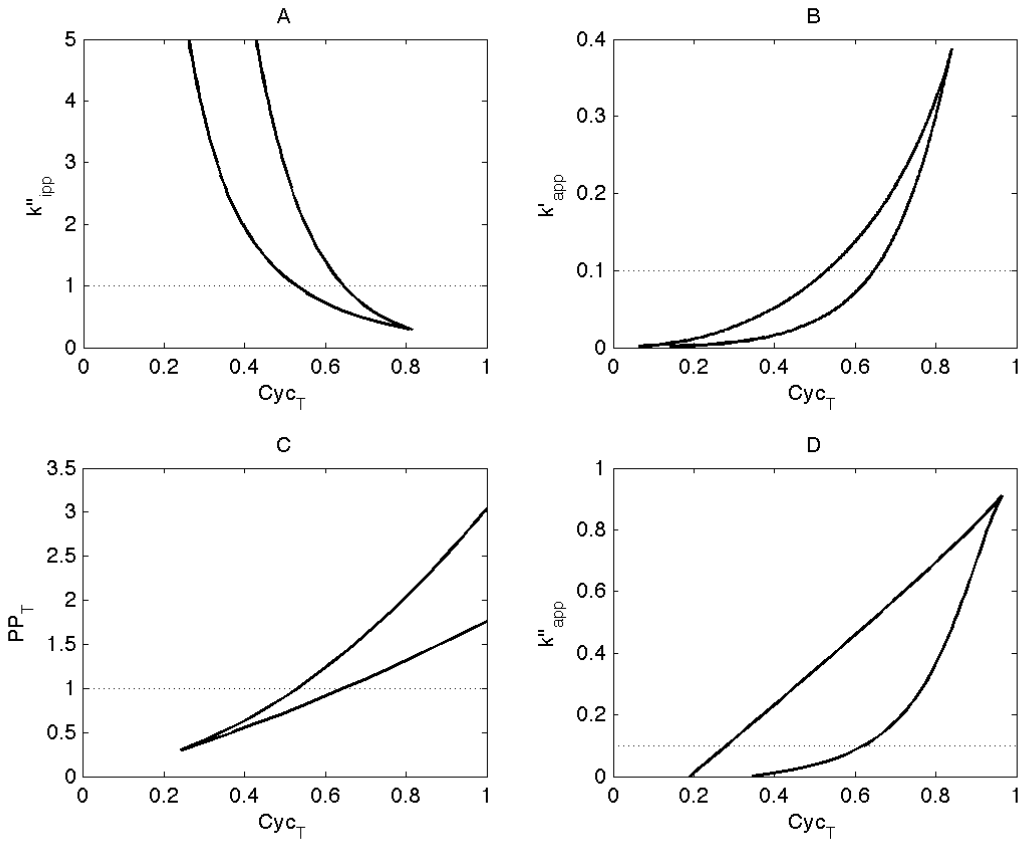

Figure 5.4. *Two-parameter bifurcation diagrams for the models of the mitotic switch with different types of PP regulation*. **A.** k''_{ipp} versus Cyc_T, for Model B. **B.** k'_{app} versus Cyc_T, for Model B. **C.** PP_T versus Cyc_T, for Model B. **D.** k''_{app} versus Cyc_T, for Model C. Other parameters as in Table 5.1 for each model.

Another interesting and biologically relevant parameter in Model B is the total amount of PP, PP_T (Figure 5.4C). Bistability is lost at low levels of PP because MPF cannot be kept inactive, as a small rise in its activity can result in Wee1 inactivation and Cdc25 activation. As PP_T increases, the bistable region becomes wider, and both cyclin thresholds move to the right. In particular, the cyclin threshold for mitotic

entry increases, suggesting that mitosis is delayed or blocked. These results agree with experimental data that indicates that reduction of the MPF-counteracting phosphatase activity leads to premature mitotic entry, while increase in its activity blocks mitosis in *Xenopus* extracts (Mochida et al., 2009). Lastly, I highlight that in order to make analogous figures, PP_T is reduced in Model A, compared to the other two models (Table 5.1). However, bistability is still present in Model B for the equivalent parameter value (Figure5.4A). A more detailed analysis of the effects of perturbations to PP activity in the mitotic switch is presented in Section 5.5.

Finally, Figure 5.4D shows the two-parameter bifurcation diagram for k''_{app}, the parameter that determines the auto-activation of PP (Model C). Bistability is possible when this parameter is equal to zero, as shown by the model without PP auto-activation (Model B). Increasing its value can initially produce an increase in the width of the bistable region, as also shown by the result in Figure 5.3I. However, further increase can lead to a reduction, and eventually loss of the bistable regime. This is because if the positive feedback of PP on its own activity is too strong, the inhibitory effect of MPF again becomes negligible, leading to a constantly active phosphatase, and thus active Wee1 and inactive Cdc25 and MPF. Therefore, it can be expected that if this feedback loop were to exist in the mitotic switch, its strength is probably fine-tuned.

In summary, this section shows that inhibition of the CDK-counteracting phosphatase activity by MPF can potentially lead to important qualitative differences in the mitotic switch, namely the occurrence of bistability. A positive feedback loop created by auto-activation of this phosphatase activity can lead to an increase of the bistable region, although the strength of this feedback is critical. In these simple models, bistability

depends on the coherent feedforward loops created in the network by PP regulation, which leads to ultrasensitive responses in the MPF/PP substrates, as I demonstrate in the next section.

These results indicate that regulation of CDK-counteracting phosphatases could be a mechanism to obtain or improve bistability in the cell cycle control system and help make the transition between interphase and mitosis more switch-like. Additionally, they again highlight the idea that opposite regulation of antagonistic enzymes and multiple feedback loops, might be important mechanisms for creation of nonlinearity and bistability in biochemical networks.

5.4. Ultrasensitivity due to coherent feedforward loops

In the previous section, I showed that PP regulation by MPF resulted in the creation of coherent feedforward loops in the mitotic switch network, which led to ultrasensitivity in the responses of Cdc25 and Wee1 to MPF. In this section, I explore this source of ultrasensitivity further, by analysing the presence of coherent feedforward loops in a general example of reversible protein phosphorylation.

As explained in Chapter 2, a feedforward loop is formed when one component of a network regulates another via two different branches, usually a direct and an indirect one (Alon, 2007b; Tyson and Novák, 2010). Here, I consider the general example of a substrate, S, that is phosphorylated by a kinase K and dephosphorylated by a phosphatase H. A coherent feedforward loop is formed when the kinase inhibits the phosphatase, because K regulates S through two different branches, directly by

phosphorylation, and indirectly by inhibition of the phosphatase that dephosphorylates S_P, the phosphorylated form of the substrate (Figure 5.5).

To show how FFLs can generate ultrasensitivity in biochemical networks, I derive an equation describing the concentration of S_P with respect to K. I start by again assuming mass action kinetics, thus disregarding sources of ultrasensitivity due to enzyme saturation. The interaction diagrams for this system with and without the feedforward loop are shown in Figure 5.5, and the following chemical equation describes the reactions relevant to the substrate:

$$S \underset{k_{dp}H}{\overset{k_pK}{\rightleftharpoons}} S_P$$

where k_p is the rate constant for phosphorylation and k_{dp} the rate constant for dephosphorylation. For simplicity, I assume that the total amount of substrate, S_T is constant, so the following conservation relation is established:

$$S_T = S + S_P \qquad 5.9$$

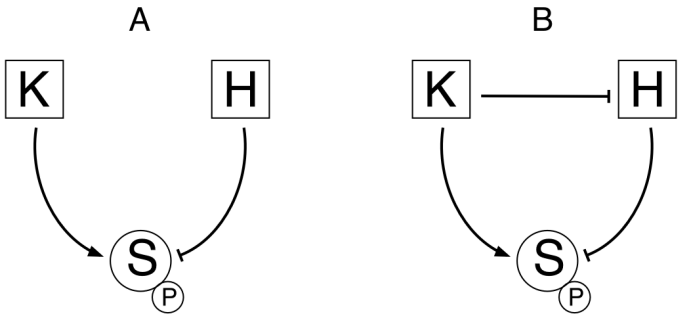

Figure 5.5. *Interaction diagrams for phosphorylation of substrate S by kinase K and dephosphorylation by phosphatase H*. **A.** No feedforward loop. **B.** Coherent feedforward loop: K promotes phosphorylation of S both directly and by inhibition of its counteracting phosphatase.

Without a regulated phosphatase and using mass action kinetics, the concentration of the phosphorylated form of the substrate, S_P can be described by the following ODE:

$$\frac{dS_P}{dt} = k_p K(S_T - S) - k_{dp} H S_P \quad 5.10$$

And therefore, at steady state, the concentration of the phosphorylated substrate is described by:

$$S_P = S_T \frac{k_p K}{k_p K + k_{dp} H} \quad 5.11$$

Next, I include the coherent FFL by allowing the kinase to inhibit the phosphatase. For simplicity, here I assume that the phosphatase is activated by another, constant phosphatase. Therefore, the ODE for the phosphatase H:

$$\frac{dH}{dt} = k_{ah}(H_T - H) - k_{ih} K H \quad 5.12$$

The concentration of active phosphatase can be calculated by assuming it is at steady state:

$$H = H_T \frac{k_{ah}}{k_{ah} + k_{ih} K} = H_T \frac{\alpha}{\alpha + K} \quad 5.13$$

Where $\alpha = k_{ah}/k_{ih}$, the ratio of the rate constants for the activation and inactivation of the phosphatase H, and also the concentration of K at which 50% of H is phosphorylated. This can be substituted in Equation 5.11, to describe the concentration of the phosphorylated substrate in the coherent FFL:

$$S_P = S_T \frac{k_p K}{k_p K + k_{dp} H_T \frac{\alpha}{\alpha + K}} \quad 5.14$$

Which leads to the following expression for the fraction of phosphorylated substrate:

$$\frac{S_P}{S_T} = \frac{\alpha K + K^2}{\alpha\beta + \alpha K + K^2} \quad 5.15$$

where $\beta = k_{dp}H_T/k_p$, which is the concentration of K at which 50% of the substrate is phosphorylated if the phosphatase was fully active (dephosphorylated). Equation 5.15 describes a nonlinear response that depends on two parameters, α and β. In the limit where $\alpha \to 0$ and $\beta \to \infty$, this equation is similar to a Hill function with Hill coefficient $n = 2$ (see Chapter 2). Of course, this situation is not possible in reality, but it can be approximated if $\beta \gg \alpha$, which implies that the phosphorylation of the phosphatase is more efficient than phosphorylation of the substrate (or that the dephosphorylation of the phosphatase is less efficient than dephosphorylation of the substrate). This is shown in Figure 5.6A-C where I plot the shape of the function described by Equation 5.15 for different values of α and β. This response can be compared to the hyperbolic response where the phosphatase is unregulated and $H = H_T$ (Figure 5.6D):

$$\frac{S_P}{S_T} = \frac{K}{\beta + K} \quad 5.16$$

And to the equivalent Hill function (Figure 5.6E):

$$\frac{S_P}{S_T} = \frac{K^2}{\beta^2 + K^2} \quad 5.17$$

For a large value of β (i.e., 10) and smaller values of α (Figure 5.6A and B), the response of the phosphorylated fraction of substrate is clearly sigmoid, and similar to the equivalent Hill function, albeit with a lower value for β. This is because the strong inhibition of the phosphatase at low values of K (given by the low α value) allows the proportion of phosphorylated substrate to be higher in the presence of the coherent

feedforward loop compared to the Hill function (Figure 5.6 D and E). However, for large values of α and/or small values of β, the ultrasensitivity in the response is much less significant, and the curves are similar to the case with no coherent feedforward loop (Figure 5.6D).

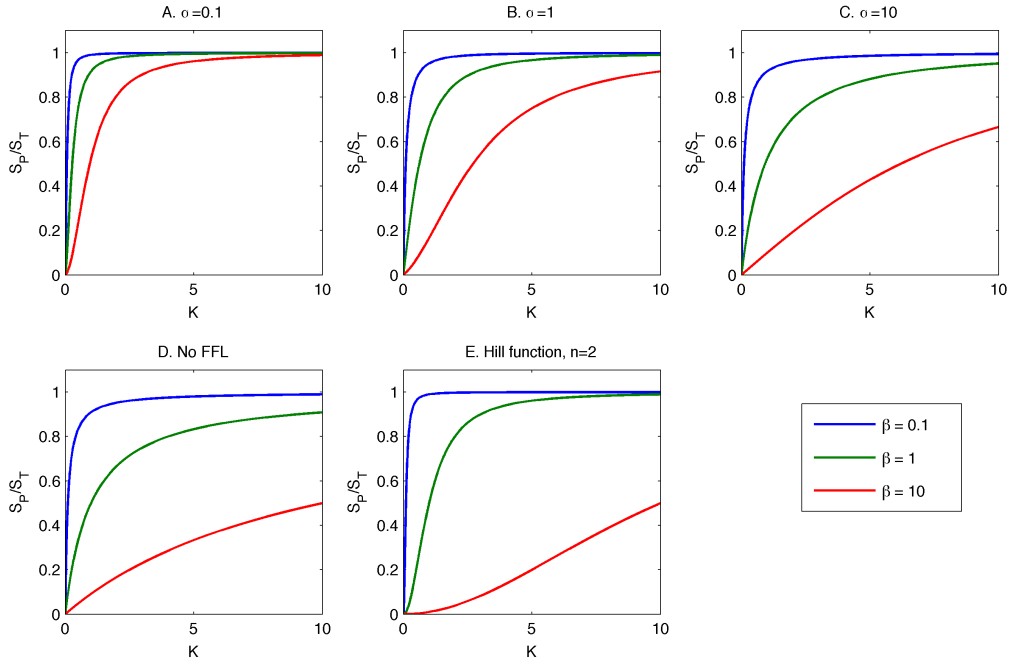

Figure 5.6. *Ultrasensitivity due to coherent feedforward loops.* **A, B, C.** Fraction of phosphorylated substrate with respect to kinase (K) activity for the coherent feedforward loop mechanism (Equation 5.15). **D.** Fraction of phosphorylated substrate with respect to kinase activity with constant phosphatase (Equation 5.16). **E.** Fraction of phosphorylated substrate with respect to kinase activity given by a Hill function with $n = 2$ (Equation 5.17). The values for α are given in the title for the relevant panels, and those for β in the legend ($\alpha = k_{ah}/k_{ih}$, the concentration of K at which 50% of H is phosphorylate; $\beta = k_{dp}H_T/k_p$, the concentration of K at which 50% of the substrate is phosphorylated if the phosphatase was fully active).

Theoretically, the maximum possible Hill coefficient for the response to SP to K with the simple coherent FFL is $n = 2$. Although this is not achievable in practice, in the model of the mitotic switch with regulated CDK-counteracting phosphatase, the slight ultrasensitivity created by the coherent FFL, together with positive feedback are

enough to allow bistability in the system. Higher apparent Hill coefficients can potentially be achieved if as in Section 5.3, the phosphatase can auto-activate. However, this also requires the inclusion of a background rate of activation for the phosphatase.

Finally, it is important to mention that although this derivation was done for the example of a protein phosphorylation system, the conclusions apply for any other reversible modification, such as acetylation and methylation. This is also the case for other mechanisms that can generate ultrasensitivity, like for example, multistep modifications (i.e. multisite phosphorylation) and zero-order ultrasensitivity (Goldbeter and Koshland, 1984, 1987; Gunawardena, 2005; Kapuy et al., 2009a).

5.5. A model of the mitotic switch with regulation of CDK counteracting phosphatase activity by Greatwall explains experimental data from *Xenopus* egg extracts

In the previous section I showed how regulation of the activity of the CDK-counteracting phosphatase could be important in contributing to ultrasensitive responses of MPF regulators and thus to bistability in the mitotic switch. In this section, I will incorporate the Greatwall kinase as another component of the mitotic switch network and use this model to simulate experimental data obtained from *Xenopus* egg extracts. Most of this work has been published together with experimental data obtained by Liliana Krasinska, Daniel Fisher and their collaborators (Krasinska et al., 2011). I also discuss some experimental results from other publications (Yu et al., 2006; Zhao et al., 2008; Mochida et al., 2009).

The new model is based on the one presented in Section 5.3. Again, only mass action kinetics is assumed for all reaction rates. Thus, the differential equation for MPF and its associated algebraic equations are the same as before (Equations 5.1, 5.5 and 5.6), but I modify the ODE for PP to incorporate its inhibition by Greatwall. Here, I assume that Greatwall phosphorylates and inactivates PP directly. It is now know that this regulation is actually indirect, exerted by the Greatwall-dependent activation of the small protein inhibitors ENSA, but for simplicity, this is not taken into account. The consequences of this assumption will be discussed later. I also assume that PP is dephosphorylated and thus inhibited by a constant phosphatase distinct from PP, a Greatwall-counteracting phosphatase that has different substrate affinity than the CDK-counteracting phosphatase. Therefore, the ODE for the Cdk1-counteracting phosphatase, PP can be written as:

$$\frac{dPP}{dt} = k_{app}(PP_T - PP) - k_{ipp}Gwl \cdot PP \qquad 5.18$$

Where k_{app} is the rate constant for dephosphorylation of PP by the hypothetical Greatwall-counteracting phosphatase, and k_{ipp} the rate constant for phosphorylation of PP by Greatwall whose active concentration is *Gwl*. To simulate experimental results, the effect of pharmacological CDK inhibitors (here referred to as RO), and the phosphatase inhibitor okadaic acid (OA) were incorporated in the model. In order to do this, the actual activity of PP and MPF is written as,

$$MPFa = \frac{MPF}{1 + RO} \qquad 5.19$$

$$PPa = \frac{PP}{1 + OA} \qquad 5.20$$

Where RO and OA are the concentrations of the added inhibitors measured as multiples of their IC_{50} for the appropriate enzyme, where the IC_{50} is the concentration of inhibitor that reduces enzyme activity by 50% in the egg extracts. The variables defined by algebraic Equations 5.19 and 5.10 are used when MPF and PP act as enzymes on other proteins, but not when they are substrates, as in the equations for their activation and inactivation (Equations 5.1 and 5.18). Incorporating this modification, the ODEs for Cdc25 and Wee1 are similar to the equations used in Section 5.3.

$$\frac{dCdc25}{dt} = V_{a25}MPFa(Cdc25_T - Cdc25) - V_{i25}PPa(Cdc25) \qquad 5.21$$

$$\frac{dWee1}{dt} = V_{awee}PPa(Wee1_T - Wee1) - V_{iwee}\,MPFa\,(Wee1) \qquad 5.22$$

The ODE for Greatwall is similar to the one for Cdc25 (Equation 5.21), since this kinase is activated by MPF-dependent phosphorylation, and for simplicity, and logical consistency, assumed to be dephosphorylated by the CDK-counteracting phosphatase PP:

$$\frac{dGwl}{dt} = k_{agwl}MPFa(Gwl_T - Gwl) - k_{igwl}PPa(Gwl) \qquad 5.23$$

Equations 5.1, 5.5, 5.6 and 5.18-23 represent the core of the model of the mitotic switch including Greatwall, and the standard parameter set is presented in Table 5.2. Parameter values were chosen to reflect qualitative features of the mitotic switch, and an appropriate time scaling to simulate experimental time courses. The interaction diagram for the model is shown in Figure 5.7A. As in all the previous

models, Cdc25 and MPF form a positive feedback loop and Wee1 and MPF a double negative feedback loop. However, there is an extra double negative feedback loop in this system, between Greatwall and PP.

Table 5.2. Parameter values for the model of the mitotic switch including Greatwall.

Parameter	Description	Value
Cyc_T	Total cyclin	0.1
PP_T	Total PP	1
k_{ipp}	Rate of PP inhibition by Greatwall	2
k_{app}	Rate of PP activation	0.2
Gwl_T	Total Greatwall	1
k_{agwl}	Rate of Greatwall activation by MPF	2
k_{igwl}	Rate of Greatwall inactivation by PP	2
$Cdc25_T$	Total Cdc25	1
k'_{25}	Rate of MPF activation by inactive Cdc25	0.02
$k^{"}_{25}$	Rate of MPF activation by active Cdc25	2
V_{a25}	Rate of Cdc25 activation by MPF	2
V_{i25}	Rate of Cdc25 inactivation by PP	2
$Wee1_T$	Total Wee1	1
k'_{wee}	Rate of MPF inactivation by inactive Wee1	0.02
$k^{"}_{wee}$	Rate of MPF inactivation by active Wee1	2
V_{awee}	Rate of Wee1 activation by PP	2
V_{iwee}	Rate of Wee1 inhibition by MPF	2
S_T	Total generic mitotic substrate	1
k_{ps}	Rate of generic substrate phosphorylation by MPF	2
k_{dps}	Rate of generic substrate dephosphorylation by PP	2
RO	Pharmacological CDK inhibitor	0
OA	Pharmacological PP inhibitor (i.e. okadaic acid)	0

As expected from previous analysis, the coherent feedforward loops in this network help to make the steady state responses of Cdc25, Greatwall and Wee1 to MPF ultrasensitive, while PP activity drops with increasing MPF in a nonlinear way (Figure 5.7B). These responses can lead to bistability in the model as shown by the three intersections of the nullclines in Figure 5.7C. The PP nullcline is the same response as in Figure 5.7B, while the shape of the MPF-nullcline depends on the Cdc25 and Wee1 feedback loops.

Figures 5.7D and E show this bistable response for both MPF and PP activities with respect to the total cyclin level. In this section, I also look at the response of a generic mitotic substrate (S) that is phosphorylated by MPF and dephosphorylated by PP. In the following, the phosphorylated form of this substrate (S_P) is used as a general marker of the mitotic state of the cell (Figure 5.7F). The differential equation for the phosphorylated form of this generic substrate is then:

$$\frac{dS_P}{dt} = k_{ps}MPFa(S_T - S_P) - k_{dps}PPa(S_P) \qquad 5.24$$

As for all the components of the system, the concentration of the phosphorylated substrate shows a bistable response with respect to Cyc_T (Figure 5.7F), with saddle node bifurcations at the same values as the cyclin thresholds for MPF activation and inactivation.

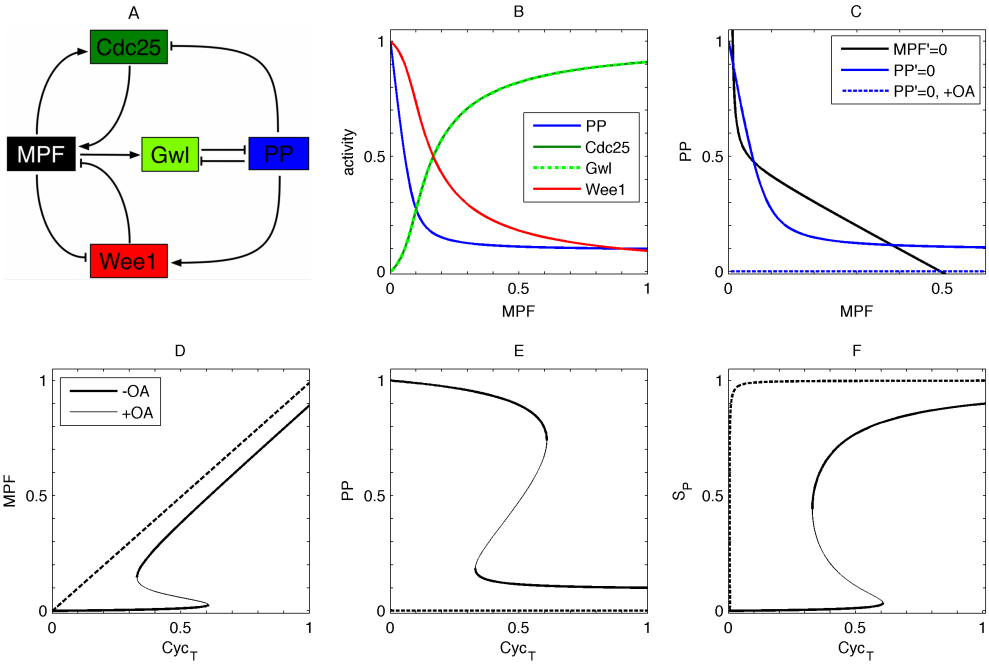

Figure 5.7. *Core of the mathematical model of the mitotic switch including Greatwall.* **A.** Interaction diagram. **B.** Response of PP, Cdc25, Greatwall and Wee1 to MPF activity. **C.** Nullclines showing bistability ($Cyc_T = 0.5$). **D, E, F.** Bistable response of MPF, PP and the concentration of a phosphorylated generic substrate, respectively, with respect to Cyc_T. **C,D,E** and **F** also show how the PP nullcline and responses change upon addition of OA ($99\times IC_{50}$).

Figures 5.7C-E also show the effect of strong PP inhibition on the system, which results in near-loss of bistability. In particular, the cyclin threshold for MPF activation is essentially lost, and virtually all Cyc_T corresponds to active MPF (Figure 5.7D). This is because without a counteracting phosphatase, low MPF activities, even at very low concentrations of total cyclin, will eventually lead to phosphorylation of Cdk1 substrates, and thus Cdc25 activation and Wee1 inhibition. This can be observed in the response of the generic mitotic substrate to Cyc_T (Figure 5.7F), which can be almost fully phosphorylated even at very low Cyc_T values. This result agrees with experimental data which shows that addition of okadaic acid to *Xenopus* extracts blocked in interphase leads to phosphorylation of mitotic substrates and premature mitotic entry at very low concentrations of CycB (Solomon et al., 1990; Krasinska et al., 2011) and is similar to previous analysis of the original Novák-Tyson model (Novák and Tyson, 1993).

In Figure 5.8A I consider further the effects of PP inhibition on the mitotic switch by showing the response of the generic mitotic substrate with respect to Cyc_T for a range of OA values. This shows that at low levels of inhibition, the response is still bistable, although the cyclin threshold for mitotic entry is significantly reduced. As PP inhibition increases, bistability and the cyclin thresholds are reduced further. A two-parameter bifurcation diagram for OA versus Cyc_T confirms these observations (Figure 5.8B). The decrease in the cyclin threshold for mitotic entry has been confirmed by experiments that show that the amount of added cyclin needed to induce mitosis in interphase *Xenopus* egg extracts is reduced upon addition of okadaic acid in concentrations not high enough to induce mitotic entry (Figure 2F from Krasinska et al 2011).

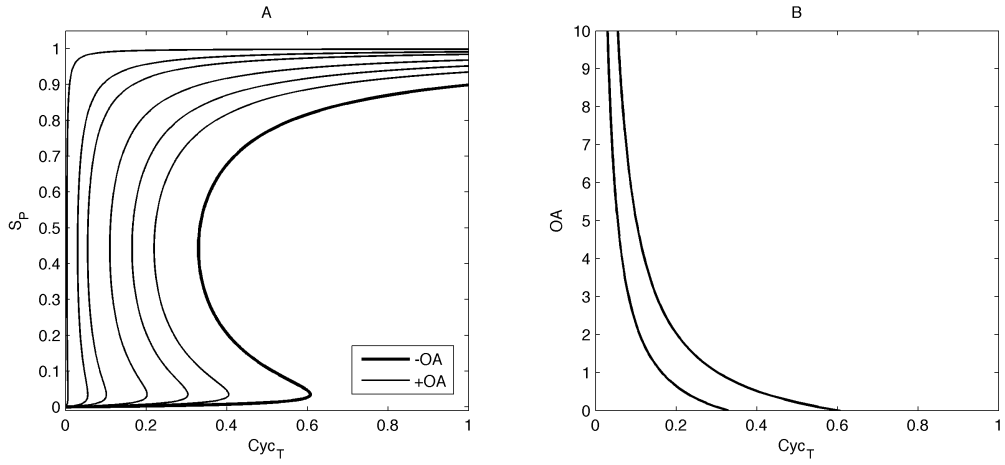

Figure 5.8. *The effect of PP inhibition on the mitotic switch*. **A.** Addition of different amounts of OA. For each curve, from right to left, *OA = 0, 0.5, 1, 2, 5, 10, 99*. **B.** Two-parameter bifurcation diagram showing the effect of okadaic acid on the cyclin thresholds for MPF activation and inactivation.

A final way to analyse the effect of PP inhibition by OA is to simulate the dynamics of the system by numerical integration of the ODEs. Figure 5.9A shows such a simulation for a *Xenopus* extract blocked in interphase by inhibition of protein synthesis (by addition of cycloheximide). I assume that there is a small level of cyclin present in these extracts (Cyc_T =0.1), as has been shown experimentally (Solomon et al., 1990). Since there is no protein synthesis and therefore Cyc_T is constant, in this simulation the system is at steady state, with inactive MPF, Cdc25 and Greatwall and active PP and Wee1. There is also a low amount of phosphorylated CDK (*Y15P*), which corresponds to the concentration of inactive Cdk1-CycB complexes, which is almost the same as the total cyclin concentration.

Upon addition of okadaic acid to an interphase extract (Figure 5.9B), Wee1 is inactivated, while Cdc25 and Greatwall are activated, after a delay, as predicted by the bifurcation analysis (Figure 5.7). MPF is also activated, although its concentration can only rise up to the low cyclin concentration present in the extract. However, as

explained before, in the absence of phosphatase activity, even this small MPF activity is enough to phosphorylate mitotic substrates. After mitotic entry, the system reaches a new steady state where MPF substrates are phosphorylated. The system remains at steady state because I do not take into account APC/C activation and cyclin degradation. The delay between the addition of okadaic acid (at time 0) and mitotic entry is due to the time it takes for the feedback loops to become engaged and allow full activation of MPF and Cdc25 and inactivation of Wee1. A similar delay can be observed for a simulation of the effect of addition of a supra-threshold concentration of CycB (Figure 5.9C), which as expected also causes phosphorylation of MPF substrates and mitotic entry. In this case, once the mitotic steady state is reached, MPF activity is much higher, but there is also a background PP activity that can lead to a slightly lower steady state level of MPF-substrate phosphorylation.

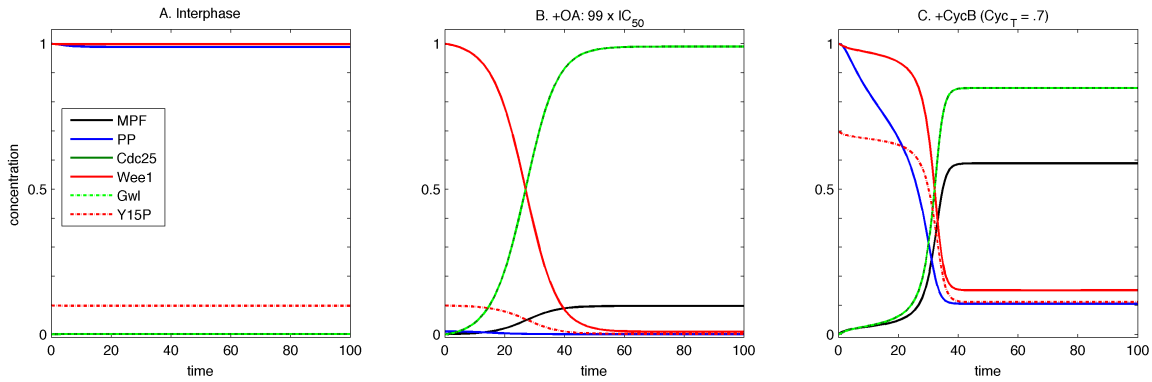

Figure 5.9. *Dynamical simulations of interphase Xenopus extracts.* **A.** Interphase (control) extract. Initial conditions: $MPF = 0, PP = PP_T, Cdc25 = 0, Wee1 = Wee1_T$, $Gwl = 0, Cyc_T = 0.1, OA = 0, RO = 0$. Also pictured is the level of phosphorylated CDK (Y15P), which corresponds to the concentration of inactive (Wee1-phosphorylated) Cdk1-CycB complex, ($Y15P = Cyc_T - MPF$). **B.** Mitotic entry caused by strong PP inhibition. Initial conditions as in A, except $OA = 99$. **C.** Mitotic entry caused by addition of CycB. Initial conditions as in A except $Cyc_T = 0.7$.

To show that CDK-dependent phosphorylation was indeed responsible for the mitotic entry induced by okadaic acid, L. Krasinska and D. Fisher performed experiments in which they tried to block such entry by addition of the CDK inhibitors NU6102 and RO-3306, here referred to as RO (Figure 3D from Krasinska et al 2011). These experiments indicated that relatively high levels of CDK inhibition were required to block entry, while lower levels only showed a delay. Time-course simulations corresponding to these experiments are shown in Figure 5.10. Panel A shows the effect of strong PP inhibition combined with low CDK inhibition. This still results in mitotic entry, but with a slight delay (compare with Figure 5.9B, without CDK inhibition). At higher concentrations of CDK inhibitor, the delay is increased further, because it takes longer for the reduced MPF activity to engage the positive feedback loops that result in its partial activation and phosphorylation of its substrates. This delay eventually appears as a block in mitotic entry within the time frame of the experiment (Figure 5.10B), and as a true block at even higher concentrations of the CDK inhibitor.

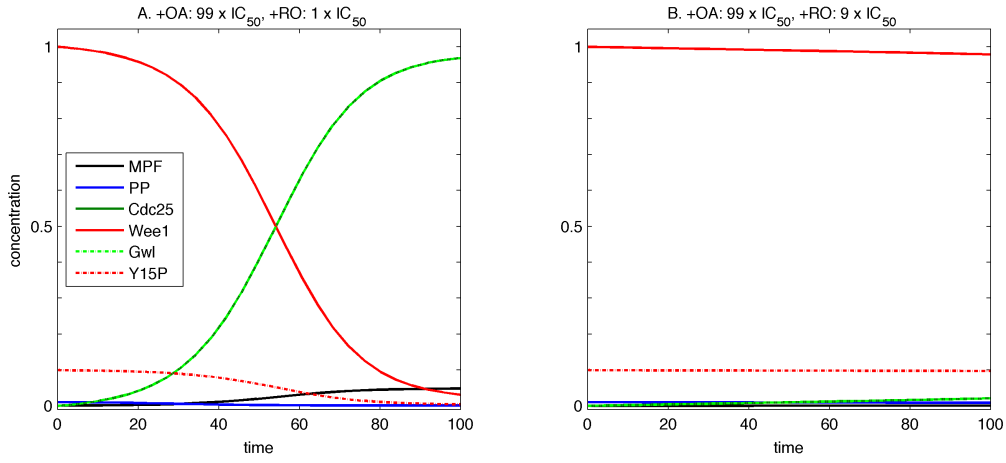

Figure 5.10. *Dynamical simulations of the effect of combined PP and MPF inhibition*. Initial conditions as for Figure 5.9A, except for the concentrations of OA and RO, specified at the top of each panel. **A.** PP inhibition and partial CDK inhibition leading to mitotic entry. **B.** PP inhibition combined with enough CDK inhibition to block mitotic entry in the time frame of the experiment.

Another experiment carried out by L. Krasinska and D. Fisher to confirm the role of CDK in the mitotic entry induced by okadaic acid was to see if such entry could be blocked by preventing MPF activation through Cdc25 depletion from the interphase extracts. Perhaps surprisingly, the results showed that entry was still possible after significant Cdc25 depletion (Figure 4B from Krasinska et al 2011). However, this result is consistent with the mathematical model, as shown in Figure 5.11. Panel A shows the response of the switch components to MPF after depletion of 90% of Cdc25. In the absence of okadaic acid, this depletion results in a very large increase in the cyclin threshold for mitotic entry, observed in the response of the generic mitotic substrate. For this example, the threshold cannot be observed at the expected scale for Cyc_T (Figure 5.11B, -OA). However, upon PP inhibition, the response becomes similar to that obtained for partial levels of PP inhibition (Figure 5.8A). Although there could still be a low cyclin threshold for mitotic entry, this may be lower than the interphase cyclin level (as in this example), which indicates that it would still be possible to induce phosphorylation of MPF substrates and mitotic entry after significant depletion of Cdc25. However, a more significant depletion of Cdc25, like the example in Figure 5.11C and D, can block okadaic acid-induced mitotic entry, when the resulting cyclin threshold is higher than the interphase cyclin level. How much Cdc25 depletion is required to block this type of mitotic entry depends on a combination of factors in the model, including the interphase cyclin level, the extent of PP inhibition and model parameters.

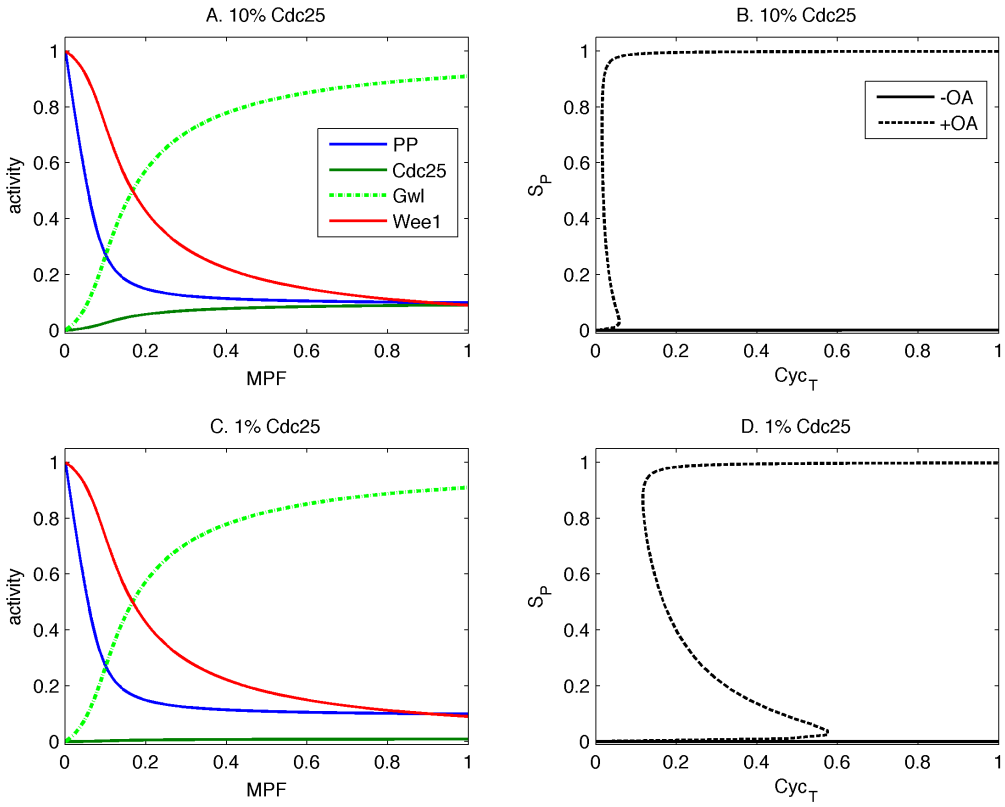

Figure 5.11. *Effect of combined Cdc25 depletion and PP inhibition on the mitotic switch.* **A.** Response of the components of the mitotic switch to MPF with 10% of the normal Cdc25 level. **B.** Response of the concentration of the phosphorylated generic mitotic substrate to Cyc_T with 10% of the normal Cdc25 level with and without okadaic acid. **C.** Like A, but with 1% of the normal Cdc25 level. **D.** Like B with 1% of the normal Cdc25 level.

Finally, I used this model of the mitotic switch to explain the results of experimental perturbations of the PP2A-B55δ and Greatwall levels. Two-parameter bifurcation diagrams can show the potential effects of addition and depletion of these proteins on mitotic entry and exit. In general, the two-parameter bifurcation diagram for PP_T for the model of the mitotic switch including Greatwall (Figure 5.12A) is similar to the PP_T versus Cyc_T two-parameter bifurcation diagram for the simple model with PP regulation (Model B) presented in Section 5.3 (Figure 5.4C). An increase in the total level of PP results in an increase of both cyclin thresholds (for MPF activation and

inactivation), as shown in Figure 5.12A. This would be expected to delay (and eventually block) mitotic entry, because more cyclin is required to flip the switch into mitosis. Indeed, experiments have shown that addition of PP2A-B55δ to cycling extracts in *Xenopus* delays mitotic entry and slows down cell cycles, eventually resulting in an interphase block when high enough concentrations are added (Mochida et al., 2009). An increase in PP during mitosis could destabilise the mitotic state and induce mitotic exit, if the cyclin threshold for mitotic exit becomes larger than the cyclin level in the mitotic state. These observations corroborate the intuitive notion that in general, an increase in the CDK-counteracting activity tends to promote the interphase state.

On the other hand, a decrease in the total level of PP reduces both cyclin thresholds in the mitotic switch (Figure 5.12A), having similar effects to inhibition of PP (Figure 5.8B). This depletion would therefore be expected to advance mitotic entry, because MPF can be activated at lower cyclin levels. This was indeed shown to be the case in cycling extracts from *Xenopus* eggs, where depletion of the PP2A regulatory subunit B55δ resulted in premature mitotic entry (Mochida et al., 2009). According to the model, PP depletion could delay or block mitotic exit, as more cyclin would need to be degraded in order to inactivate MPF. Paradoxically, experiments showing the effect of B55δ depletion on mitotic exit proved to be inconclusive, as exit was blocked when the protein was depleted in interphase, but not when it was depleted in mitosis (Mochida et al., 2009).

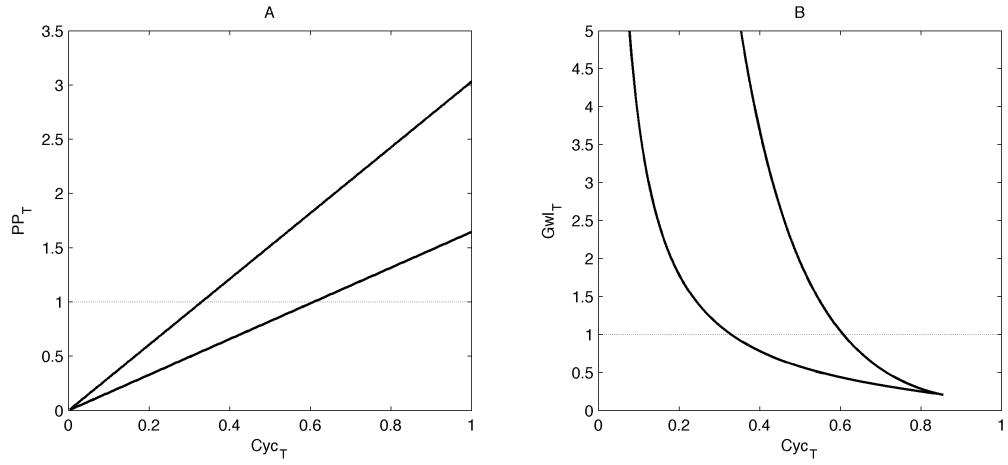

Figure 5.12. *Two-parameter bifurcation diagrams for the total concentrations of (**A**) PP (PP_T) and (**B**) Greatwall (Gwl_T), with respect to Cyc_T for the model of the mitotic switch including Greatwall*. The dashed horizontal line in each panel shows the original parameter value used for the rest of the analysis (Table 5.2).

A two-parameter bifurcation diagram for the total level of Greatwall, the PP inhibitor in this model (Figure 5.12B) shows that the result of addition or depletion of Greatwall is roughly opposite to the same perturbation for PP (Figure 5.12A). This bifurcation diagram is similar to the two-parameter bifurcation diagram for $k_{ipp}^{"}$, the rate of PP inactivation by MPF, in the simple model presented in Section 5.3 (Figure 5.4A). Thus, addition of Greatwall can decrease both cyclin thresholds and promote the mitotic state by perhaps causing an early entry and delayed exit. However, the effect on the thresholds is not as significant as PP depletion, and at very high concentrations of total Greatwall the positions of the saddle node bifurcations are insensitive to this parameter. Therefore it is possible that the effect of Greatwall addition is difficult to observe experimentally. Indeed, addition of unphosphorylated Greatwall to interphase extracts has little effect, although addition of previously activated Greatwall can indeed induce mitotic entry (Zhao et al., 2008). The effect of Greatwall depletion would be expected to be more significant, and lead to a delay in

mitotic entry or interphase block and premature exit form mitosis, due to the increase of both cyclin thresholds and eventual loss of bistability. Both of these effects have been indeed observed in *Xenopus* egg extracts (Yu et al., 2006; Zhao et al., 2008; Castilho et al., 2009; Vigneron et al., 2011).

5.6. Discussion

In the last few years there has been increasing awareness of the importance of phosphatases in processes regulated by protein phosphorylation, like the cell cycle. This is partly due to progress in our understanding of how some of the most important but general phosphatases in eukaryotic cells, like PP2A and PP1, can be regulated through binding of regulatory subunits, which can direct their subcellular localization and restrict possible substrates (Virshup and Shenolikar, 2009). This regulation can confer phosphatases specificity in time, space and substrate binding, and perhaps make the regulation of phosphatase activity as important as regulation in kinase activity in many cellular processes.

Combined with classic and modern biochemistry techniques, this increased knowledge about phosphatases has allowed the identification of specific enzymes and regulatory subunits involved in reversing CDK-dependent phosphorylation, and thus opened the doors to understanding their regulation in a relatively short period of time. Despite some early suggestions that CDK-counteracting phosphatase activity was reduced in mitosis (Kumagai and Dunphy, 1992; Clarke et al., 1993; Lee et al., 1994), little progress was made until recently, when this activity was confirmed to fluctuate in *Xenopus* egg extracts (Mochida and Hunt, 2007), and subsequently

identified as PP2A-B55δ (Mochida et al., 2009). Based on these findings, in this chapter I have shown some possible consequences of the down-regulation of CDK-counteracting phosphatase activity in mitosis, particularly how this can affect the mitotic entry switch, from a dynamical systems perspective.

According to the simple models in Section 5.3, if MPF promotes inhibition of its counteracting phosphatase, its activity has a dual effect on the phosphorylation of mitotic substrates: it directly promotes their phosphorylation and indirectly inhibits their dephosphorylation, creating coherent feedforward loops (Novák et al., 2010). This would also ensure that the kinase-to-phosphatase ratio changes sharply between interphase and mitosis, and minimizes futile cycles of phosphorylation and dephosphorylation of mitotic Cdk1 substrates, and in principle, allow a high steady state level of phosphorylation of these substrates.

Furthermore, these coherent feedforward loops can potentially generate ultrasensitivity in the response of the phosphorylation state of the mitotic substrates to MPF activity. Since Cdc25 and Wee1 are also MPF and PP substrates, this mechanism for generating ultrasensitivity could contribute to bistability in the mitotic switch. However, this is unlikely to be the only source of ultrasensitivity in these responses, and other mechanisms like multisite phosphorylation, substrate competition and saturation effects are important, as has been proposed theoretically (Goldbeter and Koshland, 1981; Gunawardena, 2005; Kapuy et al., 2009a; Domingo-Sananes and Novák, 2010). In fact, experimental evidence suggests that substrate competition and multisite phosphorylation contribute to ultrasensitivity in the responses of Wee1 and Cdc25 to Cdk1-CycB, respectively (Kim and Ferrell, 2007; Trunnell et al., 2011). However, in these experiments the proposed mechanisms have

been unable to reconstitute *in vitro* the sharpness of the response, measured as the apparent Hill coefficient. Therefore, it is possible that ultrasensitivity due to the coherent feedforward loops created by MPF-dependent inhibition of CDK-counteracting phosphatase activity significantly contributes to ultrasensitivity *in vivo*. Furthermore, this regulation might be important for the functioning of the mitotic switch by contributing to bistability, although this contribution still remains to be experimentally assessed.

It is also worth noting that inhibition of PP by MPF constitutes another example of coherent regulation of opposing enzymes, which as discussed previously seems to have an important role in generating switch-like responses (Chapter 3 and Ferrell 2008). In fact, besides feedforward loops, this regulation also creates new feedback loops in the network. In particular, MPF and PP are involved in a deeply antagonistic relationship; not only do they reverse each other's reactions, but they also form double negative feedback loops. That is MPF inhibits PP, but PP also indirectly inhibits MPF by activating Wee1 and inactivating Cdc25. This antagonism can be thought to contribute to bistability, as it helps create two characteristically different states in terms of kinase-to-phosphatase ratio: interphase with high PP and Wee1 activities and low MPF and Cdc25, and mitosis, where Cdc25 and MPF are high and Wee1 and PP have low activities.

The analysis in Section 5.3 therefore shows that down-regulation of PP by MPF during mitosis is likely to be and integral part of the mitotic switch. As in Chapter 3, this also highlights the importance of network architecture in generating particular behaviours. In this case, it again shows how coherent regulation of opposing enzymes can contribute to generating bistable switches.

It is now known that the regulation of PP by MPF is not direct, but requires intermediate components Greatwall and ENSA (Goldberg, 2010; Wurzenberger and Gerlich, 2011). Although this makes the network more complex, the main conclusions obtained by the analysis of the simple model in Section 5.3 are still valid for the model including the Greatwall kinase, presented in Section 5.5. However, this later model is useful to simulate and explain experimental data form *Xenopus* egg extracts.

It has long been known that addition of okadaic acid to *Xenopus* egg extracts leads to mitotic entry and abolishes the cyclin threshold for MPF activation (Goris et al., 1989; Félix et al., 1990; Solomon et al., 1992). These observations can be explained by assuming that okadaic acid inhibits the phosphatase that reverses CDK phosphorylations on Cdc25 and Wee1 (Novák and Tyson, 1993). This is consistent with the identification of this phosphatase as a form of PP2A (Mochida et al., 2009). In this chapter, I also showed that intermediate levels of phosphatase inhibition result in a decrease of the cyclin threshold for MPF activation. L. Krasinska and D. Fisher verified the decrease in the cyclin threshold experimentally, by showing that addition of concentrations of okadaic acid that do not result in mitotic entry, reduce the amount of CycB required to bring the extract into the mitotic state (Krasinska et al., 2011).

I also used this model to simulate the effect of combined inhibition of PP and MPF, and of inhibition of PP combined with Cdc25 depletion (Figures 5.9 and 5.10). These experiments were carried out to try to confirm that okadaic acid had an inhibitory effect on the CDK-counteracting phosphatase, and not on a different phosphatase, and that mitotic entry in these treated extracts depends on Cdk1 activity. In some regards, these experiments were “unsuccessful”, because inhibition of Cdk1 or prevention of

its activation by Cdc25 depletion did not necessarily prevent okadaic acid-induced mitotic entry. However, the analysis of the model shows that the nonlinear character of this system, can make the outcomes of such experiments difficult to predict, and that if phosphatase inhibition is strong enough, even significant CDK inhibition or Cdc25 depletion will not prevent phosphorylation of MPF substrates and mitotic entry. Therefore, there should be caution when interpreting these types of results in highly nonlinear biochemical systems.

I also looked at the effects of perturbing the levels of Greatwall in the model. In particular removal of this protein promotes the interphase state, because PP remains active. Thus, both cyclin thresholds increase, delaying mitotic entry and causing premature exit, and in this respect the model agrees with experimental results (Yu et al., 2006; Zhao et al., 2008). The model in Section 5.5 also predicts that bistability in the system can be lost due to Greatwall depletion. However, in this model bistability depends on ultrasensitivity by the coherent feedforward loops formed by MPF-dependent inhibition of PP. Therefore, when Greatwall is removed, ultrasensitivity in the responses of Wee1 and Cdc25 to MPF is eliminated, and thus bistability is lost. In reality, because there are other sources of ultrasensitivity in the system, it is possible that bistability would still be present upon Greatwall depletion, although the increase in the cyclin thresholds would still be expected. This observation could be used to experimentally assess the contribution of ultrasensitivity by the feedforward loops to bistability in this system. That is, if Greatwall depletion does indeed result in complete loss of bistability, PP regulation is likely to be a significant source of ultrasensitivity that is required for bistability in the mitotic switch.

Another aspect of Greatwall regulation in this model is the presence of a double negative feedback loop between Greatwall and PP. This is formed due to the assumption that PP removes the activating CDK phosphorylations on Greatwall, which is made for logical coherence, but has not been proved experimentally. In the next chapter, I will discuss some evidence that suggests that PP2A-B55δ may indeed dephosphorylate Greatwall. Although the existence of this feedback loop is not a requirement for bistability in the network, it can make the bistable region wider, in a similar fashion to the positive feedback loop in the simple model with auto-regulated PP in Section 5.3. Therefore, it is possible that it could make the mitotic switch more robust.

One possible consequence of the existence of this double negative feedback loop could be the existence of bistability in the response of PP to MPF, independent of MPF regulation by Cdc25 and Wee1. That is if Greatwall and PP are involved in a feedback loop, and the response of one of them is ultrasensitive, a bistable switch independent of tyrosine phosphorylation of CDK could be generated. Since Greatwall activity depends on MPF, the existence of this feedback loop could result in a bistable response of PP to MPF. Such a response could perhaps help to explain hysteresis remaining in the system when the Wee1-dependent regulation of CDK is compromised.

One potential source of nonlinearity that could lead to bistability in the Greatwall-PP double negative feedback loop is ENSA, since such stoichiometric inhibitors can cause ultrasensitive responses (Novák and Tyson, 2008). This component was not incorporated in the model for simplicity, but its inclusion could have important consequences for the mitotic switch, and should be analysed in future work. In any

case, the possible contributions of the Greatwall-PP double negative feedback loop to the mitotic switch and to the dynamics of the system still need to be rigorously assessed.

Finally, it is important to mention that so far there is evidence to support the role of PP2A-B55δ in preventing mitotic phosphorylation during interphase (Mochida et al., 2009; Castilho et al., 2009; Krasinska et al., 2011), but its role during mitotic exit is not clearly defined, since depletion of B55δ during a mitotic block does not seem to prevent exit (Mochida et al., 2009). This could be because a different phosphatase is required to dephosphorylate CDK substrates immediately after mitosis, while PP2A-B55δ is required to maintain the interphase state. In fact, other PP2A regulatory subunits, like B55α and B56, and even PP1 have been implicated in the reversal of mitotic phosphorylations during mitotic exit, in *Xenopus* eggs and in other organisms (Trinkle-Mulcahy and Lamond, 2006; De Wulf et al., 2009; Wurzenberger and Gerlich, 2011). This could create a situation analogous to the activities of the APC/C regulators that target mitotic cyclins for degradation, where in many cells Cdc20 is active during mitotic exit and Cdh1 active in interphase. However, if this were the case, then the mitotic exit that takes place after B55δ is probably reversible. Such a scenario does not necessarily invalidate the picture of the mitotic switch that I have presented here, as the interactions are still valid. However, it may have important consequences for the dynamics of mitotic exit, which still need to be addressed.

5.7. Summary

In this chapter I have analysed how the changing picture of the molecular network controlling mitotic phosphorylations can contribute to the understanding of the mitotic switch. This field has advanced quickly in the last few years, with the Greatwall pathway for phosphatase regulation being discovered during the course of this work (Goldberg, 2010).

I have shown that inhibition of CDK-counteracting phosphatase activity during mitosis may contribute to bistability and functionality of the mitotic switch. In a general framework, I have shown that coherent feedforward loops in biochemical networks can create ultrasensitive responses. This mechanism could be important in generating nonlinearity in many other biological systems.

I also analysed a model of the mitotic switch including Greatwall as the kinase responsible for regulating the activity of the CDK-counteracting phosphatase. Like in the simple models analysed before, bistability and nonlinearity in this model are generated by the network's architecture, in particular by the presence of interlinked feedback and feedforward loops. This model can qualitatively explain data obtained from *Xenopus* egg extracts, including the effects of the phosphatase inhibitor okadaic acid, combination of phosphatase inhibition and CDK inhibition or Cdc25 depletion, and changes in the concentrations of the CDK-counteracting phosphatase and Greatwall.

In the next and final chapter of this thesis, I will discuss some more general implications of the previous chapters. I will also draw on the results from the previous chapters to propose a revised model of the mitotic switch.

Chapter 6.

General discussion

6.1. Overview

In this thesis, I have developed different models of a relatively simple system, the mitotic switch that controls mitotic entry in most eukaryotic cells. The analysis of these models have been mainly concerned with understanding how bistability arises in this system and analysing factors that may affect this property, such as network architecture and sources of ultrasensitivity.

Since I have already discussed specific issues and future prospects relating to individual chapters, in this final discussion I aim to bring together concepts and ideas relevant for all the work presented previously. Based on properties studied so far and experimental evidence I will also propose an updated model of the network controlling the mitotic switch, which is a hypothesis awaiting experimental verification, and a starting point for future theoretical analysis.

6.2. General remarks and conclusions

The importance of decision-making and switches has long been familiar in biological systems. Sigmoid or ultrasensitive responses have long been recognized as

mechanisms through which a small change in a system property or signal could generate a large response (Koshland et al., 1982). A few mechanisms have been proposed to generate sigmoid responses in biochemical reaction networks, such as cooperativity in multi-subunit and allosteric proteins, enzyme saturation, which leads to zero-order ultrasensitivity, and multistep effects in mechanisms like multisite phosphorylation and signalling cascades (Goldbeter and Koshland, 1981; Koshland et al., 1982; Ferrell, 1996; Markevich et al., 2004; Gunawardena, 2005). In this thesis, I have shown that network motifs, such as coherent feedforward loops and positive feedback loops are a potential source of ultrasensitivity (Chapters 3 and 5 and Chang et al. 2010; Novák et al. 2010). This source of ultrasensitivity is related to multistep effects described previously (Koshland et al., 1982), as it relies on the action of one effector at several places in a reaction network. However, it is important to recognise the importance of this source of nonlinearity in biological systems. Even though their individual contributions may be small, the abundance of such motifs in these networks may make these sources significant nonetheless.

Ultrasensitive responses are in turn important for generating bistability (Tyson et al., 2003; Ferrell and Xiong, 2001; Angeli et al., 2004), which seems to be an important property of efficient and irreversible biological switches. As mentioned in Chapter 3, bistability is not exclusive to the mitotic switch, and has been found in other systems across very different organisms (Ninfa and Mayo, 2004; Pomerening, 2008). Bistability is probably more common than it is presently realised and it may have a role in most irreversible transitions in cells, such as developmental and differentiation switches. It probably also has an important role in 'reversible' decisions that show hysteresis, like some responses to environmental and internal

changes. Understanding these systems is therefore important if we ever want to manipulate them for therapeutic or engineering purposes.

In Chapter 4 I explored how multisite phosphorylation can create ultrasensitive responses, following on work by us and others (Gunawardena, 2005; Kapuy et al., 2009a; Wang et al., 2010). However, systems of multistep modifications can potentially be extremely versatile, and can create not only monotonic responses, but also bell-shaped curves and potentially even more complex responses (Chapter 4, Salazar et al. 2007, 2009). Although it remains to be explored whether these complex responses occur in real biochemical systems, mathematical models have proved very useful in the analysis of the potential of these multisite phosphorylation mechanisms. Furthermore, these models can also be used to predict the effects of changes in regulation and mutation of phosphorylation sites as I showed in Chapter 3. This includes the demonstration that mutations of individual, biologically relevant, phosphorylation sites can have little impact on the functioning of the system as a whole (Chapter 4, Wang et al. 2010). These mathematical models may also prove useful in trying to decipher the actual mechanisms for multisite phosphorylation that take place in cells, by understanding particular properties of individual mechanisms, such as the distribution of different phosphoforms and helping to make testable predictions.

In Chapters 3 and 5 I showed that network architecture can be important for bistability, not just due to the presence of positive feedback, but also because it can create ultrasensitivity due to the nonlinear interactions between components. In particular, coherent regulation of opposing enzymes could be an important regulatory motif, as was also proposed by Ferrell (2008). This type of regulation may

have a role in creating efficient and robust switches, and perhaps in some cases preventing unwanted futile cycles (Goldbeter and Koshland, 1987). It may also have important dynamical consequences, such as accelerating responses and transition times, but this remains to be studied.

Coherent regulation of enzymes in a network creates interlinked feedback loops and coherent feedforward loops, which I have shown can be a source of ultrasensitivity and therefore contribute to bistability. Thus, ultrasensitivity dependent on network architecture could on its own be enough to give rise to bistability in the presence of positive feedback loops. Indeed, the possibility of bistability arising from multiple, interlinked positive feedback loops was shown in parallel to this thesis (Chang et al., 2010), while I have shown here the importance of coherent feedforward loops. However, the existence of this source of ultrasensitivity does not rule out important roles of other mechanisms, such as multistep effects due to covalent modifications and signalling cascades, zero-order ultrasensitivity, cooperativity and sequestration effects. In fact, it is likely that different mechanisms contribute to create efficient biological switches.

Because of its remarkable properties, coherent regulation of opposing enzymes is likely to be widespread in biochemical networks. For almost any process that takes place in a cell, there is an opposite and counteracting process; synthesis is reversed by degradation, phosphorylation by dephosphorylation, binding by unbinding, etc. Most of these processes are regulated, and coherent regulation of opposing processes may provide robustness, along with other interesting properties shown in this thesis and by us and others (Goldbeter and Koshland, 1987; Ferrell, 2008; Chang et al., 2010; Novák et al., 2010). Based on these ideas about the importance of coherent

regulation, in the next section I describe potential additions to the mitotic switch network.

6.3. Revised model of the network controlling the mitotic switch

The picture of the molecular network controlling the mitotic switch has changed and grown over the past few years, with the incorporation of the regulation of CDK-counteracting phosphatase activity. As I explained in Chapter 5, in *Xenopus* egg extracts Cdk1-CycB indirectly down-regulates its counteracting phosphatase, PP2A-B55δ, by activating Greatwall and ENSA (Cdk1 → Greatwall → ENSA ⊣ PP2A), while PP2A-B55δ also indirectly inhibits Cdk1-CycB, by activating Wee1 (PP2A → Wee1 ⊣ Cdk1) and inhibiting Cdc25 (PP2A ⊣ Cdc25 → Cdk1) (Figure 6.1). These double negative feedback loops between Cdk1-CycB and PP2A-B55δ, together with the Cdc25-Cdk1 positive and Wee1-Cdk1 double negative feedback loops, help create two characteristically different states: interphase where PP2A-B55δ and Wee1 activities are high and Cdk1, Cdc25, Greatwall and ENSA activities are low and Cdk1 substrates remain dephosphorylated. In contrast, in mitosis, the opposite is true: Cdk1, Cdc25, Greatwall and ENSA activities are high and Wee1 and PP2A-B55δ activities are low, resulting in phosphorylation of Cdk1 substrates. Since it seems that besides B55δ, other PP2A regulatory subunits of the B55 family are involved in reversing Cdk1-dependent phosphorylation (Wurzenberger and Gerlich, 2011), in the following I refer to the Cdk1-counteracting phosphatase as PP2A-B55. The fact that the Cdk1-CycB counteracting phosphatase PP2A-B55 is regulated in a cell cycle-dependent manner can explain recent biochemical data and provides a better description of

mitotic control. Furthermore, the fact that it affects the feedback loops controlling Cdk1 activation makes this phosphatase and its regulation an integral component that shapes the mitotic switch. However, the present model is still not complete.

To fully describe a network with reversible phosphorylation each phosphoprotein must be targeted by at least one kinase and one phosphatase. So far, we know that Wee1 and Cdc25 target Cdk1, while Cdk1-CycB and PP2A-B55 target Wee1 and Cdc25. However, we also know that Cdk1 phosphorylates Greatwall and Greatwall phosphorylates ENSA, but the respective counteracting phosphatases have not yet been identified, although some hypotheses about the nature and regulation of these phosphatases can be proposed.

In the model of the mitotic switch including Greatwall, presented in Chapter 5, I suggested that since Greatwall is a Cdk1 substrate, it might be dephosphorylated, and thus inactivated, by the Cdk1 counteracting phosphatase PP2A-B55 (Figures 5.7A and 6.1). As mentioned there, if this were the case, Greatwall and PP2A-B55 would be involved in a double negative feedback loop, since Greatwall inhibits PP2A-B55 though ENSA (Greatwall⊸ENSA ⊣ PP2A) and PP2A-B55 counteracts Greatwall activation by Cdk1 (PP2A ⊣ Greatwall). This double negative feedback loop could further sharpen the ultrasensitive response of Cdk1 substrates, making the mitotic switch more robust (Chapter 5, Novák et al. 2010)

Although it is not known whether Greatwall is a PP2A-B55 substrate, some evidence suggests that this may indeed be the case. Some clues come from experiments showing that Greatwall becomes phosphorylated at very low Cdk1 activity, suggesting it may have an inhibitory effect on its counteracting phosphatase. For example, PP2A inhibition by addition of microcystin or phosphorylated ENSA to

Cdc25-depleted interphase-arrested (cycloheximide blocked) frog egg extracts causes mitotic-like Greatwall phosphorylation (Gharbi-Ayachi et al., 2010). Under these conditions, CycB levels are low and the few Cdk1-CycB dimers are inhibited by Wee1-dependent phosphorylation. Therefore if another phosphatase, not inhibited by microcystin or ENSA were responsible for Greatwall inhibition, Greatwall should remain dephosphorylated after PP2A-B55 inhibition. A related observation is that activated (phosphorylated) Greatwall induces mitosis in interphase extracts in the presence of the CDK inhibitor roscovitine (Castilho et al., 2009). As in the previous argument, this suggests that active Greatwall inhibits its own phosphatase, that is, the one that normally keeps Greatwall dephosphorylated in interphase, because otherwise active Greatwall would be quickly dephosphorylated and inactivated when placed into an extract where its activating kinase, Cdk1, is inhibited. This again points to PP2A-B55, because it is known that Greatwall inhibits it through ENSA. Another possibility would be that Greatwall inhibits yet another phosphatase that dephosphorylates Greatwall. However, another key observation that suggests that PP2A dephosphorylates Greatwall is the physical interaction of the two proteins (Vigneron et al., 2011). Since Greatwall indirectly regulates PP2A- B55 through ENSA, and there are no obvious Greatwall-phosphorylation sites on PP2A, the interaction could indicate that PP2A binds to phosphorylated-Greatwall in order to dephosphorylate it.

The other unknown phosphatase in the mitotic control switch is the Greatwall counteracting phosphatase that dephosphorylates ENSA. Reversible phosphorylation/dephosphorylation of ENSA is well established, since ENSA is phosphorylated during M-phase in *Xenopus* extracts but not in interphase, while its

amount remains constant throughout the cell cycle and the phosphorylated form does not seem to be specifically targeted for degradation (Mochida et al., 2010). Furthermore, thio-phosphorylated (stably phosphorylated) but not phosphorylated ENSA can stabilize M-phase of CSF extracts or induce M-phase in interphase extracts in the absence of Greatwall (Gharbi-Ayachi et al., 2010). This indicates that ENSA is rapidly dephosphorylated by an unknown phosphatase in the absence of its kinase Greatwall.

The activity of the Greatwall counteracting phosphatase acting on ENSA is crucial for the cell cycle control system, and we can anticipate that perturbations to this activity could have very similar effects to perturbations to the Cdk1-counteracting phosphatase. For example, inhibition of this phosphatase in interphase could lead to mitotic entry, similar to addition of okadaic acid or removal of PP2A-B55 in interphase, because a small amount of Greatwall activity could activate ENSA. By the same logic, enhanced ENSA dephosphorylation in interphase could delay mitotic entry. On the other hand increased activity of the ENSA phosphatase in mitosis could result in premature mitotic exit, due to activation of PP2A-B55 and consequent inhibition of Cdk1-CycB, while its depletion in M-phase could delay or block mitotic exit because PP2A-B55 activation gets compromised. Although cell cycle regulation of the phosphatase that inactivates ENSA is not a necessary requirement by the control system, this is a possibility that must be considered. Using the ideas about coherent regulation developed in the previous chapters, I can propose that it is likely that the activity of the Greatwall-counteracting phosphatase is inhibited during mitosis, similar to that of the CDK-counteracting phosphatase. Furthermore, this inhibition is likely to be exerted, directly or indirectly, by Cdk1-CycB.

The remaining question is the identity of this phosphatase that acts on ENSA, the Greatwall-counteracting phosphatase. Greatwall belongs to a different family of protein kinases from the CDKs, known as the AGC serine/threonine kinase family (Yu et al., 2004). Since Greatwall phosphorylates completely different sites than Cdk1-CycB, it is unlikely that the same phosphatase dephosphorylates sites targeted by these kinases, arguing against PP2A-B55 as a candidate. The characteristics of the ENSA phosphatase mentioned above, suggest that PP1 could be responsible for ENSA dephosphorylation. This would explain data that indicates that PP1 activity is required for dephosphorylation of mitotic proteins at mitotic exit (Walker et al., 1992; Wu et al., 2009).

If PP1 were indeed responsible for ENSA dephosphorylation then even more feedforward and feedback loops are created in the network, especially because PP1 is inhibited by Cdk1 (Dohadwala et al., 1994; Wu et al., 2009). In this case, Cdk1 down-regulates PP2A-B55 via two redundant arms; activation of Greatwall increases ENSA phosphorylation while inhibition of PP1 reduces ENSA dephosphorylation, which results an efficient ENSA phosphorylation and thus PP2A-B55 inhibition via a feedforward loop at mitotic entry. Furthermore, if Cdk1 phosphorylates PP1, then the obvious assumption is that PP2A-B55 acts as the Cdk1-counteracting phosphatase, which removes these inhibitory phosphates from PP1. This would create a positive feedback loop between PP2A-B55 and PP1, because PP2A activates PP1, while PP1 inhibits ENSA, thus activating PP2A (PP2A → PP1 ⊣ ENSA ⊣ PP2A) (Figure 6.1).

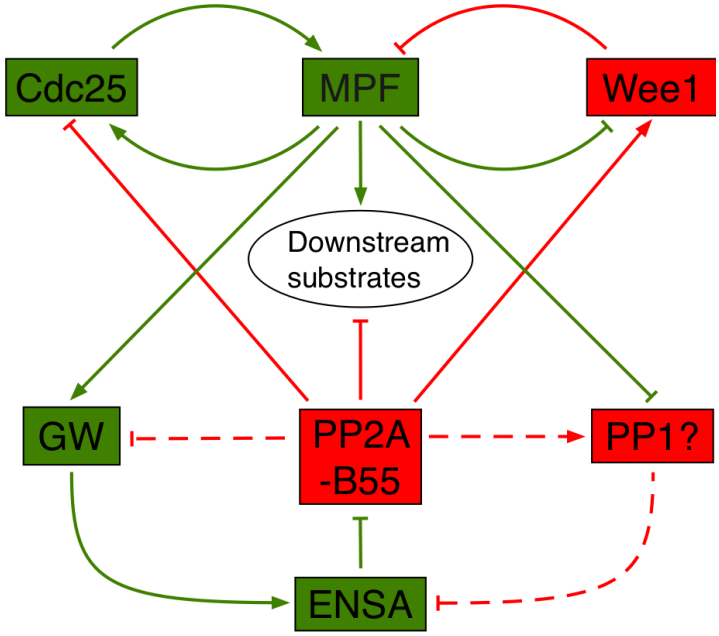

Figure 6.1. *Interaction diagram for the proposed model of the network controlling the mitotic switch*. In this model, all the molecules are phosphorylated by a regulated kinase and dephosphorylated by a regulated phosphatase. Hypothetical links in the network are shown in dashed lines.

All the players of the mitotic control switch described above, along with proven and suggested links between them are shown schematically in Figure 6.1. The proposed network has a striking symmetry in the interaction pattern of the mitotic regulators. All of the components are coherently regulated and every kinase is counteracted by a phosphatase. The mitotic regulators can be divided into two major groups, which have an antagonistic relationship with each other (Figure 6.2A). One group contains Cdk1, Cdc25, Greatwall and ENSA, which directly or indirectly increase the phosphorylation of downstream Cdk1 target proteins and thus promote M-phase. Therefore, I refer to this group as the Mitosis Promoting Factors, MPFs, to reflect the fact that not only Cdk1-CycB can promote the mitotic state. The members of the other group, Wee1, PP2A-B55 and PP1 have an opposite effect; they directly or indirectly decrease the mitotic phosphorylations by Cdk1 and thus promote interphase.

Therefore, I refer to this group as the Interphase Promoting Factors, IPFs. The central nodes in the two groups are Cdk1 and PP2A-B55, which directly influence the phosphorylation state of the downstream Cdk1-CycB/PP2A-B55 target protein that actually carry out mitosis. Besides having a negative effect on the other group, each member of a group promotes the activity of the other proteins in its own team via positive feedback loops (Figure 6.2A). This positive feedback is often direct, as is the case of Cdk1 and Cdc25 (Cdk1 → Cdc25 → Cdk1). However it can also be exerted though a long positive feedback that might contain an even number of inhibitory steps, like in the case of Cdk1 and Greatwall: Cdk1 → Greatwall → ENSA ⊣ PP2A ⊣ Cdc25 → Cdk1. Similarly, for the IPF members a relatively short positive feedback loop could connect PP2A-B55 and PP1, as described above (PP2A → PP1 ⊣ ENSA ⊣ PP2A) while there is a long positive feedback loop between PP2A-B55 and Wee1 (PP2A → Wee1 ⊣ Cdk1 → Greatwall → ENSA ⊣ PP2A).

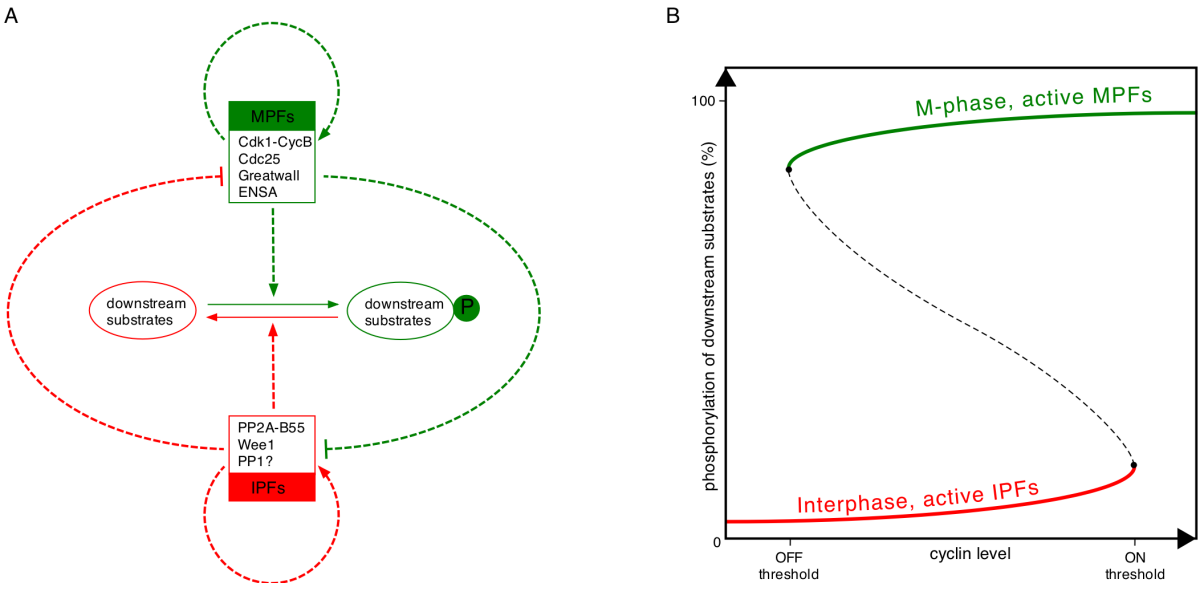

Figure 6.2. A. Scheme showing general relationships between MPFs and IPFs. Dashed lines indicate general relationships, not particular reactions. **B.** Schematic diagram of the mitotic switch showing the phosphorylation of mitotic substrates with respect to the cyclin level.

In this picture, self-activation and mutual inhibition between MPFs and IPFs could create robust bistability in the system, leading to the two characteristically different stable states, mitosis and interphase, which can be observed in the phosphorylation state of downstream Cdk1-CycB/PP2A-B55 substrates, as is shown schematically in Figure 6.2B. When IPFs are active and MPFs are inactive, the kinase-to-phosphatase ratio (Cdk1-CycB/PP2A-B55) is low and the downstream substrates remain in a dephosphorylated state, characteristic of interphase. The other possible state occurs when MPFs are high and IPFs are low, leading to a high kinase-to-phosphatase ratio and phosphorylation of mitotic phosphoproteins, the hallmarks of mitosis. Under normal circumstances, an intermediate situation where IPFs and MPFs are both partially active and most substrates only partially phosphorylated, is unstable and almost impossible to maintain. This is because as soon as one of the sides gains an upper hand, its self-activation, and inhibition of the competing side always takes the system to one of the two stable states.

Which state is actually occupied by the mitotic control system is determined by an upstream regulator of Cdk1 activity, the CycB level. Normally, at low CycB levels IPFs win over MPFs and interphase is manifested. Increasing CycB strengthens MPFs and when the cyclin threshold for activation of MPFs and inactivation of IPFs is crossed (the ON threshold), the downstream substrates are phosphorylated. Since the MPFs help each other besides down-regulating the IPFs, the M-phase state is self-stabilized. As a consequence of this self-stabilization hysteresis is present in the system, and if CycB levels decrease once the control system is in M-phase, MPFs stay active and the downstream targets remain phosphorylated. Dephosphorylation of the downstream targets requires that CycB levels drop below the cyclin threshold for inactivation of

MPFs and activation of IPFs (the OFF threshold). At this stage, Cdk1 eventually loses its power struggle to keep the MPFs active and the IPFs win.

The horizontal movement of the mitotic control system along the diagram on Figure 6.2B depends on the relative rate of CycB synthesis and degradation. If rate of synthesis exceeds the rate of degradation, the system moves to the right because the CycB level increases. If the system is in the interphase, it will move along the lower branch until CycB levels surpass the ON threshold, at which point it jumps to the mitosis state, leading to phosphorylation of the Cdk1-CycB/PP2A-B55 substrates. If degradation is faster than synthesis, the CycB level will decrease and the system moves to the left. Sooner or later, this will take the system back to the interphase state, once the OFF threshold is crossed. If synthesis and degradation are balanced, the system settles into one of the stable steady states. Which steady state is occupied depends primarily on the cyclin levels. However, due to the occurrence of hysteresis, if the CycB level is between the two thresholds, then the final state depends on where the control system was before — its history.

In this revised view of the mitotic control network, the discrete separation between the interphase and M-phase and the CycB thresholds for mitotic entry and exit are systems-level properties, arising from the underlying interconnected network, and creating a very robust switch. However, the high connectivity of the network also allows the possibility that modifications of the components and their regulation have significant effects on these systems-level properties. For example, weakening of any of the IPFs, or strengthening of the MPFs, should reduce both CycB thresholds and thereby makes the M-phase state preferable, even at low CycB levels. The opposite is also true, and strengthening of IPFs or weakening of MPFs should increase the CycB

thresholds and destabilizes the mitotic state, making interphase preferable even at high CycB levels.

Because of these effects on the CycB thresholds, external intervention can allow the mitotic control system to change between interphase and M-phase at constant CycB level by manipulation of the CycB thresholds. Significant amounts of experimental evidence support this idea that modifications of the system change the thresholds. For instance, depletion of the MPFs Cdc25, Greatwall and ENSA in interphase blocks the G2/M transition even at high CycB levels (Zhao et al., 2008; Mochida et al., 2010; Lorca et al., 2010). In contrast, their depletion in M-phase can cause dephosphorylation of mitotic substrates and destabilization of M-phase (Yu et al., 2006; Lorca et al., 2010). On the other hand, depletion or inhibition of the IPFs, PP2A-B55 and Wee1 in interphase can result in premature mitotic entry (Yu et al., 2004; Mochida et al., 2009; Lorca et al., 2010). Inhibition of PP1 blocks exit from M-phase (Wu et al., 2009), but strangely depletion of B55δ only seems to block mitotic exit when its performed in the previous interphase but not in mitosis (Mochida et al., 2009).

In summary, Figure 6.1 presents an up-to-date picture of the molecular interactions that constitute the mitotic switch, based on recent experimental data with frog egg extracts and the proposed coherent interactions between its components. This mitotic switch determines the time of mitotic entry, i.e. the length of G2 phase. Mitotic entry happens when the CycB level meets the ON threshold of the switch. The threshold is determined by the strength of the regulatory interactions and feedback loops in the network in Figure 6.1. These interactions are influenced by different surveillance mechanisms like DNA replication and/or cell size checkpoints, which can

shift the position of the turn-on threshold by affecting the abundance or activity of one or several components of the switch. Active checkpoints keep the turn-on threshold at a high (physiologically unreachable) CycB level, making it impossible for the cell to enter M-phase. The ON threshold decreases during the process of checkpoint silencing, and once CycB and threshold meet, commitment for mitotic entry takes place.

Thus, the mitotic switch can flip when CycB reaches the required level, when the threshold drops below the CycB level, or an intermediate situation. Which of these scenarios actually takes place will most likely depend on the particular cell type, organism and environmental context. Furthermore, despite the conservation of many features of the network controlling the mitotic switch from yeasts to man (Goldberg, 2010; Wurzenberger and Gerlich, 2011), the relative contributions, and perhaps even identity, of individual components might be quite variable, and it is possible that some components are yet to be discovered. However, regardless of these differences, it is important to keep in mind that the length of G2 is determined by all the components of the network of Figure 6.1 and the rate of CycB accumulation, and as we have seen, it is difficult to decide which parts are more important in an absolute sense. Understanding the similarities and differences between different organisms and cell types will require careful quantitative measurements and provide interesting topics for further research.

6.4. Future perspectives

As mentioned previously, the network proposed in Figure 6.1 is a hypothesis that requires experimental verification. A critical point at this stage is the identification of the phosphatase that dephosphorylates ENSA. The role of PP1 as the Greatwall-counteracting phosphatase could be assessed by showing it can dephosphorylate ENSA *in vitro* and seeing whether its depletion or inhibition, using specific PP1 inhibitors, such as PP1 inhibitor-2 (Virshup and Shenolikar, 2009), prevents ENSA dephosphorylation. Previous work suggests that PP1 is important for mitotic exit (Walker et al., 1992; Wu et al., 2009), but its role in mitotic entry should be reassessed, as it could yield clues about the involvement of this phosphatase in the mitotic switch. Experiments with purified components could also help to establish whether PP2A-B55 is responsible for removal of Cdk1-dependent phosphorylations on Greatwall and potentially on its counteracting phosphatase, although further verification might be needed. It is important to note that interpretation of results from experiments in this network can be difficult, due to the many connections between the different components.

Mathematical analysis of the proposed network could help this endeavour by making useful predictions about the effects of perturbations to the mitotic switch. Analysis of the network in Figure 6.1 could also be used to understand how it can generate a robust, bistable switch, and whether it has any advantages compared to a simpler network with perhaps less regulatory links. It will be also interesting to study whether incorporation of the proposed components and links can help to explain more recent experimental findings.

A combination of experimental and theoretical work will be required to complete our understanding of the mechanisms responsible for ultrasensitivity, and ultimately bistability in this system, as demonstrated by recent work (Sha et al., 2003; Pomerening et al., 2003, 2005; Kim and Ferrell, 2007; Pomerening et al., 2008; Trunnell et al., 2011). An interesting goal of this analysis would be the reconstitution of the mitotic switch *in vitro* using purified components. This could potentially guarantee a comprehensive understanding of at least the basics of this important system.

The mathematical models presented here could also be extended into more complete models of simple cell cycles (like embryonic cell cycles), or used as modules in models of more complicated cycles (like fission yeast and mammalian cell cycles). Further work could also focus on understanding dynamical and stochastic properties of the models presented in this thesis. This is important for understanding the functioning of the mitotic switch, but also to appreciate general properties of the mechanisms that create nonlinearity. There has been interest in the dynamics and robustness of systems with multisite phosphorylation, positive feedback loops and coherent feedforward loops (Mangan and Alon, 2003; Alon, 2007a; Brandman and Meyer, 2008; Salazar et al., 2010), but it would be interesting to analyse their roles in systems with bistable switches.

Finally, as I have shown here, it seems that there can be many sources of ultrasensitivity and nonlinearity in biochemical systems. There has been some analysis of how these different sources can be combined (Goldbeter and Koshland, 1984), but most current work focuses on single mechanisms. In the future, further work should address this issue, to understand whether combination and coordination

of different mechanisms can potentially add robustness and improve the functioning of biochemical systems.

6.5. Final remarks

In this thesis, I have analysed several mechanisms that may contribute to bistability in the mitotic switch. In doing so, I have also analysed some general principles and mechanisms that can contribute to bistability in biochemical systems. Many other studies have also analysed the emergence of bistable switches form a theoretical perspective and experimentally shown the existence of bistability in several biological systems (reviewed in Thomas, 1998; Tyson et al., 2003; Ninfa and Mayo, 2004; Slepchenko and Terasaki, 2004; Dubnau and Losick, 2006; Mitrophanov and Groisman, 2008; Pomerening, 2008; Ferrell et al., 2009). Together, this suggests that bistability is likely to be a common property that is relatively easy to achieve in biochemical reaction networks.

I also hope that the work shown here highlights the importance of theoretical modelling in biology. By thinking of different systems using a common framework, mathematics can help uncover common 'design' principles in biology. This provides a deeper understanding of biological systems, and should deliver a means for faster, more targeted and more efficient biological research.

References

Alon, U. 2007a. An introduction to systems biology: design principles of biological circuits. Chapman & Hall/CRC.

Alon, U. 2007b. Network motifs: theory and experimental approaches. *Nature reviews. Genetics*. 8:450-61.

Angeli, D., J.E. Ferrell, and E.D. Sontag. 2004. Detection of multistability, bifurcations, and hysteresis in a large class of biological positive-feedback systems. *Proceedings of the National Academy of Sciences of the United States of America*. 101:1822-7.

Archambault, V., X. Zhao, H. White-Cooper, A.T.C. Carpenter, and D.M. Glover. 2007. Mutations in Drosophila Greatwall/Scant reveal its roles in mitosis and meiosis and interdependence with Polo kinase. *PLoS genetics*. 3:e200.

Barik, D., W.T. Baumann, M.R. Paul, B. Novák, and J.J. Tyson. 2010. A model of yeast cell-cycle regulation based on multisite phosphorylation. *Molecular systems biology*. 6:405.

Becskei, A., and L. Serrano. 2000. Engineering stability in gene networks by autoregulation. *Nature*. 405:590-3.

Becskei, A., B. Séraphin, and L. Serrano. 2001. Positive feedback in eukaryotic gene networks: cell differentiation by graded to binary response conversion. *The EMBO journal*. 20:2528-35.

Bloom, J., and F.R. Cross. 2007. Multiple levels of cyclin specificity in cell-cycle control. *Nature reviews. Molecular cell biology*. 8:149-60.

Bollen, M., D.W. Gerlich, and B. Lesage. 2009. Mitotic phosphatases: from entry guards to exit guides. *Trends in cell biology*. 19:531-41.

Brandman, O., and T. Meyer. 2008. Feedback loops shape cellular signals in space and time. *Science (New York, N.Y.)*. 322:390-5.

Bray, D. 1995. Protein molecules as computational elements in living cells. *Nature*. 376:307-12.

Brown, D.D. 2004. A tribute to the Xenopus laevis oocyte and egg. *The Journal of biological chemistry*. 279:45291-9.

Burgess, A., S. Vigneron, E. Brioudes, J.-C. Labbé, T. Lorca, and A. Castro. 2010. Loss of human Greatwall results in G2 arrest and multiple mitotic defects due to deregulation of the cyclin B-Cdc2/PP2A balance. *Proceedings of the National Academy of Sciences of the United States of America*. 107:12564-9.

Castilho, P.V., B.C. Williams, S. Mochida, Y. Zhao, and M.L. Goldberg. 2009. The M phase kinase Greatwall (Gwl) promotes inactivation of PP2A/B55delta, a phosphatase directed against CDK phosphosites. *Molecular biology of the cell*. 20:4777-89.

Chang, D.-E., S. Leung, M.R. Atkinson, A. Reifler, D. Forger, and A.J. Ninfa. 2010. Building biological memory by linking positive feedback loops. *Proceedings of the National Academy of Sciences of the United States of America*. 107:175-80.

Chen, F., V. Archambault, A. Kar, P. Lio', P.P. D'Avino, R. Sinka, K. Lilley, E.D. Laue, P. Deak, L. Capalbo, and D.M. Glover. 2007. Multiple protein phosphatases are required for mitosis in Drosophila. *Current biology : CB*. 17:293-303.

Chen, K.C., A. Csikász-Nagy, B. Gyorffy, J. Val, B. Novák, and J.J. Tyson. 2000. Kinetic analysis of a molecular model of the budding yeast cell cycle. *Molecular biology of the cell*. 11:369-91.

Ciliberto, A., F. Capuani, and J.J. Tyson. 2007. Modeling networks of coupled enzymatic reactions using the total quasi-steady state approximation. *PLoS computational biology*. 3:e45.

Cimino, A., and J.F. Hervagault. 1987. Experimental evidence for a zero-order ultrasensitivity in a simple substrate cycle. *Biochemical and biophysical research communications*. 149:615-20.

Clarke, P.R., I. Hoffmann, G. Draetta, and E. Karsenti. 1993. Dephosphorylation of cdc25-C by a type-2A protein phosphatase: specific regulation during the cell cycle in Xenopus egg extracts. *Molecular biology of the cell*. 4:397-411.

Clifford, D.M., C.-T. Chen, R.H. Roberts, A. Feoktistova, B.A. Wolfe, J.-S. Chen, D. McCollum, and K.L. Gould. 2008. The role of Cdc14 phosphatases in the control of cell division. *Biochemical Society transactions*. 36:436-8.

Cohen, P. 2000. The regulation of protein function by multisite phosphorylation--a 25 year update. *Trends in biochemical sciences*. 25:596-601.

Coleman, T.R., and W.G. Dunphy. 1994. Cdc2 regulatory factors. *Current opinion in cell biology*. 6:877-82.

Conrad, E.D., and J.J. Tyson. 2006. No Title. *In* Modeling Molecular Interaction Networks with Nonlinear Ordinary Differential Equations. In System Modeling in Cellular Biology. Szallasi et al. eds. 97-123.

Cornish-Bowden, A. 2004. Fundamentals of enzyme kinetics. Portland Press.

Coudreuse, D., and P. Nurse. 2010. Driving the cell cycle with a minimal CDK control network. *Nature*. 468:1074-9.

Cross, F.R., V. Archambault, M. Miller, and M. Klovstad. 2002. Testing a mathematical model of the yeast cell cycle. *Molecular biology of the cell*. 13:52-70.

Csikász-Nagy, A., O. Kapuy, A. Tóth, C. Pál, L.J. Jensen, F. Uhlmann, J.J. Tyson, and B. Novák. 2009. Cell cycle regulation by feed-forward loops coupling transcription and phosphorylation. *Molecular systems biology*. 5:236.

Deibler, R.W., and M.W. Kirschner. 2010. Quantitative reconstitution of mitotic CDK1 activation in somatic cell extracts. *Molecular cell*. 37:753-67.

Dephoure, N., C. Zhou, J. Villén, S.A. Beausoleil, C.E. Bakalarski, S.J. Elledge, and S.P. Gygi. 2008. A quantitative atlas of mitotic phosphorylation. *Proceedings of the National Academy of Sciences of the United States of America*. 105:10762-7.

Devault, A., D. Fesquet, J.C. Cavadore, A.M. Garrigues, J.-C. Labbé, T. Lorca, A. Picard, M. Philippe, and M. Dorée. 1992. Cyclin A potentiates maturation-promoting factor activation in the early Xenopus embryo via inhibition of the tyrosine kinase that phosphorylates cdc2. *The Journal of cell biology*. 118:1109-20.

Dohadwala, M., E.F. da Cruz e Silva, F.L. Hall, R.T. Williams, D.A. Carbonaro-Hall, A.C. Nairn, P. Greengard, and N. Berndt. 1994. Phosphorylation and inactivation of protein phosphatase 1 by cyclin-dependent kinases. *Proceedings of the National Academy of Sciences of the United States of America*. 91:6408-12.

Domingo-Sananes, M.R., O. Kapuy, T. Hunt, and B. Novák. 2011. Switches and latches: a biochemical tug-of-war between the kinases and phosphatases that control mitosis. *Philosophical transactions of the Royal Society of London. Series B, Biological sciences*. 366:3584-94.

Domingo-Sananes, M.R., and B. Novák. 2010. Different effects of redundant feedback loops on a bistable switch. *Chaos (Woodbury, N.Y.)*. 20:045120.

Dorée, M., J.-C. Labbé, and A. Picard. 1989. M phase-promoting factor: its identification as the M phase-specific H1 histone kinase and its activation by dephosphorylation. *Journal of cell science. Supplement*. 12:39-51.

Dubnau, D., and R. Losick. 2006. Bistability in bacteria. *Molecular microbiology*. 61:564-72.

Duesbery, N.S., and G.F. Vande Woude. 1998. Cytoplasmic control of nuclear behavior during meiotic maturation of frog oocytes. *Biology of the cell / under the auspices of the European Cell Biology Organization*. 90:461-6.

Dunphy, W.G. 1994. The decision to enter mitosis. *Trends in cell biology*. 4:202-7.

Dunphy, W.G., L. Brizuela, D. Beach, and J.W. Newport. 1988. The Xenopus cdc2 protein is a component of MPF, a cytoplasmic regulator of mitosis. *Cell*. 54:423-31.

Elowitz, M.B., and S. Leibler. 2000. A synthetic oscillatory network of transcriptional regulators. *Nature*. 403:335-8.

Ermentrout, B. 2002. Simulating, analyzing, and animating dynamical systems: a guide to XPPAUT for researchers and students. SIAM.

Errico, A., K. Deshmukh, Y. Tanaka, A. Pozniakovsky, and T. Hunt. 2010. Identification of substrates for cyclin dependent kinases. *Advances in enzyme regulation*. 50:375-99.

Evans, T., E.T. Rosenthal, J. Youngblom, D. Distel, and T. Hunt. 1983. Cyclin: a protein specified by maternal mRNA in sea urchin eggs that is destroyed at each cleavage division. *Cell*. 33:389-96.

Ferrell, J.E. 1996. Tripping the switch fantastic: how a protein kinase cascade can convert graded inputs into switch-like outputs. *Trends in biochemical sciences*. 21:460-6.

Ferrell, J.E. 1999a. Xenopus oocyte maturation: new lessons from a good egg. *BioEssays : news and reviews in molecular, cellular and developmental biology*. 21:833-42.

Ferrell, J.E. 1999b. Building a cellular switch: more lessons from a good egg. *BioEssays : news and reviews in molecular, cellular and developmental biology*. 21:866-70.

Ferrell, J.E. 2002. Self-perpetuating states in signal transduction: positive feedback, double-negative feedback and bistability. *Current opinion in cell biology*. 14:140-8.

Ferrell, J.E. 2008. Feedback regulation of opposing enzymes generates robust, all-or-none bistable responses. *Current biology : CB*. 18:R244-5.

Ferrell, J.E., and E.M. Machleder. 1998. The biochemical basis of an all-or-none cell fate switch in Xenopus oocytes. *Science (New York, N.Y.)*. 280:895-8.

Ferrell, J.E., J.R. Pomerening, S.Y. Kim, N.B. Trunnell, W. Xiong, C.-Y.F. Huang, and E.M. Machleder. 2009. Simple, realistic models of complex biological processes: positive feedback and bistability in a cell fate switch and a cell cycle oscillator. *FEBS letters*. 583:3999-4005.

Ferrell, J.E., T.Y.-C. Tsai, and Q. Yang. 2011. Modeling the cell cycle: why do certain circuits oscillate? *Cell*. 144:874-85.

Ferrell, J.E., and W. Xiong. 2001. Bistability in cell signaling: How to make continuous processes discontinuous, and reversible processes irreversible. *Chaos (Woodbury, N.Y.)*. 11:227-236.

Fisher, D., and P. Nurse. 1996. A single fission yeast mitotic cyclin B p34cdc2 kinase promotes both S-phase and mitosis in the absence of G1 cyclins. *The EMBO journal*. 15:850-60.

Félix, M.A., P. Cohen, and E. Karsenti. 1990. Cdc2 H1 kinase is negatively regulated by a type 2A phosphatase in the Xenopus early embryonic cell cycle: evidence from the effects of okadaic acid. *The EMBO journal*. 9:675-83.

Gardner, T.S., C.R. Cantor, and J.J. Collins. 2000. Construction of a genetic toggle switch in Escherichia coli. *Nature*. 403:339-42.

Gautier, J., J. Minshull, M.J. Lohka, M. Glotzer, T. Hunt, and J.L. Maller. 1990. Cyclin is a component of maturation-promoting factor from Xenopus. *Cell*. 60:487-94.

Gautier, J., C. Norbury, M.J. Lohka, P. Nurse, and J.L. Maller. 1988. Purified maturation-promoting factor contains the product of a Xenopus homolog of the fission yeast cell cycle control gene cdc2+. *Cell*. 54:433-9.

Gharbi-Ayachi, A., J.-C. Labbé, A. Burgess, S. Vigneron, J.-M. Strub, E. Brioudes, A. Van-Dorsselaer, A. Castro, and T. Lorca. 2010. The substrate of Greatwall kinase, Arpp19, controls mitosis by inhibiting protein phosphatase 2A. *Science (New York, N.Y.)*. 330:1673-7.

Goldberg, M.L. 2010. Greatwall kinase protects mitotic phosphosites from barbarian phosphatases. *Proceedings of the National Academy of Sciences of the United States of America*. 107:12409-10.

Goldbeter, A. 2002. Computational approaches to cellular rhythms. *Nature*. 420:238-45.

Goldbeter, A., and D.E. Koshland. 1981. An amplified sensitivity arising from covalent modification in biological systems. *Proceedings of the National Academy of Sciences of the United States of America*. 78:6840-4.

Goldbeter, A., and D.E. Koshland. 1984. Ultrasensitivity in biochemical systems controlled by covalent modification. Interplay between zero-order and multistep effects. *The Journal of biological chemistry*. 259:14441-7.

Goldbeter, A., and D.E. Koshland. 1987. Energy expenditure in the control of biochemical systems by covalent modification. *The Journal of biological chemistry*. 262:4460-71.

Gonze, D., W. Abou-Jaoudé, D.A. Ouattara, and J. Halloy. 2011. How molecular should your molecular model be? On the level of molecular detail required to simulate biological networks in systems and synthetic biology. *Methods in enzymology*. 487:171-215.

Goranov, A.I., and A. Amon. 2010. Growth and division--not a one-way road. *Current opinion in cell biology*. 22:795-800.

Goris, J., J. Hermann, P. Hendrix, R. Ozon, and W. Merlevede. 1989. Okadaic acid, a specific protein phosphatase inhibitor, induces maturation and MPF formation in Xenopus laevis oocytes. *FEBS letters*. 245:91-4.

Graumann, P.L. 2006. Different genetic programmes within identical bacteria under identical conditions: the phenomenon of bistability greatly modifies our view on bacterial populations. *Molecular microbiology*. 61:560-3.

Gunawardena, J. 2005. Multisite protein phosphorylation makes a good threshold but can be a poor switch. *Proceedings of the National Academy of Sciences of the United States of America*. 102:14617-22.

Gérard, C., and A. Goldbeter. 2009. Temporal self-organization of the cyclin/Cdk network driving the mammalian cell cycle. *Proceedings of the National Academy of Sciences of the United States of America*. 106:21643-8.

Hansen, D.V., J.R. Pomerening, M.K. Summers, J.J. Miller, J.E. Ferrell, and P.K. Jackson. 2007. Emi2 at the crossroads: where CSF meets MPF. *Cell cycle (Georgetown, Tex.)*. 6:732-8.

Hartwell, L.H. 1991. Twenty-five years of cell cycle genetics. *Genetics*. 129:975-80.

Hartwell, L.H., J. Culotti, J.R. Pringle, and B.J. Reid. 1974. Genetic control of the cell division cycle in yeast. *Science (New York, N.Y.)*. 183:46-51.

Hartwell, L.H., and T.A. Weinert. 1989. Checkpoints: controls that ensure the order of cell cycle events. *Science (New York, N.Y.)*. 246:629-34.

Harvey, S.L., A. Charlet, W. Haas, S.P. Gygi, and D.R. Kellogg. 2005. Cdk1-dependent regulation of the mitotic inhibitor Wee1. *Cell*. 122:407-20.

He, E., O. Kapuy, R.A. Oliveira, F. Uhlmann, J.J. Tyson, and B. Novák. 2011. System-level feedbacks make the anaphase switch irreversible. *Proceedings of the National Academy of Sciences of the United States of America*. 108:10016-21.

Hershko, A. 2005. The ubiquitin system for protein degradation and some of its roles in the control of the cell-division cycle (Nobel lecture). *Angewandte Chemie (International ed. in English)*. 44:5932-43.

Hervagault, J.F., and S. Canu. 1987. Bistability and irreversible transitions in a simple substrate cycle. *Journal of Theoretical Biology*. 127:439-449.

Hochegger, H., S. Takeda, and T. Hunt. 2008. Cyclin-dependent kinases and cell-cycle transitions: does one fit all? *Nature reviews. Molecular cell biology*. 9:910-6.

Hoffmann, I., P.R. Clarke, M.J. Marcote, E. Karsenti, and G. Draetta. 1993. Phosphorylation and activation of human cdc25-C by cdc2--cyclin B and its involvement in the self-amplification of MPF at mitosis. *The EMBO journal*. 12:53-63.

Holt, L.J., B.B. Tuch, J. Villén, A.D. Johnson, S.P. Gygi, and D.O. Morgan. 2009. Global analysis of Cdk1 substrate phosphorylation sites provides insights into evolution. *Science (New York, N.Y.)*. 325:1682-6.

Hutchison, C.J., R. Cox, and C.C. Ford. 1988. The control of DNA replication in a cell-free extract that recapitulates a basic cell cycle in vitro. *Development (Cambridge, England)*. 103:553-66.

Izumi, T., and J.L. Maller. 1993. Elimination of cdc2 phosphorylation sites in the cdc25 phosphatase blocks initiation of M-phase. *Molecular biology of the cell*. 4:1337-50.

Izumi, T., D.H. Walker, and J.L. Maller. 1992. Periodic changes in phosphorylation of the Xenopus cdc25 phosphatase regulate its activity. *Molecular biology of the cell*. 3:927-39.

Jordan, D.W., and P. Smith. 2008. Mathematical Techniques: An Introduction for the Engineering, Physical, and Mathematical Sciences. Oxford University Press.

Kapuy, O., D. Barik, M.R. Domingo-Sananes, J.J. Tyson, and B. Novák. 2009a. Bistability by multiple phosphorylation of regulatory proteins. *Progress in biophysics and molecular biology*. 100:47-56.

Kapuy, O., E. He, F. Uhlmann, and B. Novák. 2009b. Mitotic exit in mammalian cells. *Molecular systems biology*. 5:324.

Kim, S.Y., and J.E. Ferrell. 2007. Substrate competition as a source of ultrasensitivity in the inactivation of Wee1. *Cell*. 128:1133-45.

Kim, S.Y., E.J. Song, K.-J. Lee, and J.E. Ferrell. 2005. Multisite M-phase phosphorylation of Xenopus Wee1A. *Molecular and cellular biology*. 25:10580-90.

Klipp, E., R. Herwig, A. Kowald, C. Wierling, and H. Lehrach. 2005. Systems biology in practice: concepts, implementation and application. Wiley-VCH.

Kornbluth, S., J. Yang, and M. Powers. 2006. Analysis of the cell cycle using Xenopus egg extracts. *Current protocols in cell biology / editorial board, Juan S. Bonifacino ... [et al.]*. Chapter 11:Unit 11.11.

Koshland, D.E., A. Goldbeter, and J.B. Stock. 1982. Amplification and adaptation in regulatory and sensory systems. *Science (New York, N.Y.)*. 217:220-5.

Koshland, D.E., and K. Hamadani. 2002. Proteomics and models for enzyme cooperativity. *The Journal of biological chemistry*. 277:46841-4.

Krasinska, L., M.R. Domingo-Sananes, O. Kapuy, N. Parisis, B. Harker, G. Moorhead, M. Rossignol, B. Novák, and D. Fisher. 2011. Protein Phosphatase 2A Controls the Order and Dynamics of Cell-Cycle Transitions. *Molecular Cell*. 44:437-450.

Kreyszig, E. 2010. Advanced Engineering Mathematics. John Wiley and Sons.

Krishnamurthy, S., E. Smith, D. Krakauer, and W. Fontana. 2007. The stochastic behavior of a molecular switching circuit with feedback. *Biology direct*. 2:13.

Kumagai, A., and W.G. Dunphy. 1992. Regulation of the cdc25 protein during the cell cycle in Xenopus extracts. *Cell*. 70:139-51.

LaPorte, D.C., and D.E. Koshland. Phosphorylation of isocitrate dehydrogenase as a demonstration of enhanced sensitivity in covalent regulation. *Nature*. 305:286-90.

Labbé, J.-C., A. Picard, G. Peaucellier, J.C. Cavadore, P. Nurse, and M. Doree. 1989. Purification of MPF from starfish: identification as the H1 histone kinase p34cdc2 and a possible mechanism for its periodic activation. *Cell*. 57:253-63.

Laurent, M., and N. Kellershohn. 1999. Multistability: a major means of differentiation and evolution in biological systems. *Trends in biochemical sciences*. 24:418-22.

Lee, M.G., and P. Nurse. 1987. Complementation used to clone a human homologue of the fission yeast cell cycle control gene cdc2. *Nature*. 327:31-5.

Lee, T., C. Turck, and M.W. Kirschner. 1994. Inhibition of cdc2 activation by INH/PP2A. *Molecular biology of the cell*. 5:323-38.

Lindqvist, A., V. Rodríguez-Bravo, and R.H. Medema. 2009. The decision to enter mitosis: feedback and redundancy in the mitotic entry network. *The Journal of cell biology*. 185:193-202.

Lohka, M.J. 1998. Nuclear responses to MPF activation and inactivation in Xenopus oocytes and early embryos. *Biology of the cell / under the auspices of the European Cell Biology Organization*. 90:591-9.

Lohka, M.J., M.K. Hayes, and J.L. Maller. 1988. Purification of maturation-promoting factor, an intracellular regulator of early mitotic events. *Proceedings of the National Academy of Sciences of the United States of America*. 85:3009-13.

Loog, M., and D.O. Morgan. 2005. Cyclin specificity in the phosphorylation of cyclin-dependent kinase substrates. *Nature*. 434:104-8.

Lorca, T., C. Bernis, S. Vigneron, A. Burgess, E. Brioudes, J.-C. Labbé, and A. Castro. 2010. Constant regulation of both the MPF amplification loop and the Greatwall-PP2A pathway is required for metaphase II arrest and correct entry into the first embryonic cell cycle. *Journal of cell science*. 123:2281-91.

Lorca, T., D. Fesquet, F. Zindy, F. Le Bouffant, M. Cerruti, C. Brechot, G. Devauchelle, and M. Dorée. 1991. An okadaic acid-sensitive phosphatase negatively controls the cyclin degradation pathway in amphibian eggs. *Molecular and cellular biology*. 11:1171-5.

Lundgren, K., N. Walworth, R.N. Booher, M. Dembski, M.W. Kirschner, and D. Beach. 1991. mik1 and wee1 cooperate in the inhibitory tyrosine phosphorylation of cdc2. *Cell*. 64:1111-22.

López-Avilés, S., O. Kapuy, B. Novák, and F. Uhlmann. 2009. Irreversibility of mitotic exit is the consequence of systems-level feedback. *Nature*. 459:592-5.

Ma, H.T., and R.Y.C. Poon. 2011. How protein kinases co-ordinate mitosis in animal cells. *The Biochemical journal*. 435:17-31.

Manchado, E., M. Guillamot, G. de Cárcer, M. Eguren, M. Trickey, I. García-Higuera, S. Moreno, H. Yamano, M. Cañamero, and M. Malumbres. 2010. Targeting mitotic exit leads to tumor regression in vivo: Modulation by Cdk1, Mastl, and the PP2A/B55α,δ phosphatase. *Cancer cell*. 18:641-54.

Mangan, S., and U. Alon. 2003. Structure and function of the feed-forward loop network motif. *Proceedings of the National Academy of Sciences of the United States of America*. 100:11980-5.

Mangan, S., S. Itzkovitz, A. Zaslaver, and U. Alon. 2006. The incoherent feed-forward loop accelerates the response-time of the gal system of Escherichia coli. *Journal of molecular biology*. 356:1073-81.

Mangan, S., A. Zaslaver, and U. Alon. 2003. The coherent feedforward loop serves as a sign-sensitive delay element in transcription networks. *Journal of molecular biology*. 334:197-204.

Mann, M., S.E. Ong, M. Grønborg, H. Steen, O.N. Jensen, and A. Pandey. 2002. Analysis of protein phosphorylation using mass spectrometry: deciphering the phosphoproteome. *Trends in biotechnology*. 20:261-8.

Markevich, N.I., J.B. Hoek, and B.N. Kholodenko. 2004. Signaling switches and bistability arising from multisite phosphorylation in protein kinase cascades. *The Journal of cell biology*. 164:353-9.

Masui, Y., and C.L. Markert. 1971. Cytoplasmic control of nuclear behavior during meiotic maturation of frog oocytes. *The Journal of experimental zoology*. 177:129-45.

Maton, G., T. Lorca, J.-A. Girault, R. Ozon, and C. Jessus. 2005. Differential regulation of Cdc2 and Aurora-A in Xenopus oocytes: a crucial role of phosphatase 2A. *Journal of cell science*. 118:2485-94.

Mayer-Jaekel, R.E., H. Ohkura, P. Ferrigno, N. Andjelkovic, K. Shiomi, T. Uemura, D.M. Glover, and B.A. Hemmings. 1994. Drosophila mutants in the 55 kDa regulatory subunit of protein phosphatase 2A show strongly reduced ability to dephosphorylate substrates of p34cdc2. *Journal of cell science*. 107 (Pt 9:2609-16.

Minshull, J., J.J. Blow, and T. Hunt. 1989. Translation of cyclin mRNA is necessary for extracts of activated xenopus eggs to enter mitosis. *Cell*. 56:947-56.

Mitrophanov, A.Y., and E.A. Groisman. 2008. Positive feedback in cellular control systems. *BioEssays : news and reviews in molecular, cellular and developmental biology*. 30:542-55.

Mochida, S., and T. Hunt. 2007. Calcineurin is required to release Xenopus egg extracts from meiotic M phase. *Nature*. 449:336-40.

Mochida, S., S. Ikeo, J. Gannon, and T. Hunt. 2009. Regulated activity of PP2A-B55 delta is crucial for controlling entry into and exit from mitosis in Xenopus egg extracts. *The EMBO journal*. 28:2777-85.

Mochida, S., S.L. Maslen, M. Skehel, and T. Hunt. 2010. Greatwall phosphorylates an inhibitor of protein phosphatase 2A that is essential for mitosis. *Science (New York, N.Y.)*. 330:1670-3.

Moreno, S., J. Hayles, and P. Nurse. 1989. Regulation of p34cdc2 protein kinase during mitosis. *Cell*. 58:361-72.

Morgan, D.O. 1997. Cyclin-dependent kinases: engines, clocks, and microprocessors. *Annual review of cell and developmental biology*. 13:261-91.

Morgan, D.O. 2007. The cell cycle: principles of control. New Science Press.

Mueller, P.R., T.R. Coleman, A. Kumagai, and W.G. Dunphy. 1995. Myt1: a membrane-associated inhibitory kinase that phosphorylates Cdc2 on both threonine-14 and tyrosine-15. *Science (New York, N.Y.)*. 270:86-90.

Murray, A.W., and M.W. Kirschner. 1989. Cyclin synthesis drives the early embryonic cell cycle. *Nature*. 339:275-80.

Murray, A.W., M.J. Solomon, and M.W. Kirschner. 1989. The role of cyclin synthesis and degradation in the control of maturation promoting factor activity. *Nature*. 339:280-6.

Murray, J.D. 2002. Mathematical biology: An introduction, Volume 1. Springer.

Nasmyth, K. 2001. A prize for proliferation. *Cell*. 107:689-701.

Nigg, E.A. 2001. Mitotic kinases as regulators of cell division and its checkpoints. *Nature reviews. Molecular cell biology*. 2:21-32.

Ninfa, A.J., and A.E. Mayo. 2004. Hysteresis vs. graded responses: the connections make all the difference. *Science's STKE : signal transduction knowledge environment*. 2004:pe20.

Novick, A., and M. Weiner. 1957. Enzyme induction as an all-or-none phenomenon. *Proceedings of the National Academy of Sciences of the United States of America*. 43:553-66.

Novák, B., O. Kapuy, M.R. Domingo-Sananes, and J.J. Tyson. 2010. Regulated protein kinases and phosphatases in cell cycle decisions. *Current opinion in cell biology*. 22:801-8.

Novák, B., and J.J. Tyson. 1993. Numerical analysis of a comprehensive model of M-phase control in Xenopus oocyte extracts and intact embryos. *Journal of cell science*. 106 (Pt 4:1153-68.

Novák, B., and J.J. Tyson. 2008. Design principles of biochemical oscillators. *Nature reviews. Molecular cell biology*. 9:981-91.

Novák, B., J.J. Tyson, B. Gyorffy, and A. Csikász-Nagy. 2007. Irreversible cell-cycle transitions are due to systems-level feedback. *Nature cell biology*. 9:724-8.

Nurse, P. 1975. Genetic control of cell size at cell division in yeast. *Nature*. 256:547-51.

Nurse, P. 1990. Universal control mechanism regulating onset of M-phase. *Nature*. 344:503-8.

Nurse, P. 2000. A long twentieth century of the cell cycle and beyond. *Cell*. 100:71-8.

Nurse, P. 2002. Cyclin dependent kinases and cell cycle control (nobel lecture). *Chembiochem : a European journal of chemical biology*. 3:596-603.

Nurse, P., P. Thuriaux, and K. Nasmyth. 1976. Genetic control of the cell division cycle in the fission yeast Schizosaccharomyces pombe. *Molecular & general genetics : MGG*. 146:167-78.

Oppenheim, A.B., O. Kobiler, J. Stavans, D.L. Court, and S. Adhya. 2005. Switches in bacteriophage lambda development. *Annual review of genetics*. 39:409-29.

Ortega, F., J.L. Garcés, F. Mas, B.N. Kholodenko, and M. Cascante. 2006. Bistability from double phosphorylation in signal transduction. Kinetic and structural requirements. *The FEBS journal*. 273:3915-26.

Ozbudak, E.M., M. Thattai, H.N. Lim, B.I. Shraiman, and A. Van Oudenaarden. 2004. Multistability in the lactose utilization network of Escherichia coli. *Nature*. 427:737-40.

O'Farrell, P.H. 2001. Triggering the all-or-nothing switch into mitosis. *Trends in cell biology*. 11:512-9.

Perry, J.A., and S. Kornbluth. 2007. Cdc25 and Wee1: analogous opposites? *Cell division*. 2:12.

Perutz, M.F., A.J. Wilkinson, M. Paoli, and G.G. Dodson. 1998. The stereochemical mechanism of the cooperative effects in hemoglobin revisited. *Annual review of biophysics and biomolecular structure*. 27:1-34.

Peters, J.-M. 2006. The anaphase promoting complex/cyclosome: a machine designed to destroy. *Nature reviews. Molecular cell biology*. 7:644-56.

Philpott, A., and P.R. Yew. 2008. The Xenopus cell cycle: an overview. *Molecular biotechnology*. 39:9-19.

Pines, J. 2011. Cubism and the cell cycle: the many faces of the APC/C. *Nature reviews. Molecular cell biology*. 12:427-38.

Pines, J., and T. Hunt. 1987. Molecular cloning and characterization of the mRNA for cyclin from sea urchin eggs. *The EMBO journal*. 6:2987-95.

Pomerening, J.R. 2008. Uncovering mechanisms of bistability in biological systems. *Current opinion in biotechnology*. 19:381-8.

Pomerening, J.R. 2009. Positive-feedback loops in cell cycle progression. *FEBS letters*. 583:3388-96.

Pomerening, J.R., S.Y. Kim, and J.E. Ferrell. 2005. Systems-level dissection of the cell-cycle oscillator: bypassing positive feedback produces damped oscillations. *Cell*. 122:565-78.

Pomerening, J.R., E.D. Sontag, and J.E. Ferrell. 2003. Building a cell cycle oscillator: hysteresis and bistability in the activation of Cdc2. *Nature cell biology*. 5:346-51.

Pomerening, J.R., J.A. Ubersax, and J.E. Ferrell. 2008. Rapid cycling and precocious termination of G1 phase in cells expressing CDK1AF. *Molecular biology of the cell*. 19:3426-41.

Queralt, E., and F. Uhlmann. 2008. Cdk-counteracting phosphatases unlock mitotic exit. *Current opinion in cell biology*. 20:661-8.

Rangone, H., E. Wegel, M.K. Gatt, E. Yeung, A. Flowers, J. Debski, M. Dadlez, V. Janssens, A.T.C. Carpenter, and D.M. Glover. 2011. Suppression of Scant Identifies Endos as a Substrate of Greatwall Kinase and a Negative Regulator of Protein Phosphatase 2A in Mitosis. *PLoS Genetics*. 7:e1002225.

Russell, P., and P. Nurse. 1986. cdc25+ functions as an inducer in the mitotic control of fission yeast. *Cell*. 45:145-53.

Sabouri-Ghomi, M., A. Ciliberto, S. Kar, B. Novák, and J.J. Tyson. 2008. Antagonism and bistability in protein interaction networks. *Journal of theoretical biology*. 250:209-18.

Salazar, C., A. Brümmer, L. Alberghina, and T. Höfer. 2010. Timing control in regulatory networks by multisite protein modifications. *Trends in cell biology*. 20:634-41.

Salazar, C., and T. Höfer. 2007. Versatile regulation of multisite protein phosphorylation by the order of phosphate processing and protein-protein interactions. *The FEBS journal*. 274:1046-61.

Salazar, C., and T. Höfer. 2009. Multisite protein phosphorylation--from molecular mechanisms to kinetic models. *The FEBS journal*. 276:3177-98.

Schmitz, M.H.A., M. Held, V. Janssens, J.R.A. Hutchins, O. Hudecz, E. Ivanova, J. Goris, L. Trinkle-Mulcahy, A.I. Lamond, I. Poser, A.A. Hyman, K. Mechtler, J.-M. Peters, and D.W. Gerlich. 2010. Live-cell imaging RNAi screen identifies PP2A-B55alpha and importin-beta1 as key mitotic exit regulators in human cells. *Nature cell biology*. 12:886-93.

Sha, W., J. Moore, K.C. Chen, A.D. Lassaletta, C.-S. Yi, J.J. Tyson, and J.C. Sible. 2003. Hysteresis drives cell-cycle transitions in Xenopus laevis egg extracts. *Proceedings of the National Academy of Sciences of the United States of America*. 100:975-80.

Shen-Orr, S.S., R. Milo, S. Mangan, and U. Alon. 2002. Network motifs in the transcriptional regulation network of Escherichia coli. *Nature genetics*. 31:64-8.

Simanis, V., and P. Nurse. 1986. The cell cycle control gene cdc2+ of fission yeast encodes a protein kinase potentially regulated by phosphorylation. *Cell*. 45:261-8.

Slepchenko, B.M., and M. Terasaki. 2004. Bio-switches: what makes them robust? *Current opinion in genetics & development*. 14:428-34.

Solomon, M.J., M. Glotzer, T. Lee, M. Philippe, and M.W. Kirschner. 1990. Cyclin activation of p34cdc2. *Cell*. 63:1013-24.

Solomon, M.J., T. Lee, and M.W. Kirschner. 1992. Role of phosphorylation in p34cdc2 activation: identification of an activating kinase. *Molecular biology of the cell*. 3:13-27.

Stegmeier, F., and A. Amon. 2004. Closing mitosis: the functions of the Cdc14 phosphatase and its regulation. *Annual review of genetics*. 38:203-32.

Strogatz, S.H. 1994. Nonlinear dynamics and chaos: with applications to physics, biology, chemistry, and engineering. Westview Press.

Sullivan, M., and D.O. Morgan. 2007. Finishing mitosis, one step at a time. *Nature reviews. Molecular cell biology*. 8:894-903.

Tang, Z., T.R. Coleman, and W.G. Dunphy. 1993. Two distinct mechanisms for negative regulation of the Wee1 protein kinase. *The EMBO journal*. 12:3427-36.

Thomas, R. 1998. Laws for the dynamics of regulatory networks. *The International journal of developmental biology*. 42:479-85.

Thomson, M., and J. Gunawardena. 2009. Unlimited multistability in multisite phosphorylation systems. *Nature*. 460:274-7.

Thron, C.D. 1996. A model for a bistable biochemical trigger of mitosis. *Biophysical chemistry*. 57:239-51.

Thuriaux, P., P. Nurse, and B. Carter. 1978. Mutants altered in the control co-ordinating cell division with cell growth in the fission yeast Schizosaccharomyces pombe. *Molecular & general genetics : MGG*. 161:215-20.

Trinkle-Mulcahy, L., and A.I. Lamond. 2006. Mitotic phosphatases: no longer silent partners. *Current opinion in cell biology*. 18:623-31.

Trunnell, N.B., A.C. Poon, S.Y. Kim, and J.E. Ferrell. 2011. Ultrasensitivity in the Regulation of Cdc25C by Cdk1. *Molecular cell*. 41:263-74.

Tsai, T.Y.-C., Y.S. Choi, W. Ma, J.R. Pomerening, C. Tang, and J.E. Ferrell. 2008. Robust, tunable biological oscillations from interlinked positive and negative feedback loops. *Science (New York, N.Y.)*. 321:126-9.

Tyson, J.J., K.C. Chen, and B. Novák. 2001. Network dynamics and cell physiology. *Nature reviews. Molecular cell biology*. 2:908-16.

Tyson, J.J., K.C. Chen, and B. Novák. 2003. Sniffers, buzzers, toggles and blinkers: dynamics of regulatory and signaling pathways in the cell. *Current opinion in cell biology*. 15:221-31.

Tyson, J.J., and B. Novák. 2002. No Title. *In* Cell Cycle Controls. In Computational Cell Biology. Fall et al, eds. 261-284.

Tyson, J.J., and B. Novák. 2008. Temporal organization of the cell cycle. *Current biology : CB*. 18:R759-R768.

Tyson, J.J., and B. Novák. 2010. Functional motifs in biochemical reaction networks. *Annual review of physical chemistry*. 61:219-40.

Tyson, J.J., and B. Novák. 2012. No Title. *In* Irreversible Transitions, Bistability and Checkpoint Controls in the Eukaryotic Cell Cycle: A Systems-level Understanding. In Handbook of Systems Biology. Walhout et al, eds.

Tóth, A., E. Queralt, F. Uhlmann, and B. Novák. 2007. Mitotic exit in two dimensions. *Journal of theoretical biology*. 248:560-73.

Ubersax, J.A., E.L. Woodbury, P.N. Quang, M. Paraz, J.D. Blethrow, K. Shah, K.M. Shokat, and D.O. Morgan. 2003. Targets of the cyclin-dependent kinase Cdk1. *Nature*. 425:859-64.

Uhlmann, F. 2003. Chromosome cohesion and separation: from men and molecules. *Current biology : CB*. 13:R104-14.

Vigneron, S., E. Brioudes, A. Burgess, J.-C. Labbé, T. Lorca, and A. Castro. 2009. Greatwall maintains mitosis through regulation of PP2A. *The EMBO journal*. 28:2786-93.

Vigneron, S., A. Gharbi-Ayachi, A.-A. Raymond, A. Burgess, J.-C. Labbé, G. Labesse, B. Monsarrat, T. Lorca, and A. Castro. 2011. Characterization of the mechanisms controlling Greatwall activity. *Molecular and cellular biology*. 31:2262-75.

Virshup, D.M., and S. Shenolikar. 2009. From promiscuity to precision: protein phosphatases get a makeover. *Molecular cell*. 33:537-45.

Voet, D., and J.G. Voet. 2004. Biochemistry, Volume 1. J. Wiley & Sons.

Voets, E., and R.M.F. Wolthuis. 2010. MASTL is the human orthologue of Greatwall kinase that facilitates mitotic entry, anaphase and cytokinesis. *Cell cycle (Georgetown, Tex.)*. 9:3591-601.

Walker, D.H., A.A. DePaoli-Roach, and J.L. Maller. 1992. Multiple roles for protein phosphatase 1 in regulating the Xenopus early embryonic cell cycle. *Molecular biology of the cell*. 3:687-98.

Wang, L., Q. Nie, and G. Enciso. 2010. Nonessential sites improve phosphorylation switch. *Biophysical journal*. 99:L41-3.

Wang, P., X. Pinson, and V. Archambault. 2011. PP2A-Twins Is Antagonized by Greatwall and Collaborates with Polo for Cell Cycle Progression and Centrosome Attachment to Nuclei in Drosophila Embryos. *PLoS Genetics*. 7:e1002227.

Wu, J.Q., J.Y. Guo, W. Tang, C.-S. Yang, C.D. Freel, C. Chen, A.C. Nairn, and S. Kornbluth. 2009. PP1-mediated dephosphorylation of phosphoproteins at mitotic exit is controlled by inhibitor-1 and PP1 phosphorylation. *Nature cell biology*. 11:644-51.

Wu, J.Q., and S. Kornbluth. 2008. Across the meiotic divide - CSF activity in the post-Emi2/XErp1 era. *Journal of cell science*. 121:3509-14.

De Wulf, P., F. Montani, and R. Visintin. 2009. Protein phosphatases take the mitotic stage. *Current opinion in cell biology*. 21:806-15.

Wurzenberger, C., and D.W. Gerlich. 2011. Phosphatases: providing safe passage through mitotic exit. *Nature reviews. Molecular cell biology*. 12:469-82.

Xiong, W., and J.E. Ferrell. 2003. A positive-feedback-based bistable "memory module" that governs a cell fate decision. *Nature*. 426:460-5.

Yang, L., W.R. MacLellan, Z. Han, J.N. Weiss, and Z. Qu. 2004. Multisite phosphorylation and network dynamics of cyclin-dependent kinase signaling in the eukaryotic cell cycle. *Biophysical journal*. 86:3432-43.

Yao, G., T.J. Lee, S. Mori, J.R. Nevins, and L. You. 2008. A bistable Rb-E2F switch underlies the restriction point. *Nature cell biology*. 10:476-82.

Yu, J., S.L. Fleming, B. Williams, E.V. Williams, Z. Li, P. Somma, C.L. Rieder, and M.L. Goldberg. 2004. Greatwall kinase: a nuclear protein required for proper chromosome condensation and mitotic progression in Drosophila. *The Journal of cell biology*. 164:487-92.

Yu, J., Y. Zhao, Z. Li, S. Galas, and M.L. Goldberg. 2006. Greatwall kinase participates in the Cdc2 autoregulatory loop in Xenopus egg extracts. *Molecular cell*. 22:83-91.

Zhao, Y., O. Haccard, R. Wang, J. Yu, J. Kuang, C. Jessus, and M.L. Goldberg. 2008. Roles of Greatwall kinase in the regulation of cdc25 phosphatase. *Molecular biology of the cell*. 19:1317-27.

Zwolak, J., N. Adjerid, E.Z. Bagci, J.J. Tyson, and J.C. Sible. 2009. A quantitative model of the effect of unreplicated DNA on cell cycle progression in frog egg extracts. *Journal of theoretical biology*. 260:110-20.

Appendix.

Publications associated with this thesis

1 Different effects of redundant feedback loops on a bistable switch.

Domingo-Sananes, M. R., and Novák, B. 2010. Chaos 20, 045120.

2 Regulated kinases and phosphatases in cell cycle decisions.

Novák, B., Kapuy, O., Domingo-Sananes, M. R., and Tyson, J. J. 2010. Current Opinion in Cell Biology 22, 801-8.

3 Protein phosphatase 2A controls the order and dynamics of cell cycle transitions.

Krasinska, L., Domingo-Sananes, M. R., Kapuy, O., Parisis, N., Harker, B., Moorhead, G., Rossignol, M., Novák, B., and Fisher, D. 2011. Molecular Cell 44, 437-450.

4 Switches and latches: a biochemical tug-of-war between the kinases and phosphatases that control mitosis.

Domingo-Sananes, M. R., Kapuy, O., Hunt, T., and Novák, B. 2011. Philosophical Transactions of the Royal Society of London. Series B, Biological sciences 366, 3584-94.